

See discussions, stats, and author profiles for this publication at:
<https://www.researchgate.net/publication/269288555>

The role of (photo)electrochemistry in the rational design of hybrid conducting polymer/semiconductor assemblies: From fundamental concepts to practical applications

ARTICLE *in* PROGRESS IN POLYMER SCIENCE · OCTOBER 2014

Impact Factor: 26.93 · DOI: 10.1016/j.progpolymsci.2014.10.003

CITATIONS

10

READS

111

2 AUTHORS, INCLUDING:



[Csaba Janáky](#)

University of Szeged

45 PUBLICATIONS 396 CITATIONS

[SEE PROFILE](#)



Contents lists available at ScienceDirect



Progress in Polymer Science

journal homepage: www.elsevier.com/locate/ppolysci

The role of (photo)electrochemistry in the rational design of hybrid conducting polymer/semiconductor assemblies: From fundamental concepts to practical applications

Q1 C. Janáky^{a,b,*}, K. Rajeshwar^c

^a Department of Physical Chemistry and Materials Science, University of Szeged, Szeged H6720, Hungary

^b MTA-SZTE "Lendület" Photoelectrochemistry Research Group, Rerrich Square 1, Szeged 6720, Hungary

Q2 ^c Department of Chemistry and Biochemistry, University of Texas at Arlington, Arlington, TX 76019, United States

ARTICLE INFO

Article history:

Received 28 March 2014

Received in revised form

28 September 2014

Accepted 7 October 2014

Available online xxx

Keywords:

Hybrid assembly

Conducting polymer

Semiconductor

Electrochemistry

Photoelectrochemistry

ABSTRACT

Hybrid materials based on conducting polymers (CPs) and inorganic semiconductors (SCs) undoubtedly constitute one of the most promising classes of new materials. The spectacular progress in this research topic has been driven by the development of novel synthetic procedures and by the large variety of applications. Beyond scientific and fundamental interest, such hybrid assemblies are attractive from technological perspectives as well, for example, in energy conversion and storage, electronics, catalysis, and optics.

This article is designed to be a critical overview for the polymer materials science community on how to employ electrosynthetic methods to obtain hybrid materials with well-designed composition and morphology. As this review illustrates, (photo)electrochemical approaches are versatile and powerful tools in the preparation of conjugated polymer-based composites, containing both elemental and compound semiconductors. Hybridization of CPs with metal oxides (TiO_2 , WO_3 , ZnO , NiO , Cu_2O , CuO , V_2O_5 , Fe_2O_3 , Fe_3O_4 , MnO_2 , SnO_2 , RuO_2), metal chalcogenides (CdS , $CdTe$, $CdSe$, Bi_2S_3), and carbon nanomaterials (nanotubes, graphene, graphene oxide) is presented. We demonstrate that both composition and nanoscale architecture of the hybrid assemblies can be precisely controlled by employing carefully designed electrochemical methods. To achieve the goal of popularizing electro- and photoelectrosynthetic procedures, particular attention will be paid to compare the as-synthesized assemblies with their counterparts obtained from other procedures. The most prominent applications of these electrosynthesized materials are highlighted, with particular focus on energy related utilization pathways.

© 2014 Published by Elsevier Ltd.

Abbreviations: CB, conduction band; CNT, carbon nanotube; CP, conducting polymer; CV, cyclic voltammetry; DS, dodecyl sulfate; DSSC, dye-sensitized solar cell; EQCM, electrochemical quartz crystal microbalance; ERGO, electrochemically reduced graphene oxide; FF, fill factor; GC, glassy carbon; GO, graphene oxide; ITO, indium tin oxide; I_{sc} , short-circuit current; LPG, liquefied petroleum gas; MIP, molecularly imprinted polymer; MWCNT, multi-walled carbon nanotubes; NP, nanoparticle; NTA, nanotube array; ORR, oxygen reduction reaction; PANI, polyaniline; PCIT, poly(3-chlorothiophene); PDNTD, poly(N,N' -di[p-phenylamino(phenyl)]-1,4,5,8-naphthalene tetra-carboxylic diimide); PDOT, poly(3,4-diethoxythiophene); PEDOT, poly(3,4-ethylenedioxythiophene); PHT, poly(3-hexylthiophene); PMT, poly(3-methylthiophene); PNMPy, poly(N -methylpyrrole); POT, poly(3-octylthiophene); PProDOP, poly(3,4-propylenedioxyppyrrole); PPy, polypyrrole; PSS, poly(styrenesulfonate); PT, polythiophene; PVK, poly(vinylcarbazole); PZC, point of zero charge; RDE, rotating disk electrode; SC, semiconductor; SWCNT, single-walled carbon nanotube; VB, valence band.

Q3 * Corresponding author at: Department of Physical Chemistry and Materials Science, University of Szeged, Szeged H6720, Hungary. Tel.: +36 62544111.
E-mail address: janaky@chem.u-szeged.hu (C. Janáky).

<http://dx.doi.org/10.1016/j.progpolymsci.2014.10.003>

0079-6700/© 2014 Published by Elsevier Ltd.

25
Contents

26	1. Introduction	00
27	2. Overview and classification of preparation methods.....	00
28	3. Electrochemical methods for the preparation of hybrid organic/inorganic assemblies	00
29	3.1. Incorporation of inorganic semiconductors into CPs during electropolymerization.....	00
30	3.2. Electrodeposition of CPs on inorganic semiconductor (nano)structures	00
31	3.2.1. Electrochemical polymerization on semiconductors	00
32	3.2.2. Photoelectrochemical polymerization	00
33	3.3. Other miscellaneous approaches	00
34	3.3.1. Electrochemical co-deposition	00
35	3.3.2. Deposition of SCs on or inside the CP layer.....	00
36	4. Selected applications of electrochemically assembled CP/SC hybrids	00
37	4.1. Solar energy harvesting (solar and photoelectrochemical cells)	00
38	4.2. Energy storage	00
39	4.2.1. Supercapacitors	00
40	4.2.2. Lithium-ion batteries	00
41	4.3. Other miscellaneous applications	00
42	4.3.1. Heterogeneous (photo-)catalysis.....	00
43	4.3.2. Sensors	00
44	4.3.3. Electrochromics.....	00
45	5. Summary	00
46	Acknowledgements	00
47	References	00
48		

49
1. Introduction

The science and technology of conducting polymers (CPs, also called conjugated polymers or synthetic metals) have traveled a long way since the modern discovery of these materials in 1976. The search for new polymers with enhanced stability, processability, and other advanced properties led to the development of subsequent generations of new materials: starting from polyacetylene, through the various heteroaromatic structures (e.g., polythiophenes, polyaniline, polypyrrole), to polymers containing more complex monomeric units [1,2]. This spectacular development was triggered both by the scientific push coming from the relevant R&D communities and a technological pull from emerging applications.

While research has been continuously developing, an increasing interest was devoted to *hybrid assemblies* based on CPs. Combination of CPs with different type of materials, such as non-conducting polymers, metals, carbonaceous materials, and inorganic compounds was successfully achieved [3–5]. Such composites proved their attractive features in a wide range of applications from organic electronics to solar cells [6], energy storage [7], and sensors [8].

In this review article, we focus on one particular segment of this broad field, namely on CP-based hybrid materials containing inorganic semiconductors (SCs). From the very early years of the study of CPs, there were scattered trials to hybridize CPs with inorganic SCs. The really impressive progress of this research field, manifests especially during the last decade, in the exponential growth of research papers published (Fig. 1). CP composites containing metal oxides (TiO_2 , WO_3 , ZnO , NiO , Cu_2O , CuO , V_2O_5 , Fe_2O_3 , Fe_3O_4 , MnO_2 , SnO_2 , RuO_2), chalcogenides (CdS , $CdTe$, $CdSe$, Bi_2S_3), and carbon nanomaterials (nanotubes, graphene, graphene oxide) have been realized. Carbon nanomaterials are included in this article because they share many similar attributes with SCs (especially related

to composite formation), although most of them behave as metallic conductors.

As will be shown later, this research field is rooted in, and has emerged based on the experience gained from flat organic/inorganic junctions. However, this was quickly followed by the study of (nano)particulate systems, and finally, more recent works are almost exclusively devoted to hybrid organized nano-architectures. These studies are motivated by the recognition that nanostructured morphology plays a key role in various applications: such as solar cells (facilitating effective exciton dissociation), supercapacitors and Li-ion batteries (faster electrolyte diffusion), electrochromics (fast response), or sensors (enhanced surface area). Therefore in this review, particular focus is on such morphological aspects, both from the fundamental and application perspectives.

There is a large pool of preparation methods that can be deployed to obtain CP/SC assemblies. As presented later, different approaches can be categorized conveniently based on whether the components are synthesized concurrently (one-pot) or separately, and if the polymer is obtained thorough chemical or electrochemical coupling. In this paper we discuss procedures where at least one component is generated *in situ* in the presence of the other component. Furthermore, from the wealth of synthetic routes we solely focus on electrochemical and photoelectrochemical methods [9,10]. This means that in all the presented procedures in this review, electrochemical or photoelectrochemical oxidation of the monomers is the first step in the formation of the CP.

As can be seen in Fig. 1B, the number of research studies employing electrochemistry to obtain hybrid assemblies follows the same trend as that shown in Fig. 1A. Further, such methods are responsible for about 10% of the overall number of studies. Importantly, while for certain materials, electrochemical approaches have become the main-stream preparation method (e.g., carbon nanomaterial/CP

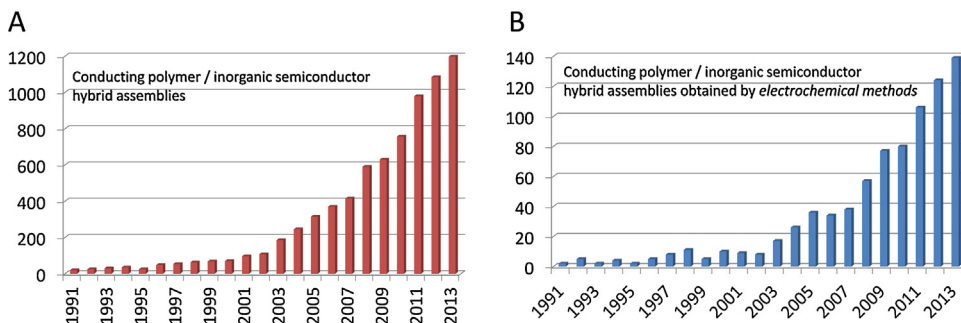


Fig. 1. Results from a literature survey using the ISI Web of Knowledge database on the number of articles published on conducting polymer-based hybrid materials; (A) in general, and (B) obtained through electrochemical methods. Note that the search was narrowed to semiconductor-containing hybrids.

composites), in other cases (chalcogenide/CP hybrids), they are not considered as widely as other (e.g., wet chemical) procedures. This also means that there are several groups of CP-based composites where electrochemistry has not been fully exploited yet. Therefore we hope that research groups actively involved in various allied areas will gain insights from the forthcoming examples, and may choose to employ electrochemical methods in the future more frequently.

As shown in this review, *in situ* electrochemical methods have several advantages over their *ex situ*-, and *in situ* chemically prepared counterparts, most importantly that the organic/inorganic interface is formed in one step during the preparation of such assemblies. Using electrodeposition, hybrid materials can be directly formed as a thin film on the electrode surface. Further, the composite structure (e.g., thickness, porosity and other morphological attributes) can be precisely controlled by electrochemical procedures. In addition, such modified electrodes have obvious benefits of strong adherence to the underlying supporting electrode and improved high mechanical stability. Application oriented benefits of the presented synthetic strategies are highlighted through comparative examples in the following sections. At the same time, however, we are aware of the drawbacks of electrochemical methods as well, most importantly that a significant portion of monomers cannot be electropolymerized. This is particularly true in the case of the recently developed bulky monomers, which are specifically designed for targeted applications (e.g., bandgap engineered polymers) [11].

2. Overview and classification of preparation methods

Prior to discussing the electrochemical methods in detail, it is worth briefly to summarize and categorize the various synthetic procedures generally employed to obtain CP/SC assemblies. A classification of variant procedures is shown in Scheme 1, where three main categories can be identified based on the time dimension of the synthesis.

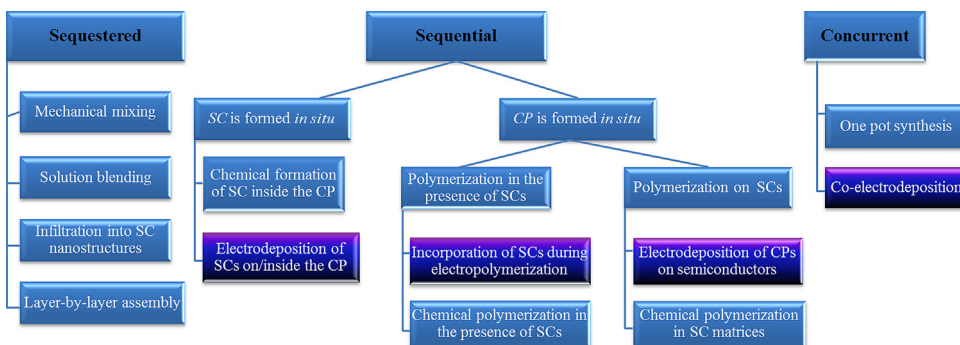
The main feature of all methods in the first category (*sequestered synthesis*) is that both the CP and SC components are synthesized separately, and the hybrid is assembled during a subsequent step, by simple or more sophisticated blending of the two components [12]. These procedures are the most commonplace due to their simplicity, and due to the fact that the resulted hybrid

material is usually solution-processible. This feature in turn facilitates mass production and processing (e.g., roll-to-roll printing using the composite dispersed in solution). Furthermore, in these methods, all the well-established synthetic procedures can be employed for each constituent separately, since their application is not affected by the presence of the other component. As for the assembly process, there is a wealth of strategies available, ranging from simple mechanical mixing of the two powders, to more complex methods such as layer-by-layer build-up or ligand exchange procedures. Last but not least, physical infiltration of CPs into SC nanostructures can also be achieved, resulting in highly ordered organic–inorganic semiconductor architectures.

According to experimental studies, however, such penetration is not that simple, the polymeric guest materials may block the pores of the nanostructured host due to simple physical limitations (e.g., hydrodynamic radius of the polymer), precluding complete pore filling, and therefore pore filling ratios as low as 0.5% have been obtained (this phenomenon will be discussed later in detail) [13]. Finally, the difference in the hydrophilic/hydrophobic nature of the two components can further hamper the application of such procedures.

In the second category of methods (*sequential*), one component of the hybrid material is generated *in situ* in the presence of its counterpart. These techniques can be further sorted on the basis of the *in situ* formed component. We focus here on strategies where the CP is synthesized *in situ* in the presence of the SC; however, the opposite sequence is also possible, namely the SC component is generated *in situ* inside the CP, either through chemical (co-precipitation) or electrochemical methods (stripping). As for the *in situ* polymerization, two distinctly different strategies can be followed. In the first group, polymerization is carried out in the presence of dispersed SC particles (either dots or other structures such as nanotubes, nanowires and nanorods), and depending on the synthesis method, either composite particles (typical for chemical polymerization), or hybrid thin films, containing SC particles are obtained (typical for electropolymerization).

For the chemical synthesis, formation of the nanocomposite is rather straightforward, because during chemical synthesis of a CP, coexisting nanoparticles act as nuclei, thus the forming insoluble oligomer chains are deposited on them. On the other hand, in the case of electrochemical



Scheme 1. Summary of the preparation routes employed to synthesize SC-containing CP-based composite materials. Darker color indicates electrochemical methods, which are discussed in this review in greater detail.

synthesis, formation of the hybrid is not that obvious, since it usually relies on the exploitation of specific interactions between the monomer/oligomer and the nanoparticles (see [Section 3.1](#)). The second major group consists of tactics where CP is *in situ* deposited either on SC electrodes, or on electrode surfaces on which SCs are immobilized.

As for the third category (*concurrent* procedures) in [Scheme 1](#), probably the easiest (and the most uncontrolled) methods belong to this group. These “one pot” methods are simply based on the *in situ* formation of *both* components, in/from one solution. Both chemical and electrochemical procedures belong to this group; however, co-electrodeposition is more frequently used. The most important drawback of this method is the very limited control over structure and morphology of the resultant composite material.

CPs are usually synthesized through oxidative coupling. In most polymerization reactions, the first step is the oxidation of the monomer, resulting in the formation of a radical cation, which reacts with another monomer or radical cation, forming a dimer. Therefore, another obvious dimension along which methods can be categorized is the way of initiation (and maintenance) of the polymerization. The two most generally applied routes are *chemical* and *electrochemical* oxidation. In the first, chemical oxidants (such as FeCl_3 or $(\text{NH}_4)_2\text{S}_2\text{O}_8$) are used to oxidize the monomer, whereas in the second one, monomers are oxidized electrochemically. Other, miscellaneous approaches, such as heat initiated polymerization [14], photopolymerization [15], or ultrasound-assisted methods [16] are also available. Note, however, that these methods are restricted to certain, special esoteric monomers.

Finally, although the particular advantages of each electrochemical method will be presented later, we briefly note that using electrodeposition composites can be directly formed as a thin film on the electrode surface. Furthermore, the film thickness, porosity and morphological features can be precisely controlled by electrochemical procedures. Also, such modified electrodes have obvious advantages of high mechanical stability and strong adherence to the underlying supporting electrode surface. For comparison, note the typical drawbacks and limitations of corresponding materials derived from chemical methods: (i) possible aggregation of the inorganic particles, resulting in a relatively small area of the organic/inorganic interface; (ii)

uncontrolled, random distribution of the particles within the polymeric matrix; and finally (iii) lack of electrical contact between the inorganic material and the supporting electrode (this hampers the application of the hybrids in many applications, e.g., electronics).

Before describing the particular electrosynthetic strategies to obtain CP based hybrid assemblies, it is useful to discuss some of the general aspects of electrochemical polymerization [17,18]. Therefore, electrochemical protocols, which are mostly employed to electropolymerize CPs are summarized and compared in [Table 1](#); typical examples for each technique are given in [Fig. 2](#). By sorting the listed approaches, two major groups can be identified: static and dynamic methods. Depending on the controlled variable, we can also distinguish between potential- and current-controlled techniques. Some of their advantages and disadvantages of these approaches are listed [Table 1](#). At this point it is important to clarify a terminological issue which is problematic in many publications, namely that cyclic voltammetry (CV) is an *electroanalytical* tool, not a *synthetic* procedure. Therefore, when potential cycling is employed to electrogenerate a CP, the correct nomenclature is either “potentiodynamic electropolymerization”, or polymerization by “potential cycling” (instead of using the term CV).

As may be seen from [Table 1](#), as well as in [Fig. 2](#), the different methods of electrochemical polymerization have markedly different features. Depending on the complexity of the procedure, a number of parameters can be varied in order to tailor the properties of the forming CP toward a targeted application. Optimization of these circumstances (e.g., potential window, sweep rate, current density, time of each potential step) is crucially important in light of the competing processes [19]. Concurrent nucleation and growth, or in other words, the formation and growth of insoluble oligomers, control the relative contribution of solution phase and solid phase polymerization. Furthermore, depending on the above listed parameters, polymer formation can also be controlled either by the polymerization kinetics or by monomer (or even dopant ion) mass transport. Note that these processes become even more important when either nanoparticles are used as dopants, or CPs are electrodeposited on nanostructured SC matrices.

Beyond the employed electrochemical technique, several other factors influence the polymerization process

Table 1

Summary and comparison of various electrochemical polymerization methods employed to obtain CPs.

Method	Controlled variable	Measured response	Advantage	Disadvantage	
Static Galvanostatic	Current density kept constant	Potential	The polymerization rate as well as overall charge density can be easily controlled and continuous growth ensured	Simple methods, easy to interpret the obtained data both qualitatively and quantitatively Potential may reach high values to keep the current constant, which can cause overoxidation. It is difficult to normalize the current in the case of nanostructured electrodes Possible inhomogeneous growth of the polymer, especially for thicker layers. The current may drop significantly in the case of longer procedures	Potential may reach high values to keep the current constant, which can cause overoxidation. It is difficult to normalize the current in the case of nanostructured electrodes The monomer concentration continuously decreases in the close vicinity of the electrode, and there is no time to replenish it. Therefore the polymerization can be limited by diffusion
Potentiostatic	Potential kept constant	Current density	As the potential is controlled, overoxidation can be avoided while speeding up polymerization		
Dynamic Current pulses	Current density periodically varied	Potential	The overall charge density can be easily controlled	There are rest periods between the polymerization steps; therefore problems caused by diffusion limitation can be avoided	Electrochemical double layer may get charged/discharged at every step More complicated than static methods; there are more parameters to consider and to optimize
Potential step	Potential periodically varied	Current density	Polymerization can be precisely controlled		
Potential cycling (potentiodynamic)	Potential cyclically varied	Current density	Polymer is under permanent electrochemical stimulus		

(Table 2), such as solvent, electrolyte, electrode material, monomer etc. All these have crucial impact on the properties of the CP ranging from molecular structure to supramolecular morphology [20]. For a hybrid, the picture gets even murkier. Two examples suffice for the challenges

which have to be overcome: (i) selection of the appropriate potential window, where the monomer gets oxidized (but the polymer will not suffer overoxidation), and at the same time the solvent, the electrolyte ions, and the SC remain chemically intact; (ii) optimization of the polymerization

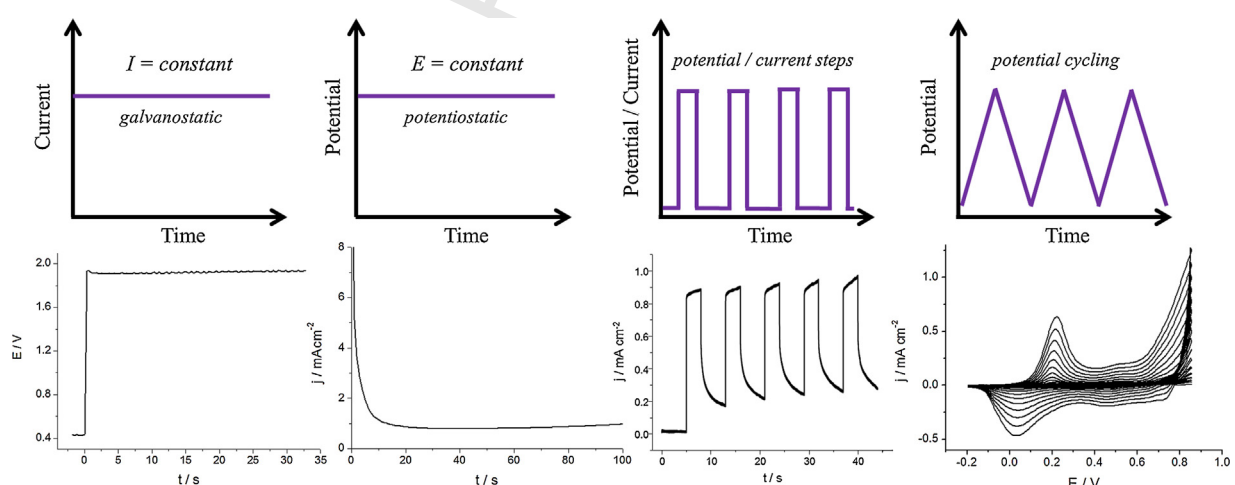


Fig. 2. Comparison of frequently employed electrochemical polymerization techniques. The controlled variables upper drawings, as well as the measured experimental responses measured data at the bottom, are shown for the various cases.

Table 2

Factors that affect electrochemical polymerization of CPs.

	General considerations, and properties it affects	Possible threat	Typical examples
Electro-chemical method	I It affects both the molecular and supramolecular structure of the polymer. By varying the synthesis parameters the thickness and the morphology of the polymer can be controlled	C areful selection of the applied potential window is indeed important to avoid overoxidation of the polymer M ass transport limitation is usually also not favored	S tatic: Potentiostatic, galvanostatic D ynamic: multiple potential steps, potentiodynamic cycling
Monomer	S ome monomers (especially the bulky ones) are not electropolymerizable O ften dimers or trimers are used as precursor, due to their lower oxidation potential M onomers with $-COOH$ and $-NH_2$ moieties are generally useful for composite preparation	L ow solubility causing mass transport limitation H igh oxidation potential may hamper electrodeposition onto SCs	O ur review is restricted to the classic heteroaromatic monomers and their derivatives (pyrrole, thiophene, aniline). Larger monomers with fused rings are not discussed here
Supporting electrolyte	I on exchange behavior of the polymer is strongly dependent of the electrolyte used during the electropolymerization (mobile vs. immobile anions) D oping level, and electroactivity is also affected M orphology, the compactness and porosity is also linked to the nature of the electrolyte	H ighly electronegative and nucleophile anions may assist overoxidation of the polymer N ote that some anions are effective dopants, others are not (especially true for multivalent anions)	I mmobile anions (PSS^- , DS^-) M obile anions (ClO_4^- , BF_4^- , PF_6^-) S mall cations (Li^+ , Na^+) B ulky cations (Bu_4N^+ , cetyl-) I onic liquids can be solvent and dopant at the same time
Solvent	A queous solutions are generally preferred, due to economic and environmental consideration. pH of the solution is crucial to obtain the conducting form of the polymer F or certain, thiophene-type monomers, non-aqueous solvents have to be utilized T he solvent affects the morphology, and even the electroactivity (memory effect)	F ormation of non-conducting polymer O xidation/reduction of the solvent	Water, A cetonitrile, nitrobenzene, propylene carbonate, nitromethane, various ionic liquids
Electrode material	A hesion of the polymer, interactions are possible between the monomer and the electrode I nterfacial properties of the polymer/electrode junction	O xidation of the electrode material D etachment of the CP L ow conductivity hampering the electrodeposition of the polymer	C lassical inert electrodes are: Pt, Au, glassy carbon, ITO coated glass E xamples for SC electrodes are presented in this review

medium, both in terms of the conducting electrolyte, as well as the solvent. Further, several monomers can only be polymerized in organic solvents; while in aqueous solutions, special emphasis should be given to the pH (it has to be optimal for both components).

3. Electrochemical methods for the preparation of hybrid organic/inorganic assemblies

3.1. Incorporation of inorganic semiconductors into CPs during electropolymerization

In the following examples, SC particles are embedded into the matrix of various CPs, through electropolymerization of the respective monomers in the presence of SCs. In these methods, compared with conventional electrogeneration of CPs, the only difference is having the (nano)particles in the polymerization media. Otherwise, similar inert working electrodes (Au, Pt, ITO, glassy carbon) and electrochemical procedures (see Table 2) are used. This one-step procedure is very attractive, because the composite can directly form *in situ* on an electrode surface, which can then be readily used as a chemically modified electrode.

The first trials in this manner relied on the simple physical entrapment of colloidal particles. Different metal oxide

particles (MnO_2 , SnO_2 , TiO_2 and WO_3) were incorporated into both polypyrrole (PPy) and polyaniline (PANI) [21–26]. The role of anions in the solution, the concentration of the SC particles, and the crucial influence of vigorous stirring, was demonstrated. The need for stirring can be rationalized by the large (micrometer) size of the SC particle, which would otherwise sediment. As for the role of pH and anions being present in the polymerization solution, detailed studies revealed that successful synthesis (e.g., high particle content in the deposited polymeric matrix) is based on optimizing interactions between the polymer and the SC particles. This interaction is usually electrostatic in nature, which means that the SC particles bearing negatively charged surfaces are incorporated into the polymer as dopants, compensating the positive charges generated in the polymer during the anodic electropolymerization. In other words, without such strong interactions, synthesis usually leads to small loadings of the built-in component, due to some occasional physical or weak chemical (dipole-dipole) interactions between the polymer and the SC particles.

Metal oxides can have different surface charge depending on the solution pH. Thus their surface $-OH$ groups can be neutral, protonated (positive surface charge), or deprotonated (negative surface charge). Some oxides (e.g.,

SnO₂, WO₃) have very low point of zero charge (PZC), consequently the pH of the oxide suspension (*without any additional electrolyte*) results in negative charges on the oxide surface. For these materials no external anions are needed as dopants, although the lack of other anions may result in lower doping levels, and thus poor electroactivity. In other cases, most importantly for TiO₂, basic conditions would be needed to ensure negative surface charge. Formation of CPs in basic solutions, however, is hampered by the presence of nucleophile OH[−] ions which lead to the formation of non-conducting polymeric species. To overcome this problem, addition of different anions (e.g., I[−] and SO₄^{2−}), having good adsorbability on the particle surface, may lead to a negatively charged surface, without disturbing electrochemical growth of the CP [22].

The effect of presence of a conducting electrolyte, however, is complex: (i) anions being adsorbed on the SC particle surface may enable their incorporation as dopants (ii) the anions can act as dopants themselves, therefore hampering incorporation of the oxide particles. In light of the possibility of such competitive doping, it is not surprising that the loaded amounts of the oxide decrease with increasing electrolyte concentration [23]. There is also good correlation between the amount of particles in the solution and in the composite, which indicates that incorporation is limited by mass transport of the SC particles. This feature was also confirmed by the fact that a slower polymerization procedure (e.g., lower current densities during the galvanostatic polymerization) results in a higher amount of the SC particle [23]. Finally, incorporation of the photoactive SC particles was confirmed by the photoelectrochemical behavior of the composite [23]. However, the anodic photocurrents were rather low (compared to both neat SC surfaces and hybrids with organized nanoscale structures, as shown in Section 3.2) predominantly due to the fact that only the CP had electrical contact with the supporting electrode (and the solution) resulting in inefficient charge carrier transport.

Based on the previous observations, and recognizing the importance of surface charge, further sophisticated surface treatments have been developed. Various small sized, and also macroions have been employed to cover the surface of the particles. It is important to emphasize that after the initial studies (mentioned above), where colloidal sized particles were incorporated, the interest turned toward nanoparticles (NPs) and other structures with nanosized dimensions. The most important features of using nano objects are the increased specific surface area, the lack of sedimentation in the suspension, and the novel properties related to the nanometer scale size of the various compounds. Besides additional studies on TiO₂ [27–33] and WO₃ [34], the group of embedded SC particles has been extended to include Bi₂S₃ [35,36], CdS [37–39], CdTe [40], Fe₂O₃ [41–43], Fe₃O₄ [44–46], MnO₂ [24], V₂O₅ [47,48], ZnO [49], and ZrO₂ [50], as listed in Table 3.

All the methods presented in Section 3.1 share at least one common attribute, namely that the incorporated SCs were prepared *before* the electrochemical polymerization. NPs of SC compounds are generally synthesized by wet chemistry. The principal advantage of these methods is that both the size and size distribution of the NPs can be

carefully controlled in the synthesis. Note that NPs are often grown in the presence of a surfactant, to prevent the nanosized particles from aggregation. Moreover, encapsulating agents may facilitate the incorporation of the coated NPs during anodic electrodeposition of the respective polymer through various interactions, as discussed earlier. Such coating species, however, may also affect the reactivity, solubility and dimension of the resulting NPs, therefore careful selection of encapsulating ions is indeed important. Despite the above advantages, application of surfactants has also an unintended effect, namely separating the inorganic and the organic semiconducting phase. In the case of electrochemically inactive surfactants, this separation may cause insulation (series resistance) between the polymer and the NPs. The existence of such an electrical barrier is particularly disadvantageous in applications based on charge transfer and/or charge separation at the organic/inorganic interface. To overcome this problem, the use of electroactive coatings has been introduced, and their effectiveness was thoroughly demonstrated [58,59].

Going another step further, nanoparticles were coated by the electroactive monomer molecules *themselves*. In this manner electropolymerization can start right at the NP surface; an intimate contact is thus ensured while aggregation is also avoided. Also note that here the driving force for the encapsulation of SC nanoparticles is not doping but the chemical interaction between the SC and the monomer/polymer components. Such chemical interactions can be facilitated through various moieties, such as –OH/–COOH, Au/S and –COOH/–NH₂, etc. This strategy was followed for preparing hybrid thin films of Fe₃O₄ and poly(3-thiophene-acetic-acid) [60]. Magnetite nanoparticles were stabilized in a non-aqueous solution through chemisorption of the monomer on their surface. The interaction of surface –OH groups of the oxide NP and the carboxyl moieties of the monomer was utilized. By this method, through simple variation of the magnetite content of the polymerization mixture, the amount of encapsulated oxide could be easily tuned, and increased up to 80% (w/w), as corroborated from electrochemical quartz crystal microbalance (EQCM) data [60]. In addition, by covering the NPs with an organic coating it was possible to carry out the electropolymerization in organic media (which is a prerequisite for certain thiophene-type monomers).

In an even more sophisticated variant of this method, a thin primary layer of the polymer/oligomer was electrodeposited on the electrode surface (shown in Fig. 3). Subsequently, electrochemical capture of CdSe semiconductor nanocrystals, with thiophene-terminated carboxylic acid capping ligands, took place at the surface of electrodeposited polythiophene film [51,52]. Due to the large size, and consequently the low diffusion coefficient of the monomer coated NPs, a multiple potential step method was employed. Initially a very short step of high potential is applied, when electrodeposition is kinetically controlled. Subsequently, a longer rest pulse is included, when the solution got enriched around the electrode surface (depletion layer). These two steps can be applied multiple times to increase the film thickness, and thus the NP loading.

A very similar approach has been followed to electrochemically attach p-aminothiophenol-functionalized CdS

Table 3

Representative examples for the incorporation of inorganic SCs into CPs during electropolymerization.

Semiconductor	Polymer	Method	Comments/ Important message	Refs.
Bi ₂ S ₃	PPy	Potentiodynamic	The lack of interaction between the components led to low inorganic content embedded in the polymer	[35,36]
CdS	PANI	Galvanostatic	The effect of the agitation of the solution was shown	[37]
		Potentiostatic	Electrolyte dependence was observed and described	[38]
CdSe	Thiophenes	Potentiodynamic	Role of stirring was emphasized	[39]
		Potentiostatic	Role of electroactive protecting shell (of the monomers) was shown	[51,52]
CdSe@ZnS	PDMDT	Potentiodynamic	The NPs were protected with –NH ₂ functionalized molecules, which can be coupled with the monomer	[53]
CdTe	PPy	Galvanostatic	A thin pre-layer of the polymer was advantageous, to avoid the need for high potential (degradation of the inorganic component was thus avoided)	[40]
CuMnO	PPy	Galvanostatic	The role of anions was shown, in light of the difference in the conductivity of the obtained hybrid	[54]
Fe ₂ O ₃	PPy	Galvanostatic	Role of the surface adsorbed anions was demonstrated	[42]
		Potentiostatic	Different anionic chelating agents were used to facilitate incorporation. Conductivity of the hybrids was compared	[43]
		Galvanostatic	Incorporation of NPs was achieved by chemical etching of the NP surface, endowing negative charge to them	[41,44]
Fe ₃ O ₄	PANI	Galvanostatic	The previous method was extended for another polymer	[55]
	PEDOT	Galvanostatic	The role of pH on the polymer formation was shown	[55]
	PPy	Galvanostatic	The mechanism was uncovered, doping type incorporation was evidenced	[44–46]
MnO ₂	PPy	Galvanostatic	The mechanism was summarized, emphasizing the role of interactions between the components	[24]
NiCoO	PPy	Galvanostatic	The polymer was immediately overoxidized during the synthesis	[56]
TiO ₂	PANI	Galvanostatic	The role of stirring was evaluated	[27]
		Potentiostatic	The polymer was immediately overoxidized	[32]
	Polyazulene	Potentiodynamic	The role of stirring, as well as the pre-deposition of a polymeric layer was studied	[31]
		Galvanostatic	The influence of TiO ₂ concentration on the incorporated amount was shown	[33]
	PPy	Galvanostatic	The crucial role of different anions, potentially adsorbed on the NP surface, was demonstrated	[22]
		Galvanostatic	Oxalic acid was used as electrolyte during the deposition	[28,29]
		Potentiodynamic	Thermal stability of the hybrid was discussed	[30]
V ₂ O ₅	PEDOT	Galvanostatic	Titanate nanotubes were incorporated	[57]
	PPy	Potentiostatic	Good discussion on the mechanical properties of the hybrid	[47]
WO ₃	PANI	Potentiostatic	Inorganic nanobeams were incorporated	[48]
	PDMDT	Potentiodynamic	Role of stirring was studied	[21]
	PPy	Galvanostatic	H-bonding contributed to the immobilization of the NPs	[34]
ZnO	NMPy	Potentiodynamic	Detailed analysis of the effect synthesis parameters on the hybrid composition and properties was given	[26]
ZrO ₂	Polymer	Potentiodynamic	The role of a surfactant in the solution was shown	[49]
			The hybrid formed a strongly adherent layer	[50]

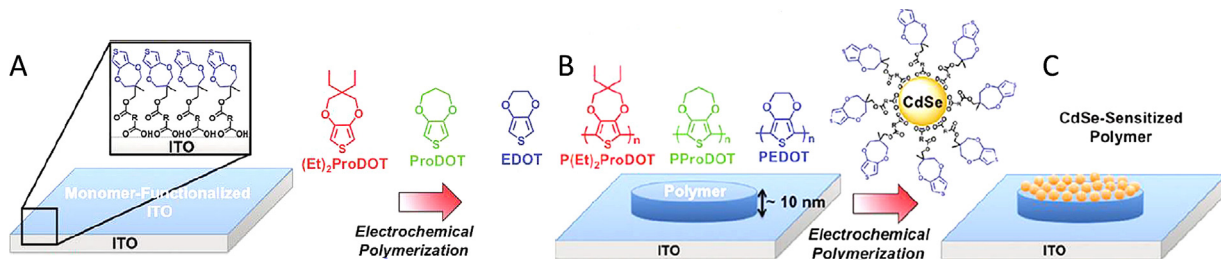


Fig. 3. Schematic illustration of the formation of different polythiophene/CdSe hybrids, using monomer coated nanoparticles, and the pre-deposited thin polymeric film (A–C). [52]. Copyright 2010, Adapted with permission from the American Chemical Society.

nanostructures to a Au electrode, which was pre-modified with a monolayer of the monomer [61]. Interestingly even ternary hybrids were realized through this approach by adding either gold NPs [62] or carbon nanotubes (CNTs) [63] to the CdS/PANI system. Importantly, these hybrids showed improved photoelectrochemical properties compared with its CNT-, and Au free counterpart due to better charge separation and charge carrier collection.

Another remarkable group of polymerization methods uses carbazole containing dendrons as precursor of the CP and as coating agent for chalcogenide NPs. Polymerization in such configuration was shown to be successful for a TiO₂/PPy system already, with the use of pyrrole-coated TiO₂ nanoparticles at the supporting electrode surface as a precursor [64]. Polymer formation is based on electrochemical crosslinking, and therefore it is different from the previously shown examples in various aspects [65,66]. As seen in Fig. 4A, monomer-coated particles were cast on the electrode surface which was subsequently exposed to potentiodynamic cycling (no additional monomers or monomer-coated NPs are available in the solution). In this procedure, the carbazole units are crosslinked both intra-molecularly and inter-molecularly within the film structure. In contrast to the previous examples, the higher current densities detected here with the increasing number of cycles do not mean increasing amount of material on the electrode, but rather step-by-step formation of the electroactive polymer as corroborated from the gradually developing electrochemical activity (Fig. 4A). Importantly, the bandgap of the organic SC can be tuned by the number of cycles (Fig. 4B).

All the previous examples share the same attribute in the sense that an external coating (either a negatively charged surfactant or an electroactive monomer) was introduced to facilitate the incorporation of the SC NPs. A somewhat different approach uses a special electrolyte or reagent for chemically modifying the SC NP surface, which subsequently leads to an interaction with the polymeric chain. This is illustrated in Fig. 5, for the specific example of chemically etched Fe₃O₄ nanoparticles, leading to a negatively charged surface. By using potassium tetraoxalate as electrolyte the magnetite nanoparticles are partially dissolved, and their surface is covered by Fe-oxalate moieties. Importantly, careful optimization of the electrolyte concentration and magnetite amount is required, to endow negative charge to the particles, but not to dissolve them completely [41,44,45].

In the case of carbon nanostructures, surface modification is even more facile. Both carbon nanotubes and graphene sheets can be chemically modified to introduce different functional groups, such as –OH, C=O, –COOH, or –NH₂. Oxygen containing moieties are usually formed by oxidative acid treatment at elevated temperatures, whereas other groups are often introduced by chemical coupling reactions [67,68]. Such modifications make these materials more hydrophilic, which allows them to be dispersed in aqueous media. Note that this is a prerequisite for their subsequent incorporation into CPs during electrosynthesis in aqueous solutions. Furthermore, these moieties can facilitate either doping type incorporation, or immobilization based on the interaction between the monomer/polymer and the surface-functionalized carbon nanomaterial [69].

In the case of graphene, the starting material is frequently graphene-oxide (GO) (note that it has a wealth of different oxygen containing moieties), which is subsequently reduced electrochemically *inside the composite material*. Representative functional groups and their respective interactions are shown in Fig. 6. Note that due to the easy surface modification, and therefore the large variety of possible interactions, this approach is widely used, so only a few representative examples are shown in Table 4.

As a partial summary, we may conclude that a wealth of examples was shown above for the incorporation of SCs into CPs, while they were electrogenerated on the surface

Table 4
Representative examples for the incorporation of carbon nanomaterials into CPs during their electrochemical polymerization.

Carbon	CP	Refs.
C60	PEDOT POT	[72] [73]
Carbon black	PPy	[74,75]
Graphene	PANI PEDOT Polypyrrole PPy	[76] [77] [78] [71,79–81]
MWCNT	PANI PEDOT PPy PMT	[70,82,83] [84–88] [89–92] [93]
SWCNT	PPy PANI	[94] [95,96]

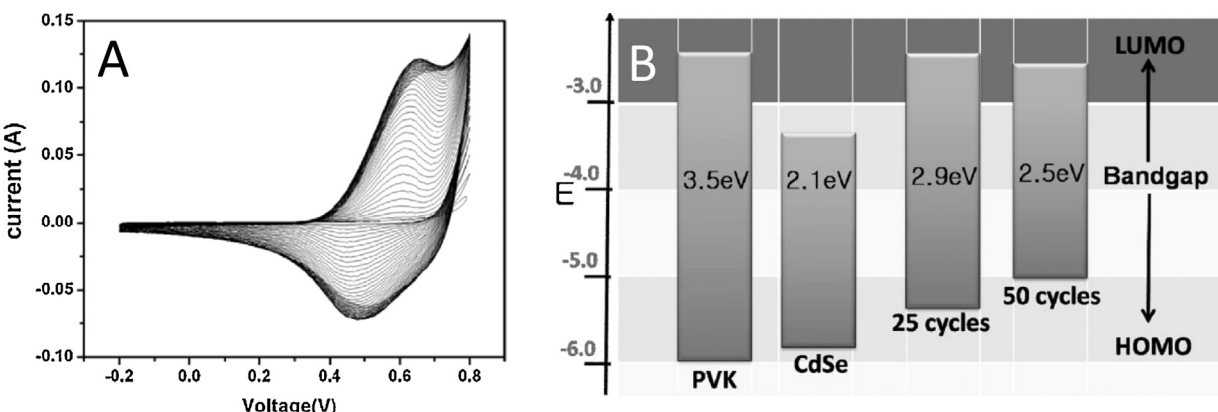


Fig. 4. Potentiodynamic curves registered during the electrochemical crosslinking of carbazole-dendron covered CdSe NPs. B: Bandgap tuning through electropolymerization. For comparison, band positions of the monomer PVK, and CdSe are also shown. [65]. Copyright 2008, Adapted with permission from John Wiley & Sons Inc.

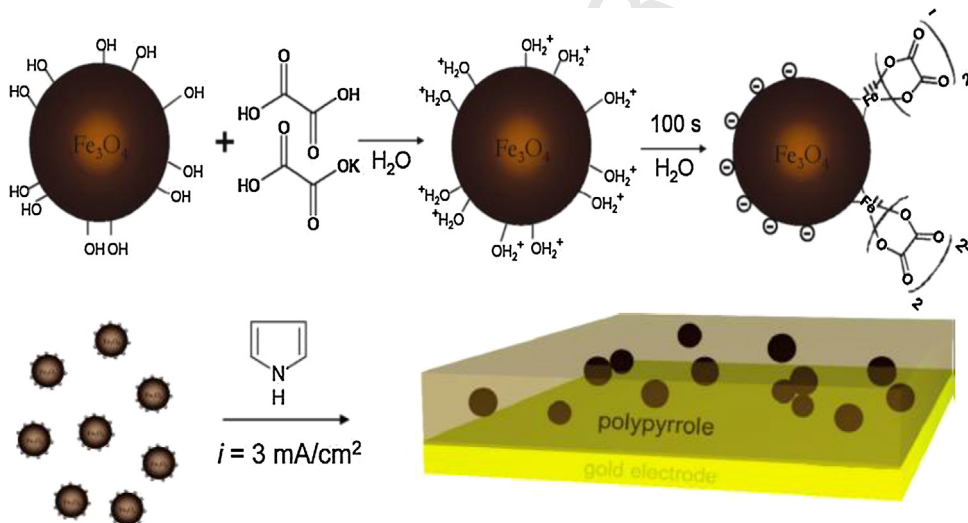


Fig. 5. Illustration of the surface modification of magnetite nanoparticles with potassium tetraoxalate electrolyte top, and of nanocomposite formation during the electrochemical polymerization bottom. [45]. Copyright 2010, Reproduced with permission from the American Chemical Society.

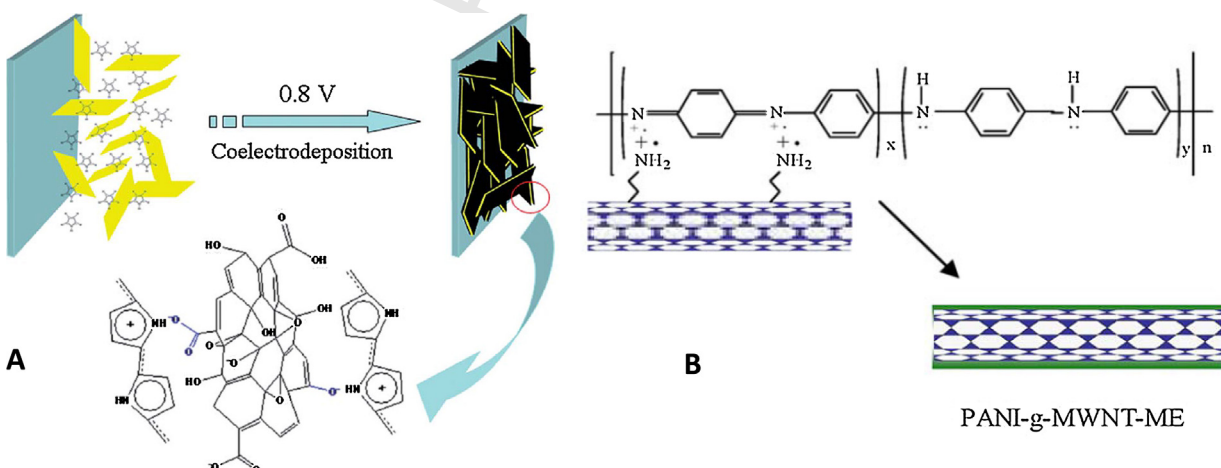


Fig. 6. Illustration of interaction between surface-modified carbon nanomaterials and CPs.

Sources, respectively: [70], Copyrights 2006, Reproduced with permission from Elsevier Ltd.; [71], Copyrights 2012, the Royal Society of Chemistry.

of conventional electrodes. All these methods, however, share some significant drawbacks and limitations, the two most important being the uncontrolled, random distribution of the (nano)particles within the polymer, and the fact that only the polymer phase has electrical contact with the supporting electrode. Consequently, use of the hybrid as an *electrode* is handicapped by both inefficient charge separation and propagation. The tactics outlined in the following sections aim at overcoming these problems, by using well-ordered SC arrays, in which both components have electrical contact with the supporting electrode.

3.2. Electrodeposition of CPs on inorganic semiconductor (nano)structures

Beyond the generally used noble metal (Pt, Au), glassy carbon (GC) and ITO-coated glass electrodes, semiconductor materials can also be used as working electrodes for the electrochemical polymerization of CPs. Such approaches are motivated by various applications, ranging from the simple protection of inorganic SC electrodes (e.g., CdS, Si) from either corrosion or photocorrosion, to photo-sensitization of oxide SCs, most importantly, TiO₂. Employing SC electrodes, however, is hampered by various facts, most importantly by their limited stability and lower conductivity, compared to their previously mentioned metal counterparts. Therefore, careful optimization of the polymerization procedure is indeed required, as demonstrated in this section. The first successful studies were carried out using flat SC surfaces; however, our particular focus is on nanostructured SCs, because the real advantages of these tactics become really prominent in the case of such architectures.

3.2.1. Electrochemical polymerization on semiconductors

In this section, electrosynthetic methods, in which SCs are used as working electrodes, are described. Importantly, in all the presented examples, electrochemical polymerization was carried out without illumination, in the dark. Studies exploiting the photoelectrochemical behavior of the SC electrode are presented in Section 3.2.2. In the early studies, CPs were electropolymerized on flat SC surfaces. In this vein, electrodeposition of CPs on elemental SCs (e.g., Si) [97], phosphides (e.g., InP) [98], metal oxides (e.g., CuO, MnO₂ or TiO₂) [99–102], different chalcogenides (including CdS, CdSe, CdTe and PbS) [103–109], as well as ternary compounds (CuInS₂ and CuInSe₂) [110,111] was accomplished.

The most important lessons learned from these studies include appreciation of the need for careful selection of the potential window, especially for those SCs which are prone to electrochemical corrosion. A notable trick to keep the SC electrode material stable is to use organic dimer or trimer instead of using the respective monomer. As mentioned earlier, the oxidation potential gradually decreases with increasing segment number due to the extended conjugation length (Fig. 7) [112]. This way, the polymerization can start at notably lower potentials, minimizing the risk of oxidizing the electrode material. Furthermore, the use of non-aqueous solutions, and especially ionic liquids, may

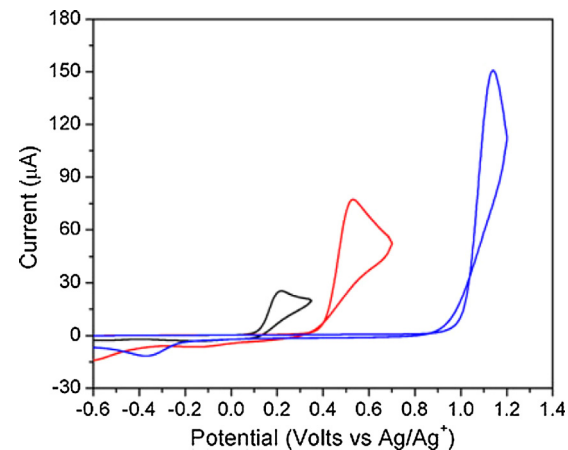


Fig. 7. Comparison of potentiodynamic polymerization curves for EDOT, bi-EDOT, tri-EDOT.
[112], Copyright 2011, Reproduced with permission from Springer.

also be viable strategies contributing factor to keep the SC electrode stable.

For electrodeposition of CPs on *nanostructured* oxide matrices, multiple challenges have to be tackled simultaneously, namely issues with mass transport limitations, and difficulties related to the low conductivity of the semiconductor matrix. Carbon nanomaterials exhibit far the highest conductivity within the studied group, which means, that for this class of materials, the limited conductivity is not an issue. Furthermore, beyond the sufficiently high conductivity, there is also a catalytic effect of carbon nanomaterials toward the electropolymerization of CPs, presumably due to π–π stacking between them and the heteroaromatic monomers. Because of this catalytic effect, deposition of CPs is favored on CNTs compared to the supporting electrode, and oxidation of the monomer (and consequently the polymerization as well) will occur at lower potentials compared to the generally used noble metal, or glassy carbon (GC) electrodes. Also note that no pretreatment of the nanocarbon is required, in contrast to the methods presented earlier, where surface groups have to be formed to ensure interaction with the polymer phase. Furthermore, there is no risk of aggregation of the nanomaterials during polymerization since they are not in the solution phase during the procedure. Table 5 lists representative examples of electrodeposited CPs on carbon nanomaterials.

In the early studies in this group, CNT films were obtained from simple drop- or spin coating of their solutions on an inert conductive surface (noble metal, ITO, GC), and were then used as working electrode for the subsequent electropolymerization of a monomer. This configuration is useful for some of the targeted applications (e.g., sensors or electrochromics), but is handicapped by both the rigidity of the supporting electrode, as well as the poor adhesion of the carbon nanomaterials, which can eventually lead to their partial desorption from the substrate. More recently, well-ordered arrays of CNTs were grown on flexible thin metal foils and used as template to electrodeposit CPs on them [122,123,127,129,139].

Table 5

Examples of electrodeposited CPs onto carbon nanomaterials.

Carbon	CP	Refs.
Carbon rods	PPy	[113]
Graphene	PANI	[114–116]
	PPy	[117–120]
MWCNT	PANI	[121–123]
	PEDOT	[124,125]
	PMT	[126]
	PPy	[127–129]
	PVK	[130,131]
Porous carbon	PANI	[132]
	PPy	[133]
SWCNT	PANI	[134–136]
	PDOP	[137]
	PHT	[138]
	PPy	[139]
	PT	[140]
	PVK	[130,131]

Such nanoarchitectures bear the advantage that every single nanotube is in direct electrical contact with the supporting electrode. Furthermore, the density of these nanotube arrays (NTAs, also called as forests or carpets) can be tuned by the synthetic parameters, and adjusted to the targeted application needs. Finally, composites based on free-standing films of CNTs and graphene have also come to the forefront of research recently. In this configuration, there is no additional supporting electrode, but self-supported films of the carbon nanomaterials are used as working electrodes (e.g., graphene or CNT papers) [114,117,136].

As for the polymerization methods, for thin films (generally up to few hundred nm, but also strongly depends on the porosity) mass transport limitation is not really an issue, therefore even static methods can be employed. To illustrate the development of a hybrid structure, we show the electrodeposition of PANI onto a continuous thin 2D film of firmly connected SWCNT bundles [136]. Such an interconnected network structure is indeed beneficial for facile electron transport and high mechanical strength of the film. As can be seen in Fig. 8, the polymer coating on the SWCNT bundles gets progressively thicker (skeleton/skin architecture), and in parallel, the pore size decreases during polymerization. As the polymerization proceeds further, the pores get filled and finally they disappear altogether.

As for thicker and dense carbon matrices, potentiodynamic protocols are generally favored because of the nanostructured character of the carbon film, which often makes diffusion of the monomer and counterion, the rate-limiting step in the electropolymerization. During continuous polymerization, all the monomer being present in the nanoporous carbon structure at the beginning of the synthesis is consumed, leading to significantly reduced electropolymerization inside the nanostructured matrix. Instead, polymerization may occur on top of the nanostructured layer, where there is a continuous supply of monomer from the bulk solution. Such top surface layer morphology of the CP is unfortunate, as it may block the functional capabilities of CNTs. Both potential cycling and current/potential pulses have been employed

to ensure even distribution of the polymer within the nanostructured template [117,122,127,129]. The key point in all these methods is the introduction of rest periods between the deposition steps, which allow for the monomer to diffuse into the carbon matrix.

If we move one step further to inorganic nanostructures, one has to tackle the challenges originating from the nanostructured character and the limited conductivity of the oxide matrix simultaneously. Due to the second feature we have to distinguish between two distinctly different mechanisms in this group (Fig. 8). In the first group, SC nanoparticles or nanostructures are grown, or immobilized on an underlying electrode surface (e.g., metal or ITO). As SCs are usually not as conductive as the supporting electrode, the growth of the polymer usually starts from the bottom of the immobilized SC layer, at the underlying electrode. In these cases the CP fills up the matrix gradually, and SC particles get entrapped in the growing polymeric layer.

Oppositely, under special conditions, electropolymerization may occur directly on the surface of the SC nanostructure. Such deposition can be envisioned for example when (i) a compact oxide layer exists underneath the nanostructured film, (ii) the SC is very conductive, (iii) the SC has a large affinity toward the monomer, (iv) monomers are chemically linked to the SC surface. Importantly, these latter methods ensure intimate contact between the two components of the hybrid assembly (vs. those in the first category) since they are in both electrical and physical contact already during formation of the polymer (Fig. 9).

Even if the previously mentioned two methods cannot be completely separated, in the following examples, the dominance of the bottom-up growth approach, starting at the underlying electrode can be seen [141–147]. In these arrangements, SC nanoparticles (usually TiO₂) are immobilized on a conducting substrate, such as ITO-coated glass electrode. As a next step, the electrodes are soaked in the monomer- and electrolyte-containing solutions (often ionic liquids, due to their inertness and favorable wetting properties), and subsequently electropolymerization is carried out. Morphological studies confirmed [142,143] deposition of the polymer inside the mesoporous SC layer, albeit, with an uneven distribution, with a densely packed layer close to the ITO substrate, and much less complete pore fillings closer to the top of the layer. This clearly reflects a disadvantage of this method, namely that the CP is growing from the substrate only and not on the SC throughout the nanoporous matrix.

Note the similarities of this configuration with that of dye-sensitized solar cells (DSSCs) [148]. This is not a coincidence, since most of these studies were motivated by the possible use of these assemblies in solid state DSSCs, where the CP may act as sensitizer or hole-transport agent or both. Finally, beyond mesoporous TiO₂ layers, similar bottom-up growth was observed for other SC/CP pairs, such as CdS nanorod array, grown on conducting gold film, with remarkably high filling ratios (with PANI, up to 76%) [149] or mesoporous film of IrO_x either immobilized on gold substrate, or grown on Ir [150].

Table 6 lists representative examples, where CPs were electrochemically deposited directly on nanostructured SC

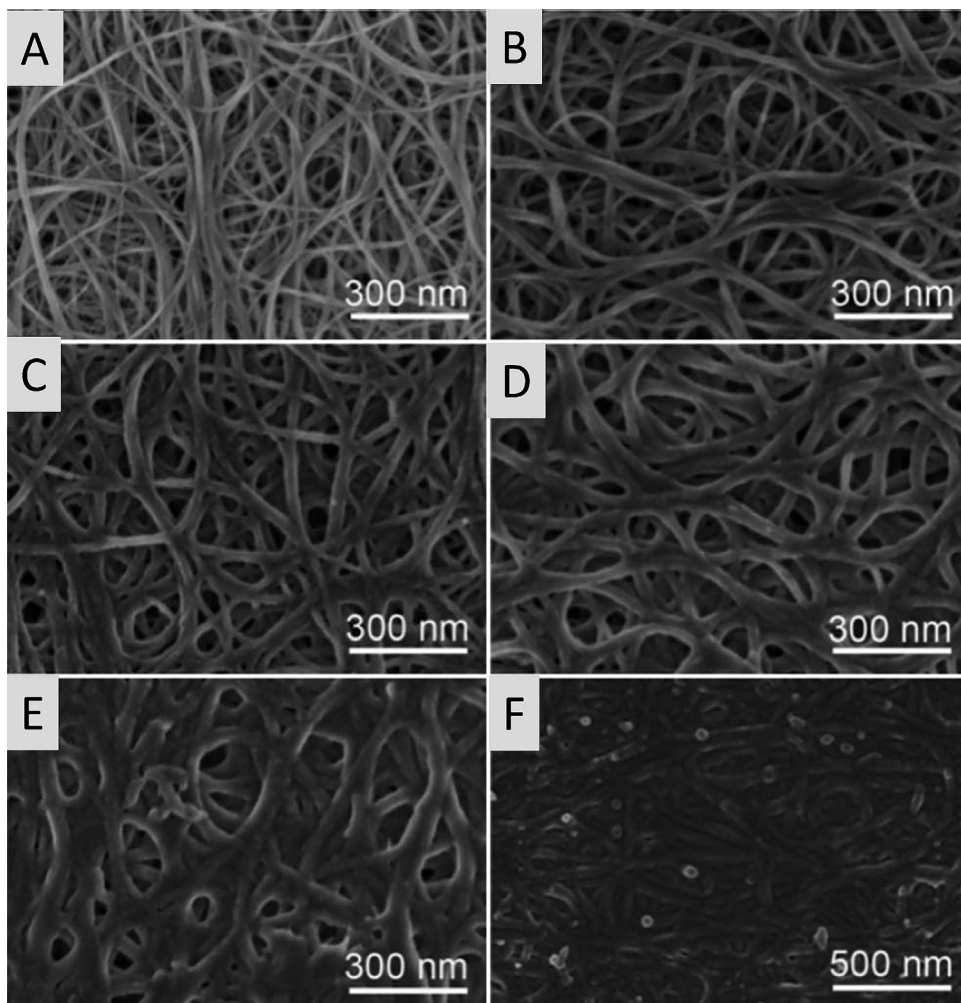


Fig. 8. Development of SWCNT/PANI structures with increasing deposition time. The evolution in the morphology can be followed from frames A to F. [136]. Copyright 2012, Reproduced with permission from the Royal Society of Chemistry.

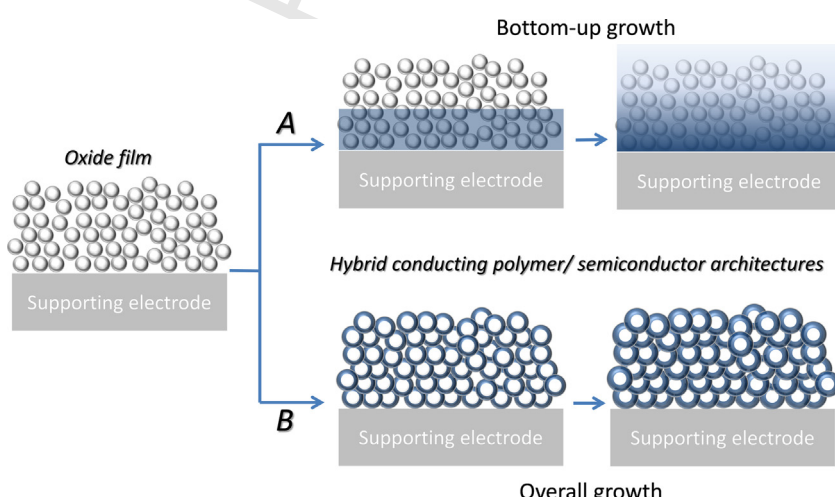


Fig. 9. Illustration of (A) bottom-up growth and (B) surface deposition of CPs on nanostructured SC matrices.

Table 6

Selected examples for direct electrodeposition of CPs on nanostructured SCs.

SC	CP	Polymerization method	SC morphology	Comments	Refs.
Co ₃ O ₄	PANI, PEDOT	Galvanostatic	Nanowire/nanoflake array	The morphology of the hybrid was controlled by the polymerization time (coaxial vs. branched)	[154]
Fe ₂ O ₃ GaAs	PPy PEDOT	Galvanostatic Potentiodynamic	Nanowire array Nanopillar array	Role of monomer concentration was shown The effect of dopant anions was demonstrated	[155] [156]
MnO ₂	PEDOT	Potentiostatic	Nanorod array	Coaxial structures were obtained, and the method was compared with other procedures	[157]
	PPy	Potentiostatic	Nanoporous	Deposition on two different oxide morphologies was compared	[158]
NiO	PANI	Potentiodynamic	Nanoflakes	Showed how porosity changes by the PANI formation	[159]
	PEDOT	Potentiodynamic	Nanoflakes	Good description on the benefits of the hybrids morphology	[160,161]
RuO ₂	PANI	Potentiodynamic	Porous	Beneficial effects of the PANI coating on the film stability was shown	[162]
Si	PPy	Galvanostatic	Nanoporous	Pore filling as well as the mechanistic details were studied	[163,164]
TiN	PANI	Galvanostatic	Nanotube array	PANI was deposited both inside, and among the nanotubes	[165]
TiO ₂	PANI	Potentiodynamic	Nanotube array	Inhomogeneous polymer deposition was observed Effect of various synthesis parameters was studied	[166,167]
	PPy	Potentiodynamic Galvanostatic	Nanorod array Nanowire array	Core-shell structures were obtained Uniform PPy shell was deposited on long TiO ₂ nanowires	[154,168] [169]
		Potentiodynamic Potential steps	Nanotube array Nanotube array	Sophisticated method to prepare MIP sensors Carefully designed multiple step protocol. Site selective deposition was also shown	[170] [171,172]
		Potentiostatic	Nanotube array	Morphology of the hybrid was not very uniform	[173]
	PEDOT	Potentiodynamic Potentiostatic	Mesoporous NTA	EQCM was used to study the hybrid Role of polymerization potential in controlling nucleation and growth was shown	[174] [175,176]
	PEDOT PHT	Potentiodynamic Potentiostatic	Mesoporous NTA	TiO ₂ film was deposited onto EQCM crystal Very slow process seemed to result in homogenous deposition	[174] [177]
	PCIT PT	Galvanostatic Potentiostatic	Mesoporous NTA	Ionic liquid was employed Thiophenes with different side chains were studied	[178] [179]
WO ₃	PANI	Potentiodynamic	Mesoporous	Role of electrolyte was shown	[180]
ZnO	PPy	Potentiostatic	Nanorod array	Good discussion on the limiting steps of the polymerization	[181]
	PEDOT PANI	Potentiostatic Galvanostatic	Nanorod array Nanorod array	Role of diffusion vs. kinetics was discussed The thickness of the deposited PANI film was monitored	[181] [182]
		Potentiodynamic	Nanowire array	Dense array of ZnO was filled to form p/n junction	[183]
ZnO@CdSe	PHT	Potentiostatic	Nanorod array	ZnO nanorods were sensitized with CdSe prior to polyhexylthiophene (PHT) electrodeposition	[184]
ZnO@CdS ZnCoO	PHT PPy	Potentiostatic Potentiodynamic	Nanotube array Nanorod array	CdS was deposited onto ZnO first An example for doped ZnO	[185] [186]

surfaces. Beyond listing the components, the employed electrochemical method, and some interesting attributes of the hybrid assemblies are also shown. Note that although a range of SCs appear in Table 6, the vast majority of the studies deal with either TiO₂ or ZnO. From a morphology perspective, SCs with various structures were studied, including interconnected configurations, such as nanoporous layers, as well as arrays of nanoflakes, nanopillars, nanorods, nanotubes, and nanowires. Such SC architectures are eminently attractive

candidates for various applications due to their ordered nanoscale structure, which greatly enhances semiconductor behavior, particularly through improved charge carrier collection due to one-dimensional vectorial e⁻ transport [151]. Moreover, through simple adjustment of the parameters of the synthetic procedures (e.g., electrochemical anodization) several key properties of the nanostructures (length, diameter, wall thickness, conductance, etc.) can be tailored toward targeted applications [152,153].

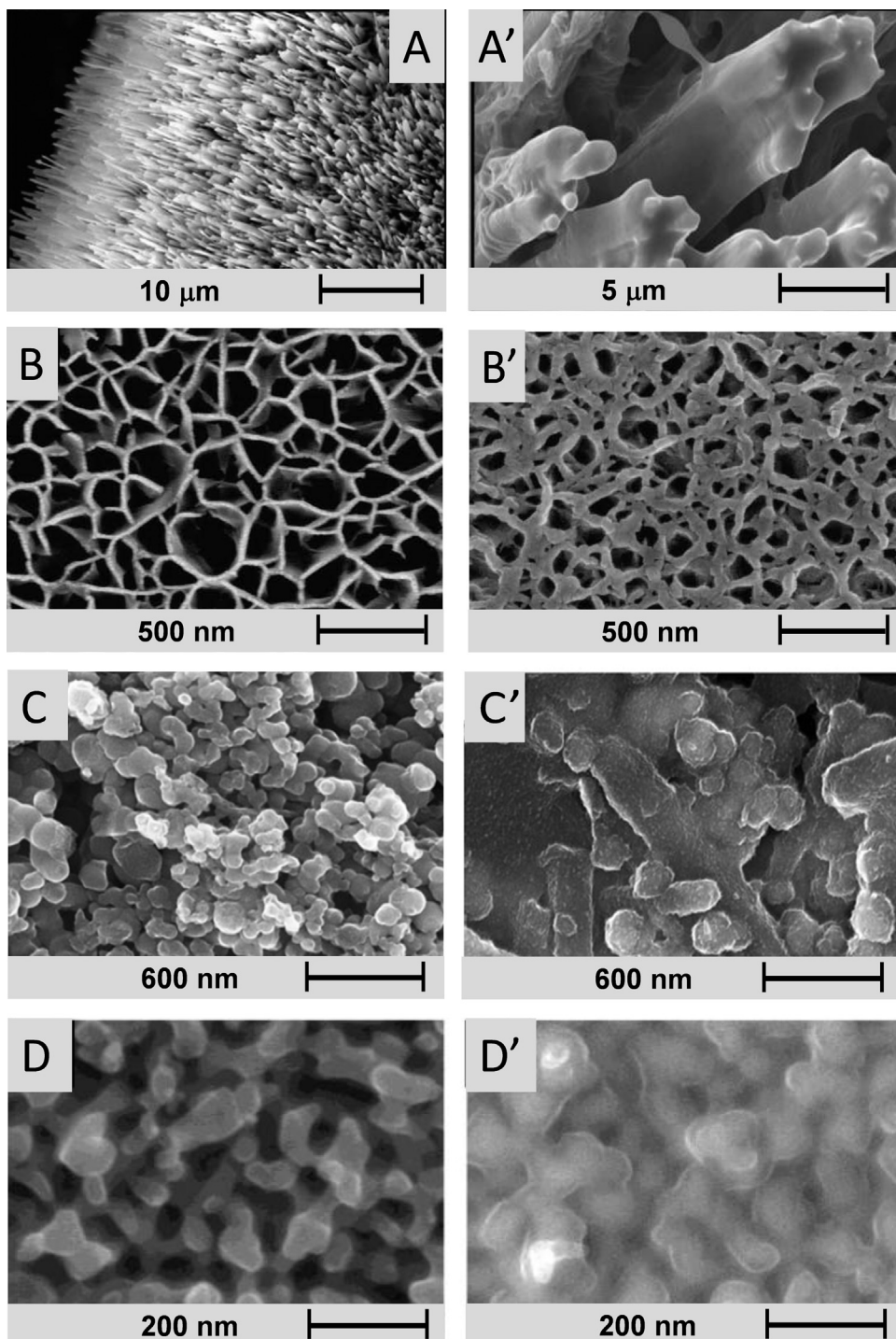


Fig. 10. Representative examples of the morphological development of CP based assemblies. The images on the left always show the parent oxide, whereas those on the right show the respective hybrid materials. (A) $\text{Fe}_2\text{O}_3/\text{PPy}$, (B) NiO/PEDOT , (C) RuO_2/PANI , (D) WO_3/PANI .
Sources (A–D), respectively: [155], Copyrights 2011, Reproduced with permission from the American Chemical Society; [160], Copyrights 2009, Elsevier Ltd.; [162], Copyrights 2011, Springer; [180], Copyrights 2012, the American Chemical Society.

When nanostructured hosts are used as working electrodes, potentiodynamic methods are favored, due to the previously shown favorable attributes. As seen in Table 6, most of the successful approaches involve either dynamic

or slow static methods, which are preferred because they afford more time to continuously replenish the solution in monomer during the polymerization, adjacent to the SC surface. In Fig. 10, representative examples of different

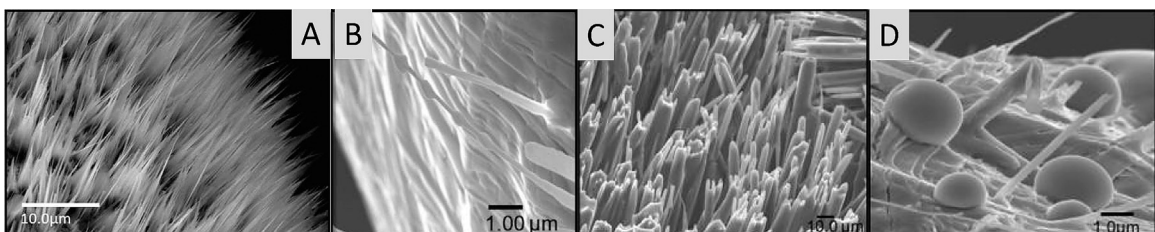


Fig. 11. Morphology of (A) the bare Fe_2O_3 nanowires and the (B–D) $\text{Fe}_2\text{O}_3/\text{PPy}$ nanostructures obtained by electrodeposition at identical current densities but with different monomer concentration, (B) 0.01 M, (C) 0.05 M, (D) 0.5 M. Note that the images are at different magnification for better visualization. [155]. Copyright 2011, Reproduced with permission from the American Chemical Society.

SC/CP hybrids made by direct electropolymerization are shown. All images share similar attributes: (i) cloudiness of the images in the hybrid case, and (ii) expansion of the dimensions of the nanoobjects (grain size, rod diameter, and wall-thickness) compared to the parent situation.

We intend to demonstrate the effect of the various synthesis parameters (see Table 2), using a different system to show the role of each parameter separately. First, to understand the role of the monomer concentration, consider the mechanism of polymer formation. As the first step, electrochemical oxidation of the pyrrole monomers leads to the formation of soluble oligomers around the electrode surface, therefore the solution inside the SC nanostructure gets saturated (note that insoluble oligomers are also forming). Subsequently, nucleation and growth begins first at favorable sites in the nanostructure, then possibly everywhere. As the next step, solid-state growth of the polymer continues and the forming polymer gradually fills the SC structure.

As nicely demonstrated for the example of Fe_2O_3 nanowires and PPy, at low monomer concentrations ($\sim 10 \text{ mM}$), polymerization is limited by the mass transport of the monomer and therefore PPy is deposited only at some favorable spots of the nanowires (such as tapered tips and kinks). If the monomer concentration is increased to medium values ($\sim 50 \text{ mM}$), polymer deposition results in a uniform, conformal coating on the individual nanowires. Finally, at rather high concentrations of pyrrole ($\sim 500 \text{ mM}$), fast and uncontrolled electropolymerization leads not only to extensive aggregation of polymer-coated nanowires, but also to the formation of large globular PPy particles attached to the nanowire surface (Fig. 11) [155].

The competition between diffusion vs. kinetics can be visualized for the example of electrodepositing PEDOT on ZnO nanowires [181]. In a very simple and demonstrative set of experiments, PEDOT was electrodeposited potentiostatically in one step and in 9 steps employing otherwise identical conditions (e.g., polymerization potential and overall charge density). The difference is striking, while in the one-step experiment PEDOT was preferably formed on the top of the ZnO nanowires, in the second case, homogenous deposition can be witnessed along the nanowires. Very similar result (namely having the polymer mostly at the top of the nanowires) was obtained even with shorter ZnO nanowires, while fast growth of the polymer was provoked by employing higher deposition currents. Importantly, in both diffusion-limited cases, mushroom-like morphologies were obtained, instead of

the homogenous coating observed for the kinetically limited experiments (Fig. 12). Similar conclusions have been drawn when diffusion limitation occurred because of using a static polymerization method instead of a dynamic one [187].

The nature of the electrolyte may also play a key role in the electropolymerization procedure. The WO_3/PANI hybrid system is a good example, since uniform deposition of PANI on nanoporous WO_3 was accomplished by recognizing the similarity in their ion-exchange properties [180]. Both components of the hybrid system are electron and proton conductors, resulting in reasonable WO_3 electroactivity in acidic solutions even in the positive potential regime, required for electropolymerization of PANI. The enhanced electroactivity of WO_3 was rationalized by the formation of tungsten-bronze phases (H_xWO_3), assisted by H^+ uptake/release as charge compensation during the $(\text{W}^{6+}/\text{W}^{5+})$ redox process. Note that electropolymerization of pyrrole in a pH-neutral medium, under otherwise identical circumstances (same WO_3 substrate), was hampered by the low electroactivity of the SC matrix [188].

Finally, the nature of the solvent also has a substantial effect on the formation of the hybrid material. Solvent molecules with higher polarity are considered to interact more closely with polar SC surfaces (e.g., ZnO or TiO_2), which hampers adsorption of the monomer molecules (thus impeding the polymerization). Furthermore, the solubility of the forming oligomers also varies in different solvents, therefore saturation (and consequent deposition on the SC) occurs in a different manner [189]. The polarity of the solvent not only affects wetting of the SC nanostructure and solubility of the oligomers, but also limits the solubility of certain monomers. Employing micellar solutions is an elegant way to overcome solubility issues, because it also facilitates transport of the monomers inside the SC host matrix [190].

Hybrids based on TiO_2 nanotube arrays (NTA) obtained by anodization deserve special consideration for multiple reasons. Notably, TiO_2 has fairly high resistance which hinders direct electrodeposition of CPs. In addition, there is an insulating compact barrier layer below the nanotubes, unlike in the examples presented above, where TiO_2 nanoparticles are immobilized directly on the conducting substrate (ITO). Despite this fact, there are a considerable number of papers published on the electrodeposition of different CPs (most importantly PPy and PANI) on TiO_2 NTAs. Most of these examples, however, suffer from major drawbacks such as uneven distribution of the polymer, and

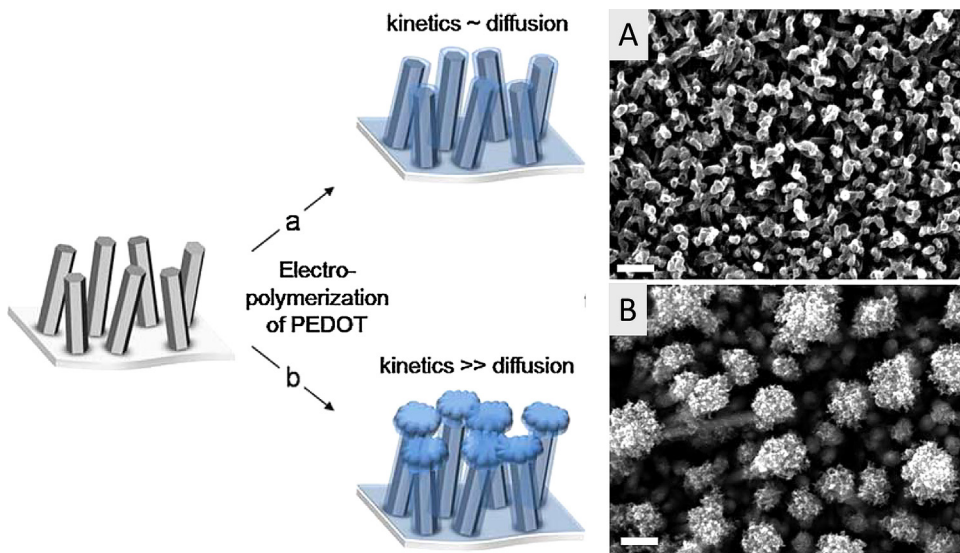


Fig. 12. Schematic and SEM illustration of the competition of kinetics and diffusion, for the example of PEDOT electropolymerization on ZnO nanowires. [\[181\]](#), Copyright 2010, Adapted with permission from Wiley.

consequently the small area of the forming p/n junction [166,167,173,177,179,191].

Recent studies demonstrated, however, that homogeneous deposition of PPy onto TiO₂ NTA can be achieved by employing a carefully designed multiple potential step protocol. Each step consisted of a short anodic pulse of very high current density (+26 mA/cm²) to ensure high nucleation density, followed by a relatively long rest period to let the solution in the NTA refill with both monomer and the electrolyte by their diffusion, and to let possible side products diffuse away. A very short cathodic step (-26 mA/cm²) was introduced to prevent change of the local pH. Note that the anodic step is short enough (10 ms) to avoid 3-dimensional growth of PPy after the nucleation step [171,172,192]. Employing high current densities (consequently high potentials), however, involves the risk of overoxidizing the forming polymer. Overoxidation means irreversible oxidation of the polymer, introducing oxygen-containing functional groups to the polymeric chains. Formation of such moieties interrupts conjugation of the polymer backbone, thus hampering its applicability in most of the considered applications due to decreased electroactivity [193,194].

The role of the template structure was also brought out by electrosynthesizing PPy on various TiO₂ NTA templates with different geometrical attributes. As depicted in Fig. 13, polymer deposition can occur *inside* the nanotubes, in the space *among* the tubes, and on top of the NTA. In principle, if the space between the tube walls is reasonably large, electropolymerization leads to filling the voids between the tubes. This behavior was rationalized by the nanoscale wetting behavior of NTA, which showed preferential wetting of the space between the nanotubes. By tailoring the properties of the TiO₂ NTA, PPy can be deposited even inside the nanotubes, if the space between the nanotubes is sufficiently reduced (this can be done by decreasing the water content of the anodization medium) and wetting inside the tubes is activated by thermal treatment [171,172].

Similarly, PEDOT was electrografted onto TiO₂ NTA by a simple but carefully optimized two-step potentiostatic growth protocol in acetonitrile-containing supporting electrolyte [195]. During a short pre-polymerization period, a relatively high constant potential ($E=1.35$ V, vs. Ag/AgCl) was applied to induce homogeneous oligomer formation. At the end of this period, electrodeposition was continued, without interrupting the current, at a lower potential (1.20 V) for longer periods. The morphology of the hybrid assembly was similar to that shown before for the TiO₂/PPy system (i.e., polymer is dominantly deposited in between the tubes). More recently it has been shown that site selective deposition of the PEDOT can be controlled by changing the polymerization parameters [175,176]. At relatively low potential, polymerization led to deposition of PEDOT inside the tubes, as well as into the void spaces. In contrast, at higher potentials, polymerization occurs in the spaces between the nanotubes *only*. Such variant behavior was rationalized by the differences in nucleation density and rate of polymerization, and a model of 3D-instantaneous and 3D-progressive nucleation and growth was proposed [175].

3.2.2. Photoelectrochemical polymerization

In the case of some oxides (including TiO₂), electrodeposition is often hampered by the low conductivity of the inorganic matrix; therefore high potentials must be applied, consequently the electrogenerated polymer is prone to overoxidation. In the quest to overcome this issue, it was recognized soon that such challenge related to the semiconducting nature of an electrode material can be turned to an opportunity. Namely, light has at least two beneficial effects with respect to the deposition of CPs on SCs. First, by illuminating the electrode (employing bandgap irradiation) the conductivity of the SC increases (photoconductivity). In addition, photogenerated holes can directly oxidize the monomer and initiate polymerization. Since this type of photoelectrochemical polymerization

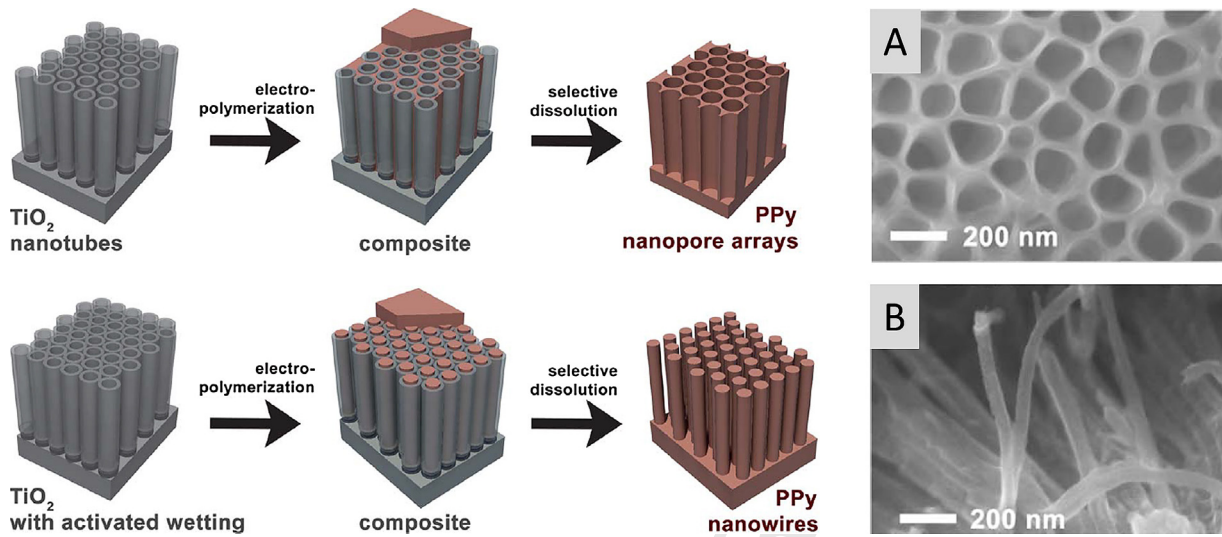


Fig. 13. Illustration of site selective electrodeposition of PPy onto TiO₂ NTA with different geometrical parameters.

[172], Copyright 2011, Adapted with permission from the Royal Society of Chemistry.

of electroactive monomers has not been reviewed yet, we briefly summarize the history and evolution of this approach. Note that photo-initiated polymerization of other, non electron-conducting polymers has been reviewed recently [196].

Photoelectrochemical polymerization dates back to the early 1980s when flat Si [197–199] and GaAs [200] surfaces were covered by PPy employing UV illumination and constant bias potential. Later the concept was extended to other SCs and CPs; thus assemblies such as CdS/PPy [201], CdS/PMT [202], GaAs/PMT [203,204], GaAs/PVP [205], and CuInS₂/PPy [206] have been realized. Subsequently hybrids based on flat oxide SCs, initially TiO₂/PPy [207,208], ZnO/PPy [209], and more recently Nb₂O₅ [210], Ta₂O₅ [211], WO₃ [137] based composites were also obtained. In these methods, photoelectrochemical polymerization occurs at the irradiated SC/electrolyte interface. When light is incident on the SC electrode, electrons from the valence band (VB) are promoted to the conduction band (CB). These electrons are drained into the external circuit by the applied external bias potential, while the photogenerated holes react with species in the solution (solvent, electrolyte anion, or monomer). The polymerization is successful if this particular species is the monomer, which gets oxidized and the polymerization starts (Fig. 14B). Then, the radical cation reacts with another radical cation (or monomer) to form dimers which can react further, either with a monomer- or oligomer radical cation and the polymer is formed. Therefore, it was recognized soon that band edge positions of the SC, as well as the oxidation potential of the species in the solution are of prime importance for the success of this method. The different process variants, the role photoexcitation, external bias potential, and that of using e⁻ scavengers, are shown in Fig. 14.

As for the role of the bias potential, note that the applied potential values are not high enough to *electrochemically oxidize* the monomer, its role is to suppress the recombination of the photogenerated charge carriers. Another

parameter to consider is that some of the SCs are prone to photocorrosion under anodic conditions, which not only leads to possible degradation of the electrode, but also lowers the efficiency of the polymerization, because only a fraction of the photogenerated holes can now oxidize the monomer. For example in the case of ZnO, much more polymer can be generated with the same charge density by electrochemical- than by photoelectrochemical polymerization [209]. Careful adjustment of the solution pH and application of additional hole-scavengers may help to suppress photocorrosion in such cases.

After the early studies on flat electrode surfaces, the concept was extended to particulate systems, more precisely to colloidal or nanoparticulate TiO₂ slurries [213,214]. In such configurations the (nano)particles are dispersed in the solution of the monomer, and possibly supporting electrolyte. Light is incident on the slurry under continuous stirring, and a thin polymeric film deposits on the surface of the NPs. Note that in these experiments no external bias potential is applied, the only driving force for charge separation is the hole scavenging property of the monomer (Fig. 14A). Sacrificial electron acceptors may also be used to enhance the effectiveness of charge separation, thus the solution is usually saturated with O₂. As a result of polymerization, coverage (only a few nm) of a thin film is formed on the NP surface. The growth of the polymer is finally terminated by both electrical and optical shielding of the deposited CP. Additional studies demonstrated the use of this method with other SCs such as CdS, CdTe [215], and (CdSe@ZnS) [216] and polymers (PEDOT) [217] as well as yielded further mechanistic details [218].

In a comparison of photoelectrochemically generated polymers with their electrochemically prepared counterparts, photoelectrochemical polymerization was found to be less dependent on the nature of the electrolyte, both in terms of the morphology and the conductivity of the formed polymer [214]. This latter was inferior compared to its electrochemically polymerized counterpart, a

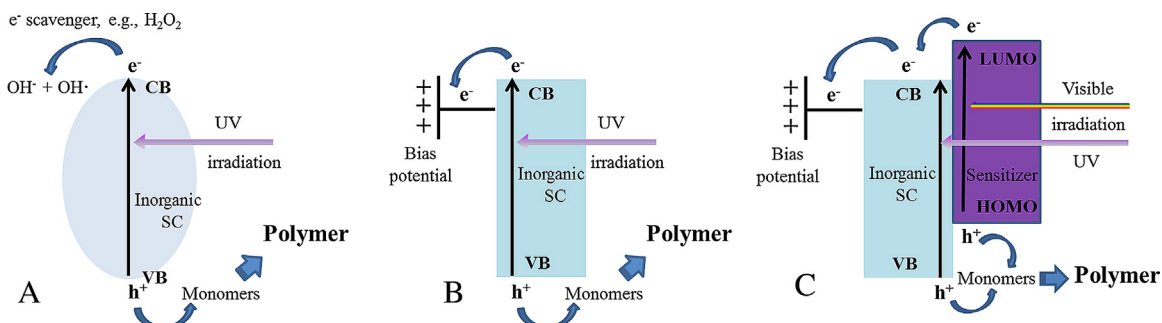


Fig. 14. Schematic illustration of (A) the photocatalytic, (B and C) photoelectrochemical polymerization of a monomer on bare and dye-sensitized semiconductor electrodes, respectively.

conclusion in accordance with earlier studies [209]. The morphology also showed significant differences, namely a more compact CP film was observed in the case of photoelectrochemical deposition, presumably due to the considerably slower polymerization procedure.

After these pioneering studies, this versatile method was somewhat forgotten, and the new wave of research was triggered by a demand for solid-state hole transporters in DSSCs, which arose after the discovery of mesoscopic DSSCs in 1991 [148]. In such solar cells, a CP can act as both sensitizer (electron donor) and even more importantly as a solid-state hole transporter [6,219,220]. From a polymerization perspective, the benefits of the previously described geometries are merged in this configuration, namely the large surface area of the nanoparticulate film, and electrochemical control with over the polymerization. In this vein, TiO₂/PPy [221–223], TiO₂/PEDOT [224,225], TiO₂/PT [15,226], and ZnO/PMT [227] hybrids were realized. In some cases, carboxyl group-containing thiophene-derivatives were initially grafted onto the TiO₂ surface and subsequent polymer growth was initiated through these moieties. Therefore, better electrical contact is envisioned between the organic and inorganic components. Interestingly, in some of the cases, polymer formation was witnessed even when UV-light was filtered out, consequently the SC component cannot be excited. In these cases, the precursor of the polymer (e.g., a dimer or oligomer) linked to the SC surface is photoexcited, and while the photogenerated e⁻ is transferred to the SC, the oxidized precursor reacts with a further monomer/dimer [226,228].

These observations bring up the next point, a more interesting variant of this method, namely when the TiO₂ NPs are already dye-sensitized before formation of the CP (Fig. 14C). In such a procedure, photoexcitation of TiO₂ and the anchored dye may occur simultaneously (under white light irradiation), or in contrast, the components can be selectively excited by irradiating with illumination of properly selected wavelengths. In practice, in most of the studies, the UV component is filtered out to avoid excitation of the SC, and only the holes, generated by the photoexcited dye are exploited (Fig. 14C). This trick not only ensures intimate contact between the photosensitizer (dye) and the hole transporter (polymer), but also

avoids photodegradation of dye by the holes from TiO₂, which have high oxidation power due to its valence band position. This is a real threat, realizing that a prominent application of such SCs is the degradation of organic dyes [229]. Studies, however, have indicated that the dye fortuitously does not decompose during photoelectrochemical polymerization [230].

In the first successful trial within this group, polypyrrole was photoelectrochemically generated onto mesoporous TiO₂ matrix on which a Ru-containing dye was immobilized by chemical bonding through its carboxyl function [231]. As a next step, a novel ruthenium dye was designed bearing pyrrole-, or thiophene functions as well as dicarboxylic acid groups as ligands. Therefore the polymerization can directly start at the dye molecule itself, bringing the dye and the hole-transporter polymer into close molecular contact. Such close contact was proven to be beneficial in terms of photoelectrochemical behavior, compared to a counterpart using a dye without monomeric moieties [232–236].

More recent efforts almost exclusively focus on PEDOT, because it possesses many favorable attributes such as high chemical stability (especially in the oxidized or doped state), small band gap energy, and good optical transparency in the electronically conducting state. For this polymer, however, the problem with the higher oxidation potential of the EDOT monomer (1.0 V vs. Ag/AgCl) means that it cannot be oxidized by the ruthenium dye (HOMO potential: 0.59 V vs. Ag/AgCl) [237]. Therefore, use of bis-EDOT [112,238] or its derivatives [239], having a lower oxidation potential (0.4 V vs. Ag/AgCl) becomes a better option.

The critical role of the dye was brought out when photoelectrochemical polymerization of bis-EDOT was carried out with two different Ru-dyes but otherwise identical circumstances [240]. Under potentiostatic conditions, the D149-sensitized TiO₂ layer gave a higher polymerization current than the Z907-sensitized TiO₂ layer. Such a difference can be rooted in the more effective charge transfer from the dye molecule to the monomer and to TiO₂. Importantly, the nature of the dye has a crucial influence on the polymerization procedure, consequently it affects the properties of the TiO₂/dye/polymer interface as well as

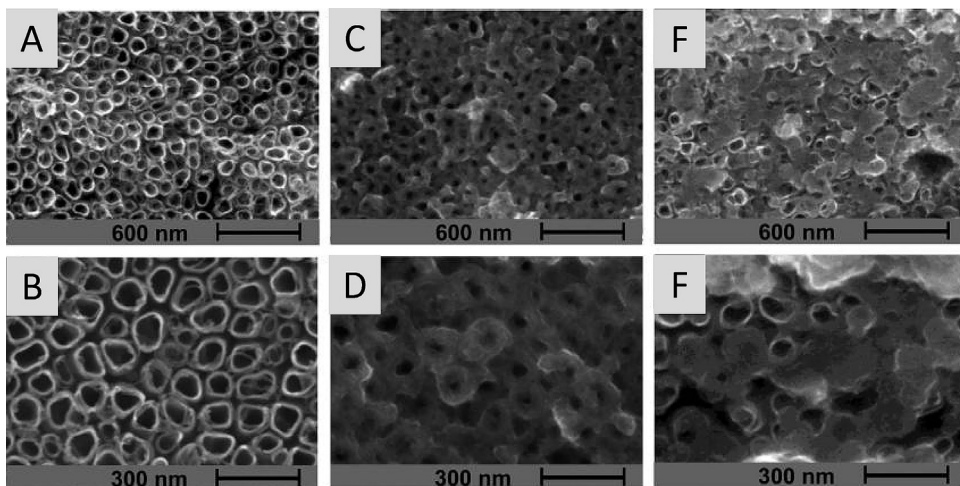


Fig. 15. SEM images of (A and B) bare TiO_2 NTA anodized at $E=20\text{ V}$; (C and D) of the corresponding TiO_2/PANI hybrid samples synthesized using 5 potentiodynamic polymerization cycles with illumination, at 50k and 100k magnification; and (E and F) without that illumination. [188]. Copyright 2012, Reproduced with permission from the American Chemical Society.

penetration of the polymer into the mesoporous TiO_2 layer (pore filling ratio) [240].

Finally, recent progress was achieved in photoelectrochemical polymerization on organized SC nanostructures. In this vein, deposition of PPy and PANI on nanoporous WO_3 and TiO_2 NTA was successfully carried out [188,241]. The most important feature of this approach is that it results in homogenous deposition of polymer, which covers the entire surface of the nanostructured SC, as can be seen both from the expansion of wall thickness and from the disappearance of nanoscopic voids in between the tubes (Fig. 15). On the other hand, the hybrid sample obtained in the absence of illumination exhibits a morphology similar to that seen in many of the papers employing general electrochemical methods in the dark, namely that the CP (in this case PANI) is randomly deposited on the substrate, even forming globular particles on the top of the TiO_2 NTA (Fig. 15). Importantly, such an alteration in the morphology results in a huge difference in the contact area of the organic/inorganic junction, which is practically equal to the surface area of the inorganic semiconductor matrix in the case of the illuminated sample, whereas it is almost negligible for its counterpart synthesized in the dark.

To rationalize the remarkable difference shown above, the contribution of electrochemical and photoelectrochemical polymerization to the formation of CP was separated, and the multiple role of external bias potential was demonstrated [188,241]. To this end, potentiodynamic polymerization cycles were run to three different potential values (1.1, 1.45 and 2.2 V), while other parameters remained unchanged (Fig. 16). Note that in the first case no direct electropolymerization occurs, whereas its gradually increasing contribution can be revealed as the potential window is extended. The increasing electroactivity can be deduced from both the increased current densities and the more expressed shape of the voltammograms. Further experiments showed the complexity of the current response under illumination, from which the mechanism of the deposition was clarified (Fig. 17). As a first step, the

aniline monomer is oxidized by photogenerated holes on the SC surface. Here the external bias potential facilitates the separation of the photogenerated excitons (by draining the photoelectrons to the back contact); hence more holes can react with the aniline monomer and oligomer to facilitate polymerization. When the potential is increased, at a certain threshold value, electrochemical growth of the polymer starts to take place. Note, however, that this threshold potential is lower than in the dark, because under illumination oligomer/polymer formation already took place at lower potentials due to photoelectrochemical deposition, thus obviating the need for electrochemical oxidation of the aniline monomer, which requires notably higher potentials. This two-step procedure is illustrated in Fig. 17.

3.3. Other miscellaneous approaches

3.3.1. Electrochemical co-deposition

In this sub-section we show examples where the precursor of each constituent is present in the initial polymerization solution. Subsequently, both components, and therefore the hybrid itself is electrogenerated in the same process in one single step. This approach has been exploited to obtain hybrids with PPy, PEDOT, and most importantly PANI; containing Fe_2O_3 [242], MnO_2 [243–248], MoO_3 [249], NiO_x [250–252], and WO_3 [253,254]. The main advantage of this approach is its simplicity and time efficiency. Also note that it is typically applied for oxide semiconductors, which can be anodically generated from their precursors in aqueous solutions. The drawback on the other hand, is limited control over simultaneously occurring processes, which results in uncontrolled size and size distribution of the SC particles, and poorly defined morphology of the hybrid.

Potentiodynamic cycling is useful to identify the potential values where polymerization and oxide formation take place. The example of PANI/ MnO_2 is shown in Fig. 18A, where during the positive potential scan, electropolymerization of aniline occurs first (from 0.7 V vs. SCE

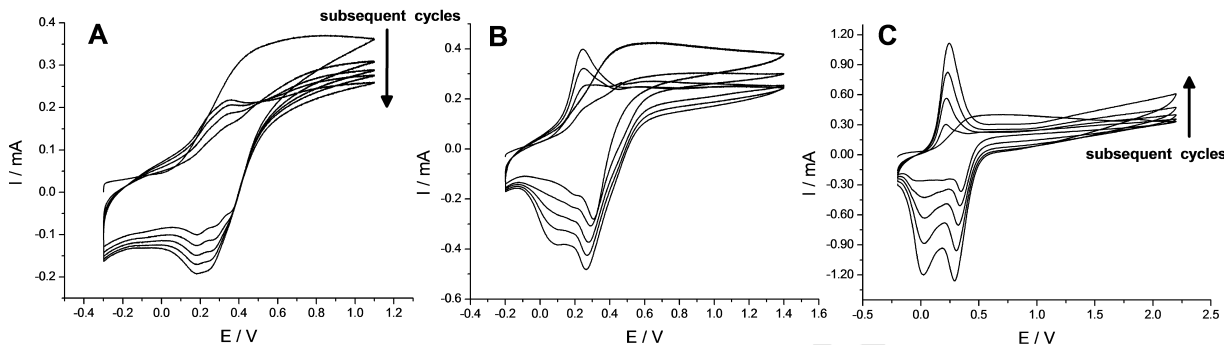


Fig. 16. Effect of the positive end expansion of the potential window, on the polymerization of aniline on TiO₂ NTA under illumination (5 cycles). [188], Copyright 2012, Reproduced with permission from the American Chemical Society.



Fig. 17. Illustration of the two steps of the photo-electrodeposition of PANI on TiO₂ NTA. [188], Copyright 2012, Reproduced with permission from the American Chemical Society.

1194 during the first scan). Upon further increase of potential up to 1.35 V vs. SCE, MnO₂ is electrogenerated on the 1195 previously formed PANI according to the following reaction: 1196 Mn²⁺ + 2H₂O → MnO₂ + 4H⁺ + 2e⁻. This 1197 procedure is repeated during subsequent cycles, leading to the 1198 formation of the hybrid layer on the electrode surface. 1199 Importantly, the mechanistic picture gets more complex 1200

when the potential regimes for formation of the constituents overlap, as can be seen for the example of MnO₂/PEDOT hybrid (Fig. 18B). Under such circumstances, careful control of the electrodeposition potential is indeed required. Note that for such a system, very small changes in the electrochemical bias potential can favor one process over the other. In this manner, the ratio of the components 1201

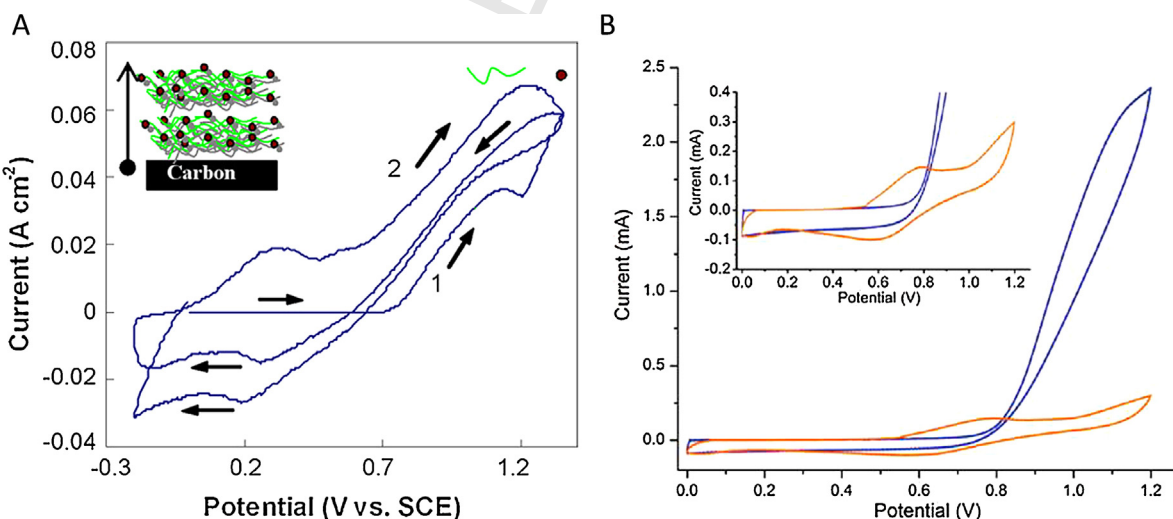


Fig. 18. Examples for electrochemical co-deposition of CP/SC hybrids, by potentiodynamic cycling. (A) MnO₂/PANI on carbon substrate. (B) MnO₂/PEDOT in alumina template. Sources, respectively: [243], Copyright 2008, Reproduced, with permission from Elsevier Ltd; [247], Copyright 2011, Reproduced, with permission from the American Chemical Society.

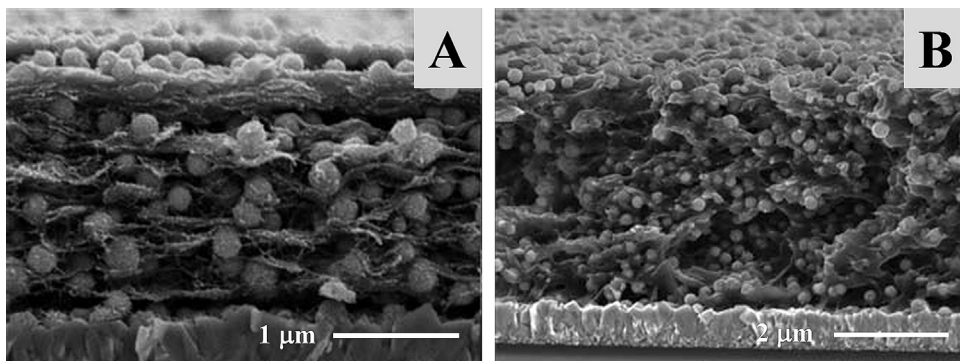


Fig. 19. Electrodeposited CdS particles inside the PEDOT host matrix from an ionic liquid solution (A) without, (B) with a pre-wetting step. [257]. Copyright 2012, Reproduced with permission from the Royal Society of Chemistry.

within the electrogenerated hybrid material can be tuned [247]. Finally, control of pH is important because it has to be optimal for polymerization, while at the same time, formation of the SC particles should not be hindered (for example by hydroxide formation).

3.3.2. Deposition of SCs on or inside the CP layer

As opposed to most of the previously described approaches, the CP component can also be synthesized as a first step, and subsequently hybridized with the inorganic component. Such composite formation can be facilitated either by the electroactivity of the CP film or by that of the underlying supporting electrode. In the first case the SC is generated inside the CP, assisted by its electrochemical transformation. In the second case, the inorganic component grows from the substrate and fills the pores of the CP (note that this procedure mirrors that where the CP fills the nanoparticulate TiO₂ matrix, see Section 3.2.1). This second method is especially attractive for SCs which are not stable at the highly positive potentials where CPs are usually electrosynthesized.

As mentioned earlier, CdS is prone to both electrochemical and photocorrosion. Therefore its formation within a previously deposited CP film is favored vs. the previously shown approaches. In this manner, the cation exchange behavior of a PPY/PSS layer was exploited first. Having a large immobile polyion (PSS⁻) as dopant, Cd²⁺ ions can be incorporated in the polymer upon cathodic polarization. Note that by applying a carefully selected potential, only the polymer is reduced (and not the Cd²⁺ ions), and therefore the metal cations can be incorporated to compensate the negative charges of the built-in macroanions. Subsequently, addition of bisulfide ions (HS⁻) led to the formation of CdS particles at various sites throughout the PPY matrix [255].

CdS formation was achieved in the opposite order as well, namely exposing the bisulfide ion-doped PPY to Cd²⁺ containing solutions [255]. Alternatively, Cd was electrodeposited onto poly(3,4-dioctyloxythiophene) (PDOT) and subsequently chemically transformed into CdS [256]. Finally, direct electrodeposition of CdS from its precursors (cadmium acetate and sodium thiosulfate) in an ionic liquid was also achieved, under galvanostatic conditions at elevated temperatures (120 °C). The synthesis resulted in

relatively large-sized CdS particles throughout the whole PEDOT host matrix (Fig. 19) [257].

Cuprous oxide (Cu₂O) is a good example of an oxide in which the metal can have different oxidation states. Importantly, electropolymerization is hampered on this SC, since the formation of CuO (cupric oxide) is favored under oxidative conditions. Therefore the opposite strategy was followed: Cu₂O was cathodically electrodeposited in the porous CP layer. At the same time, however, under cathodic polarization most CPs are in their neutral, insulating state, thus the growth of the SC occurs from the substrate electrode, and the forming oxide fills the pores of the CP. By careful adjustment of the deposition potential, the formation of different Cu-species (Cu, Cu₂O, CuO) can be tuned [258–260] as well as hybrids with various morphologies can be obtained [261].

Oppositely, when SCs are electrogenerated anodically, the electroactivity of the CP template can be exploited, as they are conductive in their oxidized (doped) state. For example electrodeposition of SnO₂ nanocrystals on PPY nanowire was carried out under galvanostatic conditions ($\text{Sn}^{2+} - 2\text{e}^- \rightarrow \text{Sn}^{4+} + 4\text{OH}^- \rightarrow \text{Sn}(\text{OH})_4 \rightarrow \text{SnO}_2 + \text{H}_2\text{O}$). The such formed 3D nanostructured SnO₂@PPY composite exhibits a rough surface indicating that the PPY nanowires are covered with SnO₂ nanoparticles [262].

Similarly, RuO₂ can be oxidatively deposited from solutions containing Ru³⁺ ions. RuO₂/PEDOT composite nanotubes were electrogenerated using porous alumina template [263]. As the first step, EDOT was electropolymerized and PEDOT nanotubes were formed. Subsequently, RuO₂ was formed inside the nanotubes through potential cycling; more precisely, RuO₂ was electrodeposited on the inner walls of the polymeric tubes [263]. RuO₂ electrodeposition was achieved on PANI films as well, both under potentiodynamic [264] and galvanostatic [265] conditions. In the same vein, MnO₂ was hybridized with PANI [266], PEDOT [267], PMT [268] and even PEDOT-PANI assemblies [269].

The previous approach can be followed by subsequent deposition of another polymeric layer, obtaining a sandwich structure [270]. Through tuning the deposition conditions, the thickness of each layer, and consequently the properties of the hybrid assembly can be controlled. Furthermore, even sequential deposition can be achieved,

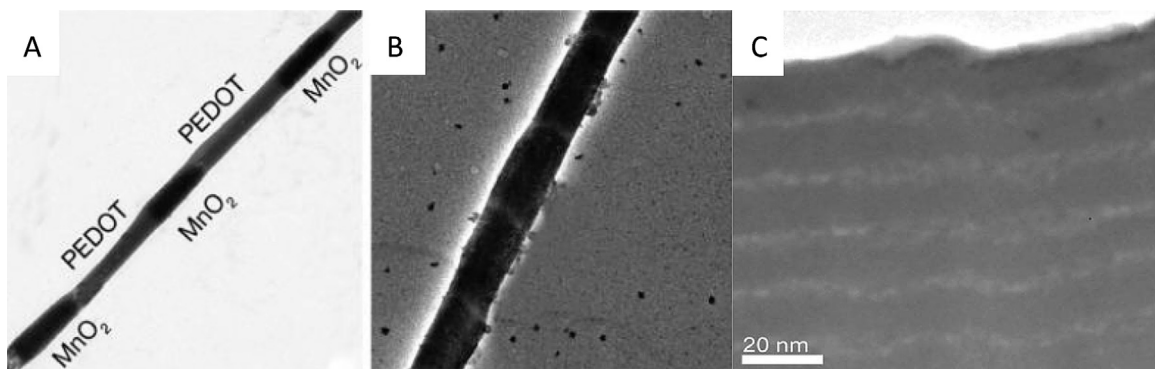


Fig. 20. Formation of multiple heterojunctions by sequential electrodeposition. (A and B) $\text{MnO}_2/\text{PEDOT}$, (C) graphene/PEDOT.

Source: (A and B) [247] Copyright 2011, Adapted with permission from the American Chemical Society; (C) [272], Copyright 2012, Adapted with permission from the Royal Society of Chemistry.

by subsequently repeating the deposition steps for the SC and the polymer [271]. If a template is also used, then nanostructures containing multiple heterojunctions can be obtained (Fig. 20A and B) [247]. Such a multilayer formation can be also seen on the example of a graphene/PEDOT system, where graphene layers were introduced between PEDOT layers of different thickness (Fig. 20C) [272].

An interesting and also promising variant of this method is when both the CP and graphene are deposited on the electrode surface at the anodic and cathodic ends of the potentiodynamic cycles respectively. This approach is enabled by the fact that graphene oxide (GO) can be reduced at negative potentials, whereas oxidative polymerization of aniline takes place in the anodic regime. This separation of the two processes allows layer-by-layer formation of the hybrid assembly. Furthermore, just by switching the direction of the potentiodynamic cycle, the order of the layers can be controlled [273].

4. Selected applications of electrochemically assembled CP/SC hybrids

4.1. Solar energy harvesting (solar and photoelectrochemical cells)

Finding alternative earth abundant solar cell materials beyond Si has been at the leading edge of research for many years. There are three distinctly different solar cell configurations in which assemblies of organic and inorganic SCs can be deployed (Fig. 21). First, the high absorption coefficient of CPs makes them possible candidates to be used in a combination with n-type inorganic SCs (typically TiO_2 , ZnO , and CdSe) to form simple and inexpensive hybrid organic-inorganic solar cells [274–276]. In such arrangements, the p-type semiconductor polymer acts both as an electron donor and as a hole transporter. The theoretically achievable efficiencies are predicted to be as high as 12% [275], but until now the performances obtained for real cells remain well below these expectations (1–4%). It is also worth noting that for the preparation of materials in this group, chemical methods dominate over electrochemical processes, most importantly due to the larger variety of

possible polymers that can be combined with the SC NPs [276].

In the second case (Fig. 21B), CPs are employed as solid-state hole transporter materials in DSSCs [219,277]. This is an attractive approach, because by replacing the homogeneous redox couple (I_3^-/I^-) by a solid-state hole conductor, it is possible to avoid use of the liquid electrolyte. This is indeed important, since many of the drawbacks of conventional DSSCs, such as leakage, low thermal stability, and corrosion of the counterelectrode are related to the presence of the liquid electrolyte. What is equally important, a steep rise in the power conversion efficiencies was witnessed during the last decade for this type of solar cell. Note that while the first trials resulted in efficiencies only about 0.1% [231], the latest cells exhibit 7.1% [278], which is in the range of values obtained with molecular hole transporters (7.2% with Spiro-OmeMAD [279]). Molecular dyes can be either the regularly employed Ru-containing benchmark dyes (N3 or Z907) or other, more environmentally friendly candidates (porphyrins). The rapid rise depicted in Fig. 22 is predominantly rooted in the development of photoelectrochemical polymerization techniques, achieving careful interfacial engineering in the hybrid materials.

Most recently, quantum-dot [280,281] and perovskite sensitized solar cells [282,283] have come to the forefront of research. Impressive power conversion efficiencies were obtained (up to 15%) using perovskite sensitizer and solid state hole-transporter [282,283]. Although CPs were proven to be efficient in this configuration as well [220,284], their use has been restricted to the infiltration of the polymer, and no in situ electrochemical or photoelectrochemical polymerization methods have been employed yet. Such studies are in progress in our research groups, with particular focus on the structure/property relationships of oxide/perovskite/CP interfaces.

In some cases, both polymer and the redox electrolyte are present in the cell (Fig. 21C), and in such configurations CP acts as a surface modifier to enhance interfacial charge transfer, and thus suppress recombination [184,185,285,286]. Finally, electrodeposited CNT/CP and graphene/CP hybrids are also used as the counterelectrode in DSSCs [125,287–289]. This research is fueled by the high price of Pt, and aims to find cheap alternatives with

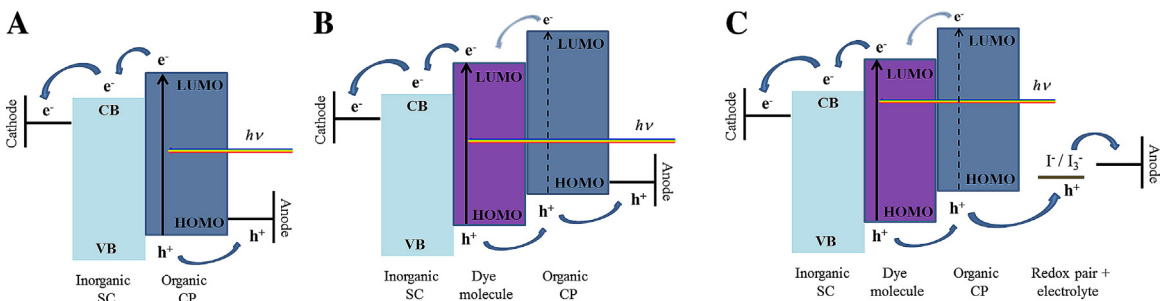


Fig. 21. Illustration of different solar cell configurations containing inorganic SCs and CPs.

high specific surface area, and reasonable catalytic activity toward the reduction of I_3^- .

It is well known that nanostructuring play a key role in the performance: laminar device structures only show limited efficiencies (<1%) due to the small interfacial area. Also, as the exciton diffusion length in most CPs is in the range of 5–10 nm, enlargement of the interfacial area is of prime importance to avoid extensive carrier recombination. In this vein, various strategies have been developed to create nanostructured heterojunctions with large area, ensuring efficient charge separation at the interface and charge carrier transport [290]. One such method is to make bulk heterojunctions by blending inorganic NPs with the CP [274]. This approach works for CdS and CdSe, however, for oxide NPs, most importantly for TiO_2 , it usually results in devices with low performance, due to the small area of the heterojunction, caused by NP agglomeration.

As an alternative approach, CPs can be infiltrated into nanostructured SC matrices, using solutions of the pre-synthesized CP. However, as mentioned earlier, this approach is hampered by the large size of the CP, by the difference in the hydrophilic/hydrophobic character of the two components. Consequently, often very low pore-filling ratios have been observed [13]. Various studies have dealt with the role of pore filling, and although the conclusions are controversial in the sense whether the nanostructured oxide host has to be fully filled or not, there is an agreement that uniform distribution of the infiltrated CP is crucially

important [291–293]. Due to these facts, *in situ* approaches are favored to generate CPs inside nanostructured oxide matrices, bringing the organic and inorganic component into intimate contact both at the physical and electronic level [294,295]. As an example, short circuit currents (J_{SC}) of a solid-state DSSC containing photoelectrochemically generated PEDOT was about 20 times higher than that of its counterpart having chemically polymerized PEDOT as hole transporter [237].

As already shown in the previous sections, the nature of the doping ion plays a key role in determining the properties of the electrogenerated CP, and this has substantial impact on the solar cell devices as well. For example, solid-state DSSCs have been fabricated based on TiO_2 , and employing PEDOT as a hole transporter, using various anions [296,297]. Importantly, the anions already affect the photoelectrochemical polymerization procedure, as can be deduced from the overall charge passed through during the synthesis. These variances, however cannot fully explain the differences observed in the solar cell performance. It was found that dopant anions in the PEDOT hole-conductor have great influences on $I-V$ curves, conductivity, and impedance as well. The most vital finding of these studies is probably the linear dependence of conversion efficiency on the logarithm of the conductivity of the hole transporting polymer [296,297].

The strong effect of the anions was also demonstrated for hybrids synthesized by dark electrodeposition

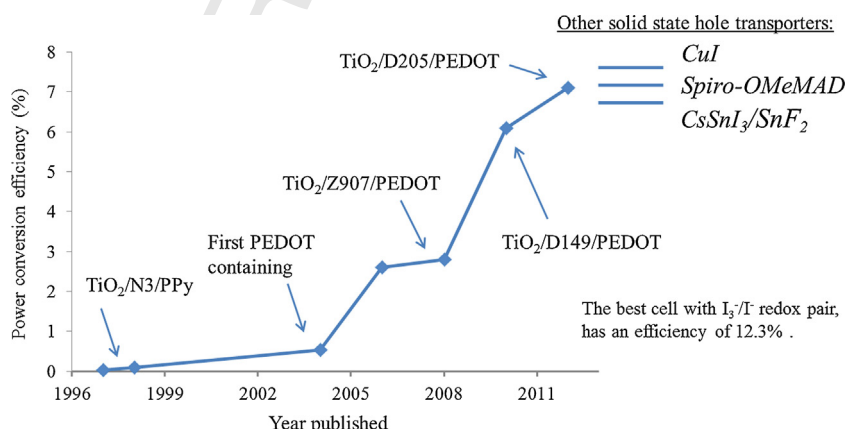


Fig. 22. Development of power conversion efficiencies in solid-state DSSCs, using CP as a hole transporter. Highest efficiencies obtained with solid-state inorganic as well as molecular hole transporters are shown as benchmarks.

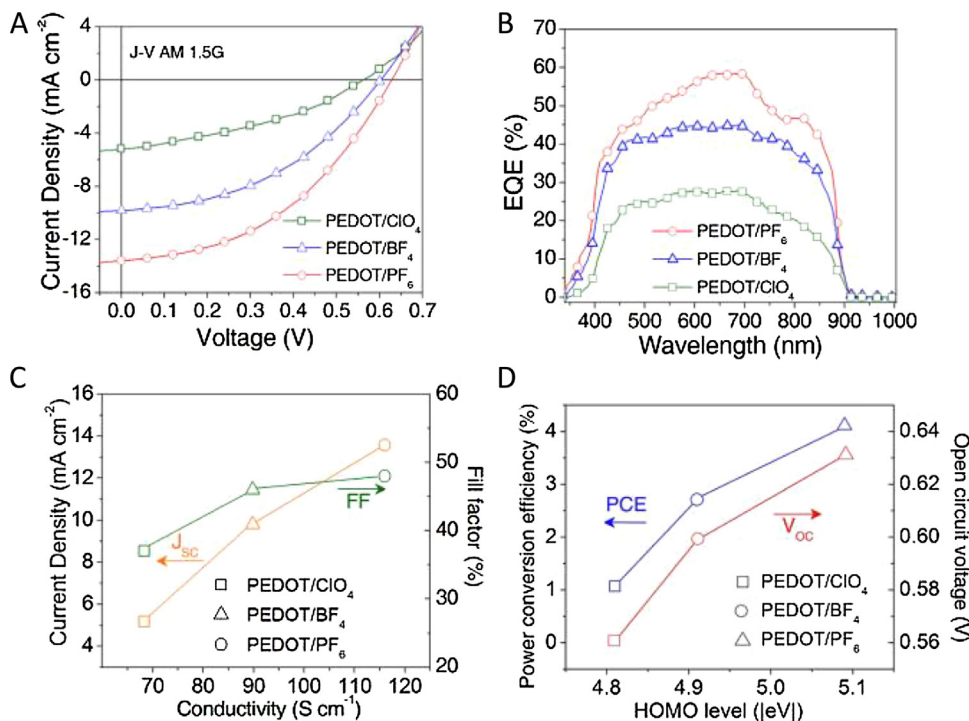


Fig. 23. Dependence of solar cell parameters of GaAs/PEDOT devices on the dopant ion.

[156], Copyright 2012, Reproduced with permission from the American Chemical Society.

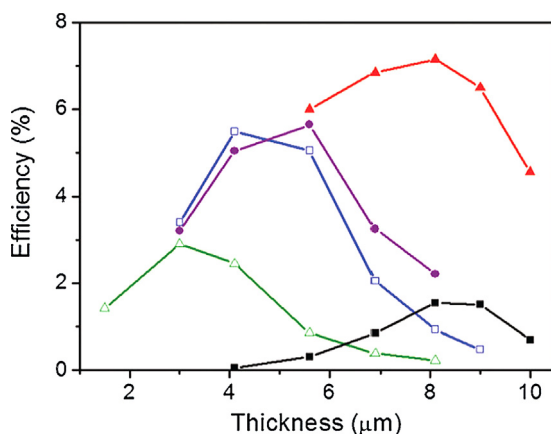
[104,156]. For example, in a recent study a nanostructured organic/inorganic solar cell was constructed by electrodepositing PEDOT on a GaAs nanopillar array using potentiodynamic cycling [156]. Five different dopant ions were studied (dodecyl-sulfate, poly(styrenesulfonate), ClO₄⁻, BF₄⁻, PF₆⁻), and it was found that both the properties of the CP, as well as that of the organic/inorganic interface are affected by the nature of the dopant anion. Most importantly, charge transport properties of electro-generated PEDOT exhibited a strong dependence on the dopant ion, and the conductivity values ranged between 21 and 116 S cm⁻¹. As depicted in Fig. 23, all the important parameters describing solar cell performance are strongly influenced by the properties of the CP, thus short circuit current (J_{sc}), fill factor (FF), external quantum efficiency (EQE) and the open circuit voltage (V_{oc}) show a clear and strong dependence on the nature of the dopant ion.

Parameters of the employed electrochemical method also exert an important effect on the solar cell performance. As discussed before, in the case of photoelectrochemical polymerization methods, the applied external bias potential may have dual contribution to the polymer formation. Such involvement can be envisioned either through direct electrochemical polymerization, or by draining the photogenerated electrons, therefore providing more holes to oxidize the monomer. In most of the studies where actual solar cell devices are fabricated, bias potential values are selected where only the second mechanism contributes to the polymerization [298]. This is mainly because in these configurations TiO₂ NPs were immobilized on conducting glass, and therefore electrochemical growth of the CP

would occur on that, possibly causing short circuit in the cell. On the other hand, in Section 3.2.2, we showed that electropolymerization results in polymers with superior conductivity and electroactivity compared to counterparts generated purely by photoelectrochemical polymerization. Therefore future studies along this avenue may be useful, with oxide structures where short circuiting is not an issue (e.g., NTAs, having a compact barrier layer below the tubes).

To illustrate the complexity of such systems and the role of multiple parameters, we show another example, namely the role of thickness of the hybrid layer. In conventional DSSCs, relatively thick TiO₂ layers (up to 10 μm) are used, to ensure sufficient light absorption. At such thicknesses mass transport limitation of bis-EDOT (or any other) monomer may hamper the polymerization at the deeper regions of the layer. This limitation not only results in inadequate pore filling, but also in an uneven distribution of PEDOT throughout the oxide matrix. Such effect was observed, when increasing thickness of the TiO₂ film first resulted in higher power conversion efficiencies, but after a certain threshold, the opposite trend was observed [240]. Solubility of the monomer can be increased by using organic solvents or aqueous micellar solutions. This latter method in an environmentally friendly and cheap alternative, and relies on the solubilization of the monomers using micelles (e.g., sodium dodecyl sulfate) [299].

Furthermore, a recent study [278] demonstrates that the picture is even more complicated, since diffusion of the monomer is not the only factor which hinders polymerization at the deeper areas of relatively thick TiO₂ films.



Q7 Fig. 24. Power conversion efficiencies of PEDOT based solid-state DSSCs with different mesoporous TiO_2 film thicknesses, synthesized under different light illumination black: 740 nm, red: 670 nm, blue: 605 nm, green: 540 nm and purple: continuous spectral light. (For interpretation of the references to color in this figure legend, the reader is referred to the web version of the article.)

[278], Copyright 2012, Reproduced with permission from the PCCP owner societies.

Hybrid layers obtained under monochromatic illumination outperformed their counterparts synthesized under continuous wavelength illumination. Interestingly, for different thickness different wavelengths were shown to be optimal. Such behavior was shown to be related to the difference in the absorption properties of the TiO_2 /dye layer for the different wavelengths. The consequence of this decrease is shown in Fig. 24; the optimal illumination wavelength is seen to be different for each layer thickness [278].

Overall, we may conclude that all solid-state solar cell devices will receive more and more attention in the future. The importance of high polymer loading is underlined by the fact that in solid-state DSSC using PEDOT as hole transporter, dye regeneration kinetics was found to be orders of magnitude slower than its counterparts having either I_3^-/I_2 redox couple or small molecule hole transporters [300]. Such slow dye regeneration limits the short circuit current, and this was attributed to low pore-filling (approximately 20%), and thus a low polymer/sensitizer ratio.

4.2. Energy storage

4.2.1. Supercapacitors

CP-based hybrids are eminently attractive candidates for energy storage. CPs have very good prospects in this application because of their pseudocapacitive behavior. This potential, however, has not been fully exploited yet, due to some handicaps of CPs, most importantly related to their relatively low cycling stability and limited mobility of anions in bulk CP layers. Hybridization with different inorganic materials aims to overcome these limitations. In most of the available examples, both components can contribute with their intrinsic electroactivity but the real synergy stems from other aspects of hybrid formation.

Two distinctly different categories can be identified: there are hybrids where both constituents exhibit

electroactivity in the same potential regime (e.g., MWCNT/PHT, see Fig. 25A), while in other cases the components have complementary electroactivity, therefore the hybrid is electroactive in a wider potential window (e.g., WO_3/PANI , see Fig. 25B). Importantly, in the case of appropriately designed composites, the specific capacitance of the hybrid is not just a linear combination of that of the constituents, but in optimal cases the specific capacity of the hybrid can be higher than that of its components. What is equally important, the composites usually have smaller charge transfer resistance than the pure polymer, which further enhances the performance in electrochemical capacitors.

As excellent reviews are available on this body of research [7,301], we only cite studies where electrochemical synthesis methods have contributed to some special, application-related benefit. As seen in Table 7, dominantly carbon nanomaterials (e.g., nanotubes or graphene) and metal oxides (such as MnO_2 or RuO_2) are combined with CPs for the purpose of electrochemical charge storage. This is not a surprise given that these are the most frequently applied materials in their own right.

In general, the advantage of electrochemical polymerization is the lack of added oxidants and binders as CPs and their hybrids are directly formed on the electrode. Consequently, the resistance between the CP-based active material and the current collector is smaller than in their chemically prepared counterparts. These notions have been realized in a pioneering study, where among the three methods used for preparing CNT/PEDOT composites (mechanical mixing, chemical polymerization, electrodeposition) the electrochemical method gave the best capacitor performance [84]. Table 7 compiles various hybrid assemblies with possible use as electrochemical capacitors. The highest specific capacitance values obtained in each study are also compared.

First-generation hybrids incorporated the carbon component into the CP matrix during electrodeposition [309]. Besides the contribution of the intrinsic capacitive behavior of the carbons, the enhanced behavior (especially in terms of durability) of the hybrid is generally attributed to the higher conductivity and stability of the composites compared to their bare CP counterparts. Such improvement is due to better charge-transfer and the porous structure of composites, facilitating rapid ionic transport. However, co-polymerization suffers from aggregation of the nanomaterials, as well as from the uneven distribution of the carbon component within the polymer matrix. Furthermore, due to lack of connection between the incorporated conductive materials, large electrode resistances are observed. To overcome these drawbacks, and to gain additional benefits from the hybridization, CPs were electrodeposited on *nanostructured* carbon substrates. The advantages of this method were shown for example on different highly porous carbon/PANI composites, and summarized as follows [132]:

- Easy handling compared with powdered carbon
- Binder-free and conductive-agent-free electrode preparation

Table 7

Electrogenerated CP-based assemblies as electrochemical capacitors.

Carbon	CP	Comment	Capacity	Refs.
GO	PPy	Free standing electrodes were obtained by doping type incorporation of GO	356 F/g at 0.5 A/g	[71]
Graphene	PANI	PANI nanorods are electrodeposited onto a self-standing graphene paper	763 F/g at 1 A/g	[302]
Graphene	PANI	3D porous structure was filled with increasing amounts of PANI	716 F/g at 0.47 A/g	[115]
Graphene	PANI	Free standing and flexible electrode. The effect of PANI amount was also shown	233 F/g	[114]
Graphene	PANI	This flexible electrode had high capacity and excellent stability	970 F/g at 2.5 A/g	[116]
Graphene	PANI	Attractive one step electrodeposition	640 F/g at 0.1 A/g	[303]
Graphene	PANI	Fast doping/dedoping of PANI was observed due to the morphology of the hybrid	725 F/g at 10 A/g	[76]
Graphene	PPy	Structure–property relationship for hybrids obtained by continuous and pulsed electrodeposition was evaluated	237 F/g at 10 mV/s	[117]
Graphene	PPy	Sulfonated graphene sheets were incorporated, resulting in improved electrical properties	285 F/g at 0.5 A/g	[80]
MWCNT	PANI	PANI was infiltrated into fibers of aligned carbon nanotubes	274 F/g at 2 A/g	[304]
MWCNT	PANI	The advantages of highly ordered NTAs were demonstrated. The role of filling ratio on the capacitance as well as the stability was also discussed	1030 F/g at 5.9 A/g	[122,123]
MWCNT	PEDOT	Several different compositions were studied, and the superior performance of electrodeposited hybrids was demonstrated	150 F/g	[84]
MWCNT	PPy	The contribution of increasing amounts of PPy was shown for this self-supporting membrane	427 F/g at 5 mV/s	[128]
MWCNT	PPY	Very thick NTA films are used and defects were introduced before polymer deposition	587 F/g at 3 A/g	[129]
MWCNT	PPy, PANI, PEDOT	Different polymers were studied, and the PANI containing composite showed the best durability	No data	[83]
Porous carbon	PANI	Hierarchically porous carbon monolith was used as an effective support for PANI deposition	360 F/g at 20 mA/g	[132]
SWCNT	PANI	The effect of hybrid composition on the capacitance and conductivity was studied	473 F/g at 5 mA/cm ²	[135]
SWCNT	PANI	Skeleton/skin morphology, effect of the change in porosity on the capacitance was shown	236 F/g at 20 mV/s	[136]
SWCNT	PDOP	An adhesive layer was introduced between the CP and the CNTs	151 F/g	[137]
MnO ₂	PEDOT	Electrochemical behavior was correlated with the morphology and crystal structure of the hybrid electrodes	285 F/g at 20 mV/s	[157]
MnO ₂	PMT	Role of polymeric underlayer was studied, and compared with MnO ₂ deposited onto Ti	218 F/g at 20 mV/s	[268]
MnO ₂	PEDOT	Morphological considerations on the performance were given	199 F/g at 10 mV/s	[267]
MnO ₂	PANI	Contribution of the individual components to the capacitance in the hybrid configuration was studied	715 F/g at 5 mA/cm ²	[266]
MnO ₂	PEDOT	Sequential deposition of multilayers was achieved, and capacitive properties of the various structures were compared	487.5 F/g at 1 mA/cm ²	[270]
MnO ₂	PEDOT	Hybrid coaxial nanowires were formed, and both symmetric and asymmetric capacitor devices were assembled	210 F/g	[305,248]
MnO ₂	PPy	Redox performance of the hybrid significantly exceeded that of its constituents	620 F/g at 5 mV/s	[245]
MnO ₂	PANI	Dependence of the specific capacitance on the hybrid composition was shown	532 F/g at 2.4 mA/cm ²	[244]
MnO ₂ -C	PANI	The hybrid was deposited onto activated carbon, and performance was studied in organic electrolyte	413 F/g at 5 mV/s	[246]
RuO ₂	PEDOT	Hybrid nanotubes were formed in Al ₂ O ₃ template, and RuO ₂ had very high contribution in the hybrid configuration	664 F/g at 5 mA/cm ²	[263]

Table 7 (Continued)

Carbon	CP	Comment	Capacity	Refs.
RuO ₂	PPy	Vertically well-aligned cone-shaped nanostructures of PPy were coated by a thin film of RuO ₂	302 F/g at 0.5 mA/cm ²	[306]
RuO ₂	PANI	Porous PANI provided a high surface area substrate for RuO ₂ growth	605 F/g at 10 mV/s	[265]
RuO ₂ .C	PANI	Specific capacitance significantly decreased at higher scan rates	708 F/g at 5 mV/s	[162]
RuO ₂ .C	PANI	RuO ₂ and PANI were co-immobilized on porous double-shelled carbon spheres	531 F/g at 1 mA/cm ²	[264]
TiO ₂	PPy	TiO ₂ NTA was used, and PPy did not have well defined electroactivity in the hybrid	179 F/g at 1.85 mA/cm ²	[192]
TiO ₂	PT	Polythiophene was infiltrated into TiO ₂ NTA, therefore it had high surface area	640 F/g at 5 mV/s	[307]
WO ₃	PANI	Good performance in asymmetric capacitor configuration	168 F/g at 1.28 mA/cm ²	[254]
WO ₃	PANI	Interaction of PANI with WO ₃ improved stability	No data	[308]

- Facile synthesis
 - Controlled growth of active materials by limited pore spaces
 - Optimal performance (specific capacitance, power and energy densities, excellent cycling stability).

Importantly, all these characteristics apply for other nanostructured carbon hosts as well, such as CNT arrays or three-dimensional graphene structures. The capacitance of an electrode depends among other factors, on the resistance of electron transfer between the electroactive material and current collector and the ease of electrolyte migration. Consequently, a good compromise has to be found between the deposited amount of polymer and the pore size and density. This latter is an important parameter, because it ensures that all the deposited polymer is accessible to the electrolyte phase, as demonstrated by the example of interconnected SWCNT/PANI hybrid [136]. In another example, the amount of PANI electrodeposited inside a three-dimensional matrix of electrochemically reduced graphene oxide (ERGO) was varied, by increasing the number of potentiodynamic deposition cycles [115]. As seen in Fig. 26, there is an optimal loading of PANI, over which the capacitance does not increase further, and even decreases mainly due to pore blocking.

Among metal oxides, MnO₂ and especially RuO₂ are very attractive for charge storage, as they have an extraordinary high charge capacity. When combining them with CPs, the aim is generally to obtain hybrids with high surface area using nanoscale distribution of the components. For example, a co-deposited MnO₂/PPy composite outperformed both of its components in terms of specific capacitance, with reasonable stability at the same time [245]. Careful study of sequential electrodeposition of different MnO₂/PEDOT hybrids proved the importance of both under- and over-laying PEDOT film, below, and above a MnO₂ layer respectively [246]. Such a sandwich structure was beneficial from two aspects: the thin inner layer of PEDOT acted as a flexible binder to the current collector, whereas the outer film protected MnO₂ from being detached. Due to these favorable contributions, the hybrid held 95.5% of its charge capacity over 1500 cycles [246].

In the case of RuO₂, higher specific capacitance values are often obtained for the hybrid than for its components, due to the large surface area of the oxide in the hybrid configuration [162]. Very similar trends were revealed for PPy nanotubes having an ultrathin coating of RuO₂ on their surface [306]. Ternary composites have also been fabricated by depositing both the CP and RuO₂ on high surface area carbon substrate [162,264]. In another study, both the inner

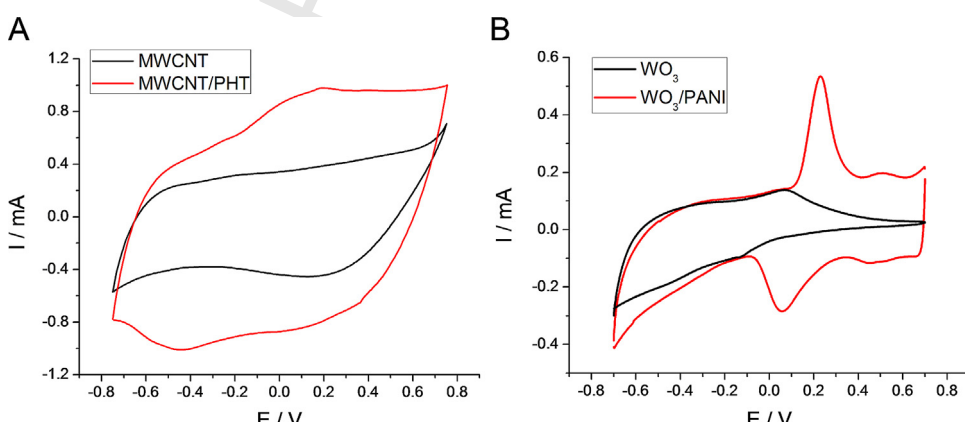


Fig. 25. Examples for hybrid charge-storage materials where the constituents have (A) overlapping, (B) complementary electroactivity.

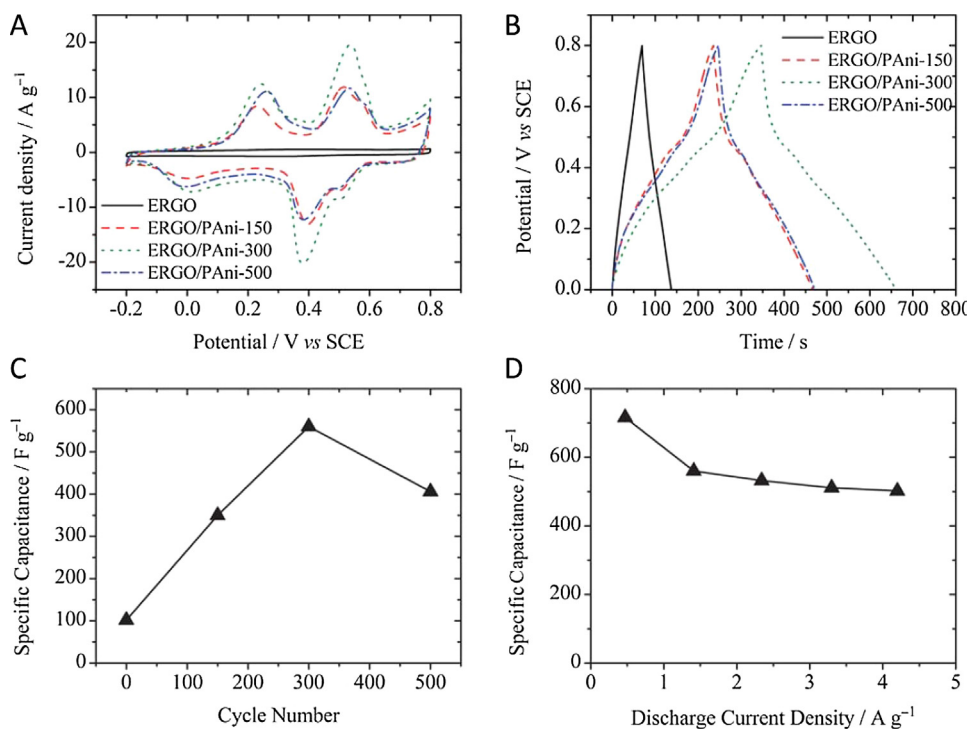


Fig. 26. Electrochemical properties of electrochemically reduced graphene oxide ERGO, and ERGO–PANI composite electrodes. (A) CV curves at the scan rate of 5 mV/s; (B) galvanostatic charge–discharge curves at a current density of 1.4 A/g; (C) specific capacitance of ERGO–PANI-300 at different charge/discharge current densities. [115], Copyright 2012, Reproduced with permission from the Royal Society of Chemistry.

and outer surfaces of PEDOT nanotubes were decorated with RuO₂ NPs. In these configurations, the mechanical properties of the components are mutually reinforced; the flexible PEDOT prevents the RuO₂ detaching from the current collector while the rigid oxide avoids collapse and aggregation of the nanotubes [263]. The charge-storage mechanism of RuO₂/PEDOT composite nanotubes as well as the advantages of the organized nanoscale structure is schematically shown in Fig. 27A.

More recently, other oxides (WO₃ and TiO₂) have also been studied in this manner (see Table 7). TiO₂ NTAs appear

to be particularly promising in this respect, due to their high surface area and chemical/electrochemical stability. Such composites may offer short migration path for the dopant ions and also improve the effectiveness of electron transfer, resulting in a high electrochemical capacitance (e.g., 640 F/g for TiO₂/PT hybrid) [169,307].

4.2.2. Lithium-ion batteries

This application area is not as well developed as those discussed before, but there are still some notable examples as presented below. There are also emerging concepts,

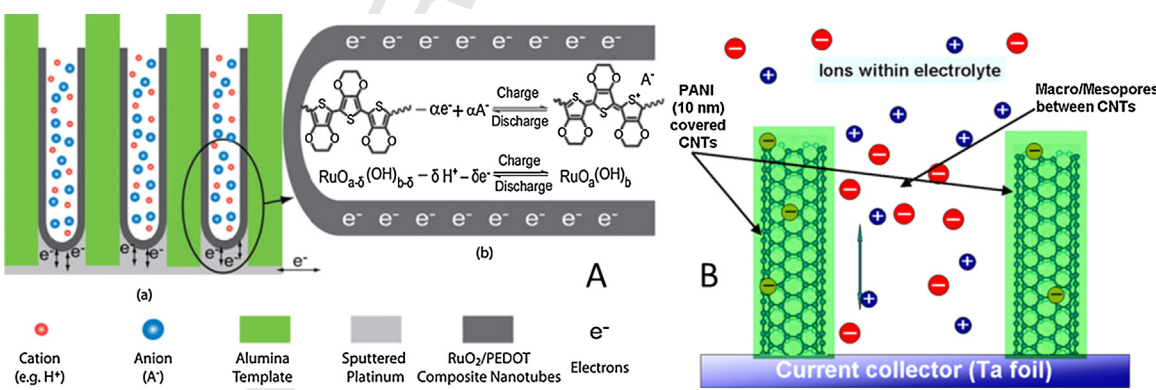


Fig. 27. Role of organized nanostructures in enhanced capacitive properties due to effective ion transport. (A) RuO₂/PEDOT composite nanotubes, (B) CNT array/PANI hybrid.

Sources, respectively: [263], Copyright 2010, Reproduced with permission from the PCCP owner societies; [123], Copyright 2009, Reproduced with permission from Elsevier Ltd.

such as combining solar cells with Li-ion batteries in one electrochemical cell resulting in a solar rechargeable battery [225,310]. In general, transition metal oxides are attractive candidates as active materials in Li-ion batteries due to their high capacity (over 700 mAh/g) even at high charge–discharge current density. However, in most of the cases, a very quick decrease in their capacity can be observed during repeated discharge–charge cycles, due to the low conductivity of these oxide semiconductors. Therefore, hybrids with carbons, metals or even CPs have been developed. In such composites CPs improve both Li-ion intercalation capacity and accessibility, mechanical stability, and conductivity of the electrode compared to the parent oxide. Furthermore, CPs have an additional advantage, as they not only act as the conducting network but also as the active material, because of their ion-exchange properties.

For example, MnO_2 particles in a PPy film worked well as an active material, giving an increase in the charge–discharge capacity over that of PPy itself. These electrodes had only one potential plateau during both charge and discharge cycles, which indicated that the redox transformation of both components take place in the same potential regime [24,311]. NiO/PEDOT films were also studied, and exhibited weaker polarization and better cycling performance as compared to the bare oxide (best specific capacity: 520 mAh/g) [161]. Importantly, the presence of PEDOT enhanced the conductivity of the electrode, and contributed to the improved stability of the porous NiO during the cycling [161]. PPy nanowires were uniformly decorated by SnO_2 nanocrystals forming organized nanostructures to be applied in Li-ion batteries. This assembly exhibited a reversible capacity of 690 mAh/g, and what is equally important, most of its electroactivity (622 mAh/g) was retained even after 80 cycles. The advanced properties was enabled by multiple factors, most importantly by the advantages of the three-dimensional architecture of the PPy nanowire support, in terms of facile charge carrier transport, high porosity, and enhanced stability [262].

Lithium ion intercalation/de-intercalation of TiO_2/PPy and $\text{TiO}_2/\text{PEDOT}$ hybrids was studied [174]. The improved Li-ion intercalation was attributed to the higher conductivity of the hybrid compared to mesoporous TiO_2 [174]. Vanadium pentoxide is probably one of the most extensively studied materials, and its hybrids with PPy, PANI and PEDOT have been evaluated for their application in this vein. In all the cases, a better mechanical flexibility during the expanding/shrinking cycles of discharge/charge was observed. $\text{V}_2\text{O}_5/\text{PANI}$ composite films showed a specific capacity of 270 mAh/g, with very small fading (ca., 3.4%) [312]. As for $\text{V}_2\text{O}_5/\text{PPy}$ composites (294 mAh/g), the performance of electrodeposited and chemically generated samples was compared, and the electrochemically assembled electrode displayed superior performance in terms of both cycle stability and specific capacity [313]. Finally, V_2O_5 nanobeams were embedded into PEDOT and the kinetics of lithium transport was analyzed [47].

Most recently, a novel ternary composite anode composed of Si NPs embedded in a three-dimensional hierarchically porous PPy framework containing SWCNTs has been realized [314]. This Si/PPy/CNT showed

high-performance, because of exploiting the benefits if each component, namely the high surface area of the CP, the ultrahigh specific capacity of Si, and the high electric conductivity of the SWCNTs. The as-prepared ternary electrode exhibited long-term stability because of the presence of the CP helped to avoid major degradation of the Si particles during lithium insertion/extraction [314].

4.3. Other miscellaneous applications

4.3.1. Heterogeneous (photo-)catalysis

CPs can be used as a support for both photo- and electrocatalysts, due to their porosity and potentially high surface area, especially in their nanostructured form. Metal NPs are the most frequently used additives for such purposes, but studies with inorganic SCs and carbon nanostructures can also be found in the literature. Furthermore, CPs have intrinsic electrocatalytic activity toward different reactions, for example, oxygen reduction reaction (ORR) [315]. Such activity can be synergistically combined with that of the immobilized inorganic NPs, as shown in the following examples.

A wide range of ternary transition metal oxides have been incorporated into CPs in this vein, including $\text{Cu}_{1.4}\text{Mn}_{1.6}\text{O}_4$ or $\text{Ni}_x\text{Co}_{3-x}\text{O}_4$ [54,56], and their improved efficiency in ORR was demonstrated. In addition, it was found that the presence of oxide NPs avoids degradation of the polymeric matrix, caused by the formation of HO_2^- during ORR. This is a vital point in view of applications because chemical and mechanical degradation is a major drawback of polymeric materials in these applications (note the similarity with PEMFCs [316]). The nature and concentration of the dopant anions play a key role in ORR, due to their effect on the structural, morphological, and electronic properties of the hybrid assembly. Electrocatalytic reduction of other species, such as ClO_3^- and BrO_3^- were performed on WO_3/PANI [317] and MoO_3/PANI [249] composites, respectively. With the purpose of possible fuel cell applications, electrooxidation of different fuels, such as methanol [251], ethanol [251,252], and also polyhydroxyl compounds [250] were tested on NiO_x -containing CP electrodes. In all the cases the catalytic activity was facilitated by the $\text{Ni}(\text{II})/\text{Ni}(\text{III})$ redox transition of the NiO_x nanoparticles, dispersed in the CP matrix.

In some cases, the catalytic efficiency can be further enhanced by illumination, due to the semiconductor properties of either the CP, or the embedded NPs, or occasionally both. For example, CPs (being p-type SCs) are known to photoreduce dissolved oxygen [318]. In the case of a $\text{Fe}_3\text{O}_4/\text{PPy}$ composite, the built-in oxide resulted in higher currents, because of the electroreduction of H_2O_2 , formed in the reaction between the photogenerated electron and oxygen. Rotating disk electrode (RDE) studies indicated the dominance of the 4 e^- reduction pathway for O_2 for the overall process. In addition, electrocatalytic reduction of H_2O_2 (as the intermediate of the ORR) was also studied, and the $\text{Fe}_3\text{O}_4/\text{PPy}$ hybrid showed 7.5 times larger catalytic activity compared to neat PPy [45,46].

CPs can also be used as sensitizers of inorganic photocatalysts (similar to their application in hybrid organic/inorganic solar cells). In this manner TiO_2 NTAs

were decorated by various thiophene derivatives [179] and PANI [166], and tested under visible light irradiation for photoelectrochemical degradation of 2,3-dichlorophenol and Rhodamine B, respectively. One particularly important finding was that the side chain of the polymer affects the photocatalytic efficiency, due to differences in interfacial properties, and consequently in the charge transfer. Again, electrodeposition is particularly useful here, since it directly results in better electronic contact between the two components (see above).

As for carbon nanomaterials, their incorporation can also enhance the catalytic performance related to the polymer, because such hybrids exhibit improved electrical conductivity, electrochemical capacitance, and mechanical strength. SWCNT/PPy were used in ORR and, a mixture of two-electron and four-electron processes was observed [94]. Electrodeposited composites (having a thin net-like structure) were found to outperform their chemically synthesized counterparts, because of morphological differences [94]. Similar conclusions were drawn for MWCNT/PMT hybrids for the electrooxidation of NADH [126]. The real advantages of carbon nanomaterials however, can be exploited in ternary hybrids, in which beyond the CP and the carbon, a third, catalytically active component (e.g., metal NPs) is also present. In such configurations, the advantages of each constituent are mutually reinforced: CP provides a common flexible platform, the carbon nanomaterial enhances the electronic conductivity, and metal/inorganic nanoparticles contribute with their catalytic activity. In this manner among others, SWCNT/PANI/Pt [319,320], MWCNT/PANI/Au [321] and graphene/PEDOT/Co [322] assemblies were realized through electrodeposition, and tested for the oxidation of formic acid, methanol, ascorbic acid and nitrite-ions, respectively.

4.3.2. Sensors

The first applications of CP-based assemblies in this area were demonstrated in conductivity sensors, where the interaction between the analyte and the electrode material (usually in the gas phase) results in a change of the electrical conductivity. Chemical reactions (doping/dedoping) as well as physical (e.g., solvation/desolvation) changes are responsible for the observed resistivity alterations. Hybridization aims to extend sensing to a wider range of analytes to enhance sensitivity, and to achieve better selectivity [8].

For example, photoelectrochemically generated TiO₂/PPy was demonstrated to outperform its bare polymeric counterpart as a humidity sensor [323]. The surface morphology as well as the interaction between PPy and doped TiO₂ NPs resulted in higher sensitivity (impedance changed almost two orders of magnitude), and much better linearity in the semi-logarithmic response curve. The PPy component has much higher surface area in the hybrid configuration, which is indeed important when sensing is based on the reduced conductivity due to water adsorption. Co-deposited graphene oxide/polypyrrole composite films were employed for the detection of volatile organic compounds [78]. The presence of the carbon component improved the mechanical properties

of the polymer and ensured a continuous and porous morphology. A chemoresistor-type vapor sensor demonstrated fast, linear and reversible response to toluene with high sensitivity and selectivity [78]. Detection of liquefied petroleum gas (LPG) was performed using a series of SC/PANI heterojunctions, containing CdTe [107], CdS [105] and PbS [109] respectively. In these studies, changes in the *I-V* curves were correlated with the LPG concentration and the response alteration were rationalized in terms of the modification of the organic/inorganic interface.

In electrochemical sensors, application of CP-modified electrodes was first demonstrated in potentiometric sensors, most importantly in ion selective electrodes [324]. As for voltammetric/amperometric detection, considerable interest manifested toward hybrid materials due to their selectivity, sensitivity and homogeneity, strong adherence to electrode surface and chemical stability [325]. We omit examples from this last group for two reasons: (i) these hybrids are very similar to those shown in the previous section, used as electrocatalysts, (ii) this topic has been reviewed recently [326]. The conclusion of the review was that electrodeposited composites exhibited superior performance both in terms of sensitivity and detection limits compared to that of the chemically synthesized samples [326].

4.3.3. Electrochromics

Many of the widely utilized electrochromic materials are either inorganic oxide SCs (most importantly WO₃) [327] or CPs. Note that the whole color palette has been covered using CPs by now [328]. The main advantages of inorganic materials are the relatively fast color switching, durability, and long term stability, but their use is hampered by their narrow color variation and low coloration efficiencies. This latter, together with the high contact resistance in the device, results in the need of high electrical power input to reach the required color change. On the other hand, CPs exhibit high coloration efficiencies at relatively lower redox switching potentials, on a short timescale. Their relatively low environmental stability (especially in the oxidized state) and mechanical strength, however, are important drawbacks from an application perspective. Therefore, it was soon recognized that in hybrids, the complementary properties can be exploited, and the synergies fully utilized [329]. Such synergies predominantly stem from the combination of the flexibility and functionality of the CP with the mechanical strength and chemical stability of the inorganic SC [330]. The assembling method, as well as the resulted (nanoscale) morphology is of prime importance as shown in the examples below.

The first realization of electrochromic hybrid assemblies relied on the incorporation of WO₃ particles into both PPy [23] and PANI [253]. The composite films were blue in color at negative potentials (due to the color of the inorganic component) and multicolored from green to violet at positive potentials. Importantly, there is an electrochromic window between the WO₃ coloration and PANI coloration, which opens an opportunity to their use in multicolor displays. In this vein, WO₃ particles were embedded to additional polymers [34], and PANI

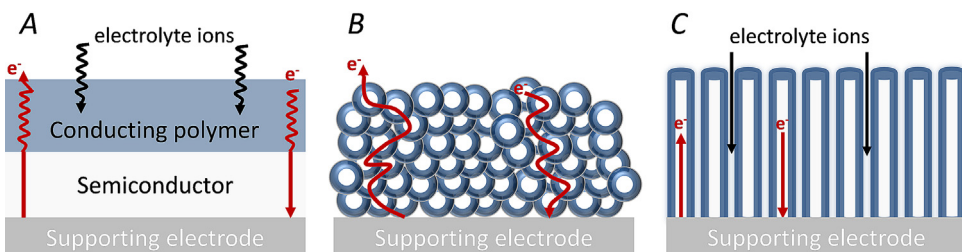


Fig. 28. Comparison of (A) flat, (B) nanoparticulate and (C) nanostructured device configuration for electrochromic applications. The possible ion and electron transport routes are also shown.

1899 was also electrodeposited on the WO_3 surface [308,331].
 1900 TiO_2 -containing hybrids have also been obtained, containing PANI [168], and various thiophene derivatives
 1901 [142,146,178]. In these cases a major advantage is the
 1902 increased stability of the CP in the hybrid configuration.
 1903

1904 The improved stability during the redox transformation
 1905 is predominantly related to the hybrid architecture (CP is
 1906 infiltrated into mesoporous TiO_2), as the nanoparticulate
 1907 matrix acts as a skeleton, keeping the polymer intact and
 1908 avoiding its detachment. Notably, use of ionic liquid as
 1909 an electrolyte is also likely to contribute to the enhanced

1910 lifetime. In addition, significantly faster electrochromic
 1911 response was obtained in the case of a nanostructured
 1912 TiO_2/PPy hybrid compared to the neat PPy layer [223].
 1913 Similarly, an interconnected array of NiO nanoflakes was
 1914 employed as the host matrix for both PANI and PEDOT, and
 1915 subsequently used as electrochromic materials [159,160].

1916 In summary, the most important lessons learned from
 1917 the previous studies can be summarized as follows:

1918 \checkmark The inorganic compound may contribute with its intrinsic
 1919 electroactivity coupled with the color change. This may

Table 8

Direct examples of performance enhancement in selected applications of electrogenerated conducting polymer–inorganic semiconductor nanocomposites relative to cases when other, non-electrochemical synthesis methods were applied.

Hybrid material	Application	Remarks	Refs.
$\text{TiO}_2/\text{dye}/\text{PEDOT}$	Hole-transporter in solid state DSSC	Short circuit currents (I_{sc}) of a solid-state DSSC containing photoelectrochemically generated PPy was about 20 times higher, than that of its counterpart having chemically polymerized PPy as hole transporter	[237]
CNT/PEDOT	Supercapacitor	Because of the lack of added oxidants and binders, resistance between the CP-based active material and the current collector is smaller than in their chemically prepared counterparts. For example among three compositionally identical CNT/PEDOT composites made by different methods (mechanical mixing, chemical polymerization, electrodeposition) the electrochemical method gave the best capacitance results	[84]
$\text{V}_2\text{O}_5/\text{PPy}$	Li-ion battery	The performance of electrodeposited and chemically generated $\text{V}_2\text{O}_5/\text{PPy}$ composite samples was compared, and the electrochemically assembled electrode displayed superior performance in terms of both cycle stability and specific capacity	[313]
SWCNT/PPy and MWCNT/PMT	Electrocatalysis	Electrodeposited SWCNT/PPy composites (having a thin net-like structure) were found to outperform their chemically synthesized counterparts in ORR, because of morphological differences and enhanced mechanical strength. Similar conclusions were drawn for MWCNT/PMT for the electrooxidation of NADH	[94,124]
Various CNT/CP and SC/CP hybrids	Electrochemical sensing	By comparing similar composite materials prepared by different techniques, those obtained through electrochemical methods show superior performance to their chemically synthesized counterparts in electrochemical sensing. Almost all the composites that exhibit the lowest detection limits within their group toward the sensing of a certain benchmark analyte have been obtained electrochemically	[326]

or may not coincide with the polymer properties in terms of coloration window (potential) and the resulting colors.

✓ Improved stability of the polymer because of the intimate contact with the inorganic component.

✓ Better charge carrier transport due to the organized network structure, which can act as a “freeway” for the charge carriers (see also Fig. 28). Also the nano-dimension of the polymer can avoid limitations from the small exciton diffusion length in CPs.

✓ Porous hybrid structures facilitating diffusion/migration of ions and resulting in faster coloration times (Fig. 28B and C).

Finally a related phenomenon, namely, photochromism of SC-containing CP films is noted. In the case of TiO₂ [27,332] or CdS [37] containing films, their coloration was observed upon illumination. In this case, alteration of the PANI oxidation level (and the coupled color change) was not caused by external electrochemical stimulus (bias potential) but by photogenerated electrons from the SC particles. Upon generation of excitons, the photoelectrons reduce the oxidized PANI, while the photoholes are consumed by a hole scavenger (methanol) in the solution phase.

5. Summary

Introduction of new functional materials into CPs, or deposition of CPs on SC surfaces aims to result in advanced properties in various aspects. The success of such hybridization however, critically depends on the control attained over the composition and nanoscale morphology of the hybrid assembly and especially the interface between the components. In this review we have demonstrated the power of electrochemistry for obtaining hybrid materials based on CPs and SCs. Through careful control over the electrochemical synthesis parameters, the resultant hybrid can be tuned toward a targeted application. What is equally important, electrochemistry is a relatively mild method, and it does not require use of additional chemicals for the polymer synthesis. As demonstrated in this review, there is a wealth of possible electrochemical approaches to be employed, each of them having particular advantages and drawbacks. Opportunities with less frequently used approaches, such as photoelectrochemical polymerization, may attract increasing interest in the future, especially in light of its usefulness for less conductive SC electrode substrates.

The above listed attractive attributes of CP/SC composites have re-sparked much attention on such hybrid assemblies to be deployed in various applications ranging from solar energy conversion, energy storage, sensors, and electrochromics. Particular stress was given to applications, in which the hybrid can be directly used as a modified electrode. Table 8 highlights a set of CP/SC nanocomposite systems where the electrogenerated hybrids outperformed counterparts obtained by other synthetic procedures. Examples of performance enhancement in selected applications are by no means exhaustive but only representative of the range examined. It is impressive that these nanocomposites show superior performance whether the

application considered is solar energy conversion (solar and photoelectrochemical cells), electrochromics (smart windows), (photo)catalysis (environmental remediation, solar fuel generation, or sensors), or charge storage (electrochemical capacitor, Li-ion battery).

Uncited reference

[212].

Acknowledgements

CJ is grateful to his former PhD advisor and mentor Prof. Csaba Visy, who inspired him to enter the fascinating world of conducting polymer based hybrid assemblies. Equally important he taught me that human qualities are as important as intellectual stature and that training of younger generations of emerging researchers and new scientific achievements must go hand in hand. CJ also gratefully acknowledges funding support of the European Union under FP7-PEOPLE-2010-IOF, Grant Number: 274046. This research was also supported in the framework of TÁMOP 4.2.4.A/2-11-1-2012-001 “National Excellence Program—Elaborating and operating an inland student and research personal support system” key project. KR thanks the National Science Foundation (CHE-1303803) for partial funding support.

References

- [1] Heeger AJ. Semiconducting polymers: the Third Generation. *Chem Soc Rev* 2010;39:2354–71.
- [2] Inzelt G, Pineri M, Schultze J, Vorotyntsev M. Electron and proton conducting polymers: recent developments and prospects. *Electrochim Acta* 2000;45:2403–21.
- [3] Gangopadhyay R, De A. Conducting polymer nanocomposites: a brief overview. *Chem Mater* 2000;12:608–22.
- [4] Rajeshwar K, de Tacconi NR, Chenthamarakshan CR. Semiconductor-based composite materials: preparation, properties, and performance. *Chem Mater* 2001;13:2765–82.
- [5] Gomez-Romero P. Hybrid organic–inorganic materials – in search of synergic activity. *Adv Mater* 2001;13:163–74.
- [6] Skompska M. Hybrid conjugated polymer/semiconductor photovoltaic cells. *Synth Met* 2010;160:1–15.
- [7] Wang G, Zhang L, Zhang J. A review of electrode materials for electrochemical supercapacitors. *Chem Soc Rev* 2012;41:797–828.
- [8] Hatchett DW, Josowicz M. Composites of intrinsically conducting polymers as sensing nanomaterials. *Chem Rev* 2008;108:746–69.
- [9] Malinauskas A, Malinauskiene J, Ramanavicius A. Conducting polymer-based nanostructured materials: electrochemical aspects. *Nanotechnology* 2005;15:R51–62.
- [10] Li C, Bai H, Shi G. Conducting polymer nanomaterials: electrosynthesis and applications. *Chem Soc Rev* 2009;38:2397–409.
- [11] Liang Y, Yu L. Development of semiconducting polymers for solar energy harvesting. *Polym Rev* 2010;50:454–73.
- [12] Reiss P, Couderc E, Girolamo J, Pron A. Conjugated polymers/semiconductor nanocrystals hybrid materials – preparation, electrical transport properties and applications. *Nanoscale* 2011;3:446–89.
- [13] Bartholomew GP, Heeger AJ. Infiltration of regioregular poly[2,2-(3-hexylthiopene)] into random nanocrystalline TiO₂ networks. *Adv Funct Mater* 2005;15:677–82.
- [14] Koh JK, Kim J, Kim B, Kim JH, Kim E. Highly efficient, iodine-free dye-sensitized solar cells with solid-state synthesis of conducting polymers. *Adv Mater* 2011;23:1641–6.
- [15] Huisman CL, Huijser A, Donker H, Schoonman J, Goossens A. UV polymerization of oligothiophenes and their application in nanostructured heterojunction solar cells. *Macromolecules* 2004;37:5557–64.

- [16] Kowsari E, Faraghi G. Ultrasound and ionic-liquid-assisted synthesis and characterization of polyaniline/Y₂O₃ nanocomposite with controlled conductivity. *Ultrason Sonochem* 2010;17: 718–25.
- [17] Rajeshwar K. Electrochemistry of conducting polymers. In: Skotheim T, Elsenbaumer RL, Reynolds JR, editors. *Handbook conducting polymers*. 2nd ed. New York: Marcel Dekker Inc.; 1998. p. 531–89.
- [18] Heinze J, Frontana-Uribe B, Ludwigs S. Electrochemistry of conducting polymers—persistent models and new concepts. *Chem Rev* 2010;110:4724–71.
- [19] Zhou M, Heinze J. Electropolymerization of pyrrole and electrochemical study of polypyrrole: 1. Evidence for structural diversity of polypyrrole. *Electrochim Acta* 1999;44:1733–48.
- [20] Sabouraud G, Sadki S, Brodie N. The mechanisms of pyrrole electropolymerization. *Chem Soc Rev* 2000;29:283–93.
- [21] Yoneyama H, Hirao S, Kuwabata S. Preparation and electrochemical properties of WO₃-incorporated polyaniline films. *J Electrochem Soc* 1992;139:3141–6.
- [22] Kawai K, Miura N, Kuwabata S, Yoneyama H. Electrochemical synthesis of polypyrrole films containing TiO₂ powder particles. *J Electrochem Soc* 1990;137:1793–6.
- [23] Yoneyama H, Shoji Y. Incorporation of WO₃ into polypyrrole, and electrochemical properties of the resulting polymer films. *J Electrochim Soc* 1990;137:3826–30.
- [24] Kuwabata S, Kishimoto A, Tanaka T, Yoneyama H. Electrochemical synthesis of composite films of manganese dioxide and polypyrrole and their properties as an active material in lithium secondary batteries. *J Electrochim Soc* 1994;141:10–5.
- [25] Beck F, Dahlhaus M, Zahedi N. Anodic codeposition of polypyrrole and dispersed TiO₂. *Electrochim Acta* 1992;37:1265–72.
- [26] Beck F, Dahlhaus M. Anodic formation of polypyrrole/tungsten trioxide composites. *J Appl Electrochim* 1993;23:781–9.
- [27] Kuwabata S, Takahashi N, Hirao S, Yoneyama H. Light image formations on deprotonated polyaniline films containing titania particles. *Chem Mater* 1993;5:437–41.
- [28] Ferreira C, Domenech S, Lacaze P. Synthesis and characterization of polypyrrole/TiO₂ composites on mild steel. *J Appl Electrochim* 2001;31:49–56.
- [29] Lenz D, Delamar M, Ferreira C. Application of polypyrrole/TiO₂ composite films as corrosion protection of mild steel. *J Electroanal Chem* 2003;540:35–44.
- [30] Liu YC, Huang JM, Tsai CE, Chuang TC, Wang CC. Effect of TiO₂ nanoparticles on the electropolymerization of polypyrrole. *Chem Phys Lett* 2004;387:155–9.
- [31] Ilieva M, Ivanov S, Tsakova V. Electrochemical synthesis and characterization of TiO₂-polyaniline composite layers. *J Appl Electrochim* 2007;38:63–9.
- [32] Zubillaga O, Cano FJ, Azkarate I, Molchan IS, Thompson GE, Skeldon P. Synthesis of anodic films in the presence of aniline and TiO₂ nanoparticles on AA2024-T3 aluminium alloy. *Thin Solid Films* 2009;517:6742–6.
- [33] Latonen RM, Meana Esteban B, Kvarnström C, Ivaska A. Electrochemical polymerization and characterization of a poly(azulene)-TiO₂ nanoparticle composite film. *J Appl Electrochim* 2008;39:653–61.
- [34] Wei H, Yan X, Li Y, Gu H, Wu S, Ding K, Wei S, Guo Z. Electrochromic poly(DNTD)/WO₃ nanocomposite films via electropolymerization. *J Phys Chem C* 2012;116:16286–93.
- [35] Rincón M, Hu H, Martínez G. Effect of Bi₂S₃ nanoparticles in the protection mechanism of polypyrrole thin films. *Synth Met* 2003;139:63–9.
- [36] Rincón M, Hu H, Martínez G, Suárez R, Banuelos JG. Bi₂S₃ nanoparticles in polypyrrole thin films electropolymerized on chemically deposited bismuth sulfide electrodes: synthesis and characterization. *Sol Energy Mater Sol Cells* 2003;77:239–54.
- [37] Yoneyama H, Tokuda M, Kuwabata S. Photo-induced electrochromic reactions of deprotonated polyaniline containing cadmium sulfide particles. *Electrochim Acta* 1994;39: 1315–20.
- [38] Pethkar S, Patil R, Kher J, Vijayamohanan K. Deposition and characterization of CdS nanoparticle/polyaniline composite films. *Thin Solid Films* 1999;349:105–9.
- [39] Madani A, Nessark B, Boukherroub R, Chehimi MM. Preparation and electrochemical behaviour of PPy-CdS composite films. *J Electroanal Chem* 2011;650:176–81.
- [40] Gaponik NP, Talapin DV, Rogach AL, Eychmüller A. Electrochemical synthesis of CdTe nanocrystal/polypyrrole composites for optoelectronic applications. *J Mater Chem* 2000;10:2163–6.
- [41] Garcia B, Lamzoudi A, Pillier F, Nguyen H, Le T, Deslouis C. Oxide/polypyrrole composite films for corrosion protection of iron. *J Electrochem Soc* 2002;149:B560–6.
- [42] Bidan G, Jarjayes O, Fruchart J, Hannecart E. New nanocomposites based on "tailor dressed" magnetic particles in a polypyrrole matrix. *Adv Mater* 1994;6:152–5.
- [43] Jarjayes O, Fries P, Bidan C. New nanocomposites of polypyrrole including γ-Fe₂O₃ particles: electrical and magnetic characterizations. *Synth Met* 1995;69:343–4.
- [44] Pailleret A, Hien NTL, Thanh DTM, Deslouis C. Surface reactivity of polypyrrole/iron-oxide nanoparticles: electrochemical and CS-AFM investigations. *J Solid State Electrochim* 2007;11: 1013–21.
- [45] Janáky C, Endrodi B, Berkési O, Visy C. Visible-light-enhanced electrocatalytic activity of a polypyrrole/magnetite hybrid electrode toward the reduction of dissolved dioxygen. *J Phys Chem C* 2010;114:19338–44.
- [46] Bencsik G, Janáky C, Endrődi B, Visy C. Electrocatalytic properties of the polypyrrole/magnetite hybrid modified electrode towards the reduction of hydrogen peroxide in the presence of dissolved oxygen. *Electrochim Acta* 2012;73:53–8.
- [47] Song HM, Yoo DY, Hong SK, Kim JS, Cho WI, Mho SI. Electrochemical impedance analysis of V₂O₅ and PEDOT composite film cathodes. *Electroanalysis* 2011;23:2094–102.
- [48] Kim Y, Ta Q, Dinh H, Aum PK, Yeo I, Cho II W, Mho S. Cyclic stability of electrochemically embedded nanobeam V₂O₅ in polypyrrole films for Li battery cathodes. *J Electrochim Soc* 2011;158:A133–8.
- [49] Mahmoudian MR, Basirun WJ, Alias Y, Khorsand Zak A. Electrochemical characteristics of coated steel with poly(N-methyl pyrrole) synthesized in presence of ZnO nanoparticles. *Thin Solid Films* 2011;520:258–65.
- [50] Chaudhari S, Patil P. Use of poly(o-toluidine)/ZrO₂ nanocomposite coatings for the corrosion protection of mild steel. *J Appl Polym Sci* 2007;106:220–9.
- [51] Shallcross RC, D'Ambruoso GD, Korth BD, Hall HK, Zheng Z, Pyun J, Armstrong NR. Poly(3,4-ethylenedioxothiophene)-semiconductor nanoparticle composite thin films tethered to indium tin oxide substrates via electropolymerization. *J Am Chem Soc* 2007;129:11310–1.
- [52] Shallcross RC, D'Ambruoso GD, Pyun J, Armstrong NR. Photoelectrochemical processes in polymer-tethered CdSe nanocrystals. *J Am Chem Soc* 2010;132:2622–32.
- [53] Wei H, Yan X, Li Y, Wu S, Wang A, Wei S, Guo Z. Hybrid electrochromic fluorescent poly(DNTD)/CdSe@ZnS composite films. *J Phys Chem C* 2012;116:4500–10.
- [54] Nguyencong H, Elabbassi K, Gautier J, Chartier P. Oxygen reduction on oxide/polypyrrole composite electrodes: effect of doping anions. *Electrochim Acta* 2005;50:1369–76.
- [55] Janáky C, Kormányos A, Visy C. Magnetic hybrid modified electrodes, based on magnetite nanoparticle containing polyaniline and poly(3,4-ethylenedioxothiophene). *J Solid State Electrochim* 2011;15:2351–9.
- [56] Cong HN, de la Garza Guadarrama V, Gautier JL, Chartier P. Ni_xCo_{3-x}O₄ mixed valence oxide nanoparticles/polypyrrole composite electrodes for oxygen reduction. *J New Mater Electrochim Syst* 2002;40:35–40.
- [57] Herrasti P, Kulak AN, Bayvkina DV, de Léon CP, Zeckonyte J, Walsh FC. Electrodeposition of polypyrrole-titanate nanotube composites coatings and their corrosion resistance. *Electrochim Acta* 2011;56:1323–8.
- [58] Milliron D, Alivisatos A, Pitois C, Edder C, Frechet J. Electroactive surfactant designed to mediate electron transfer between CdSe nanocrystals and organic semiconductors. *Adv Mater* 2003;15:58–61.
- [59] Mitsumori M, Nakahodo T, Fujihara H. Synthesis of chiral hybrid nanotubes of magnetite nanoparticles and conducting polymers. *Nanoscale* 2012;4:117–9.
- [60] Janáky C, Visy C, Berkési O, Tombácz E. Conducting polymer-based electrode with magnetic behavior: electrochemical synthesis of poly(3-thiophene-acetic-acid)/magnetite nanocomposite thin layers. *J Phys Chem C* 2009;113:1352–8.
- [61] Granot E, Patolsky F, Willner I. Electrochemical assembly of a CdS semiconductor nanoparticle monolayer on surfaces: structural properties and photoelectrochemical applications. *J Phys Chem B* 2004;108:5875–81.
- [62] Yildiz HB, Tel-Vered R, Willner I. Solar cells with enhanced photocurrent efficiencies using oligoaniline-crosslinked Au/CdS nanoparticles arrays on electrodes. *Adv Funct Mater* 2008;18:3497–505.

- [63] Ovits O, Tel-Vered R, Baravik I, Wilner OI, Willner I. Photoelectrochemical cells based on bis-aniline-crosslinked CdS nanoparticle–carbon nanotube matrices associated with electrodes. *J Mater Chem* 2009;19:7650–65.
- [64] Roux S, Soler-Illia GJ, Demoustier-Champagne S, Audebert P, Sanchez C. Titania/polypyrrole hybrid nanocomposites built from in-situ generated organically functionalized nanoanatase building blocks. *Adv Mater* 2003;15:217–21.
- [65] Park Y, Taranekar P, Park JY, Baba A, Fulghum T, Ponnappati R, Advincula RC. Hybrid CdSe nanoparticle–carbazole dendron boxes: electropolymerization and energy-transfer mechanism shift. *Adv Funct Mater* 2008;18:2071–8.
- [66] Frau AF, Park Y, Pernites RB, Advincula RC. Nanocomposite p-n junction polycarbazole CdSe/TiO₂ thin films on ITO via electrochemical crosslinking. *Macromol Mater Eng* 2012;297:875–86.
- [67] Okpalugo TT, Papakonstantinou P, Murphy H, McLaughlin J, Brown NMD. High resolution XPS characterization of chemically functionalised MWCNTs and SWCNTs. *Carbon* 2005;43:153–61.
- [68] Chua CK, Pumera M. Covalent chemistry on graphene. *Chem Soc Rev* 2013;42:3222–33.
- [69] Oueiny C, Berlioz S, Perrin FX. Carbon nanotube–polyaniline composites. *Prog Polym Sci* 2013;39:707–48.
- [70] Santhosh P, Manesh K, Gopalan A, Lee K. Fabrication of a new polyaniline grafted multi-wall carbon nanotube modified electrode and its application for electrochemical detection of hydrogen peroxide. *Anal Chim Acta* 2006;575:32–8.
- [71] Zhu C, Zhai J, Wen D, Dong S. Graphene oxide/polypyrrole nanocomposites: one-step electrochemical doping, coating and synergistic effect for energy storage. *J Mater Chem* 2012;22:6300–6.
- [72] Nasybulin E, Cox M, Kymmissis I, Levon K. Electrochemical codeposition of poly[thieno(3,2-b)thiophene] and fullerene: an approach to a bulk heterojunction organic photovoltaic device. *Synth Met* 2012;162:10–7.
- [73] Kim SY, Lee KH, Chin BD, Yu JW. Network structure organic photovoltaic devices prepared by electrochemical copolymerization. *Sol Energy Mater Sol Cells* 2009;93:129–35.
- [74] Wampler WA, Wei C, Rajeshwar K. Electrocomposites of polypyrrole and carbon black. *J Electrochem Soc* 1994;141:L13–5.
- [75] Wampler WA, Wei C, Rajeshwar K. Composites of polypyrrole and carbon black. 2. Electrosynthesis, characterization and influence of carbon black characteristics. *Chem Mater* 1995;7:585–92.
- [76] Hu L, Tu J, Jiao S, Hou J, Zhu H, Fray DJ. In situ electrochemical polymerization of a nanorod-PANI-graphene composite in a reverse micelle electrolyte and its application in a supercapacitor. *Phys Chem Chem Phys* 2012;14:15652–6.
- [77] Österholm A, Lindfors T, Kauppila J, Damlin P, Kvarnström C. Electrochemical incorporation of graphene oxide into conducting polymer films. *Electrochim Acta* 2012;83:463–70.
- [78] Zhang L, Li C, Liu A, Shi G. Electrosynthesis of graphene oxide/polypyrene composite films and their applications for sensing organic vapors. *J Mater Chem* 2012;22:8438–43.
- [79] Scott CL, Zhao G, Pumera M. Stacked graphene nanofibers doped polypyrrole nanocomposites for electrochemical sensing. *Electrochim Commun* 2010;12:1788–91.
- [80] Liu A, Li C, Bai H, Shi G. Electrochemical deposition of polypyrrole/sulfonated graphene composite films. *J Phys Chem C* 2010;114:22783–9.
- [81] Si P, Chen HL, Kannan P, Kim DH. Selective and sensitive determination of dopamine by composites of polypyrrole and graphene modified electrodes. *Analyst* 2011;136:5134–8.
- [82] Guo D, Li H. Well-dispersed multi-walled carbon nanotube/polyaniline composite films. *J Solid State Electrochem* 2005;9:445–9.
- [83] Peng C, Jin J, Chen GZ. A comparative study on electrochemical co-deposition and capacitance of composite films of conducting polymers and carbon nanotubes. *Electrochim Acta* 2007;53:525–37.
- [84] Lota K, Khomenko V, Frackowiak E. Capacitance properties of poly(3,4-ethylenedioxythiophene)/carbon nanotubes composites. *J Phys Chem Solids* 2004;65:295–301.
- [85] Bhandari S, Deepa M, Srivastava AK, Lal C, Kant R. Poly(3,4-ethylenedioxythiophene) (PEDOT)-coated MWCNTs tethered to conducting substrates: facile electrochemistry and enhanced coloring efficiency. *Macromol Rapid Commun* 2008;29:1959–64.
- [86] Bhandari S, Deepa M, Srivastava AK, Joshi AG, Kant R. Poly(3,4-ethylenedioxythiophene)-multiwalled carbon nanotube composite films: structure-directed amplified electrochromic response and improved redox activity. *J Phys Chem B* 2009;113:9416–28.
- [87] Mousavi Z, Bobacka J, Lewenstam A, Ivaska A. Poly(3,4-ethylenedioxythiophene) (PEDOT) doped with carbon nanotubes as ion-to-electron transducer in polymer membrane-based potassium ion-selective electrodes. *J Electroanal Chem* 2009;633:246–52.
- [88] Luo X, Weaver CL, Zhou DD, Greenberg R, Cui XT. Highly stable carbon nanotube doped poly(3,4-ethylenedioxythiophene) for chronic neural stimulation. *Biomaterials* 2011;32:5551–7.
- [89] Chen G, Shaffer M, Coleby D, Dixon G, Zhou W, Fray DJ, Windle AH. Carbon nanotube and polypyrrole composites: coating and doping. *Adv Mater* 2000;12:522–6.
- [90] Hughes M, Chen G, Shaffer M, Fray DJ, Windle AH. Electrochemical capacitance of a nanoporous composite of carbon nanotubes and polypyrrole. *Chem Mater* 2002;14:1610–3.
- [91] Wang J, Musameh M. Carbon-nanotubes doped polypyrrole glucose biosensor. *Anal Chim Acta* 2005;539:209–13.
- [92] Zhang X, Zhang J, Liu Z. Conducting polymer/carbon nanotube composite films made by in situ electropolymerization using an ionic surfactant as the supporting electrolyte. *Carbon* 2005;43:2186–91.
- [93] Hughes M, Chen GZ, Shaffer MSP, Fray DJ, Windle AH. Controlling the nanostructure of electrochemically grown nanoporous composites of carbon nanotubes and conducting polymers. *Compos Sci Technol* 2004;64:2325–31.
- [94] Wei P, Tanabe H. Synergy effects between single-walled carbon nanotubes and polypyrrole on the electrocatalysis of their composites for the oxygen reduction reaction. *Carbon* 2011;49:4877–89.
- [95] Huang J, Li X, Xu J, Li H. Well-dispersed single-walled carbon nanotube/polyaniline composite films. *Carbon* 2003;41:2731–6.
- [96] Wei D, Kvarnstrom C, Lindfors T, Ivaska A. Electrochemical functionalization of single walled carbon nanotubes with polyaniline in ionic liquids. *Electrochim Commun* 2007;9:206–10.
- [97] Intelmann CM, Syritski V, Tsankov D, Hinrichs K, Rappich J. Ultrathin polypyrrole films on silicon substrates. *Electrochim Acta* 2008;53:4046–50.
- [98] Aydoğan Ş, Sağlam M, Türüt A. Current-voltage and capacitance-voltage characteristics of polypyrrole/p-InP structure. *Vacuum* 2005;77:269–74.
- [99] Wang X, Shi G, Liang Y. Low potential electropolymerization of thiophene at a copper oxide electrode. *Electrochim Commun* 1999;1:536–9.
- [100] Bahloul A, Nessark B, Chelali NE, Groult H, Mauger A, Julien CM. New composite cathode material for Zn/MnO₂ cells obtained by electro-deposition of polybithiophene on manganese dioxide particles. *Solid State Ionics* 2011;204–205:53–60.
- [101] Bahloul A, Nessark B, Habelhames F, Julien CM. Preparation and characterization of polybithiophene/β-MnO₂ composite electrode for oxygen reduction. *Ionics* 2010;17:239–46.
- [102] Idla K, Inganäs O, Strandberg M. Good adhesion between chemically oxidised titanium and electrochemically deposited polypyrrole. *Electrochim Acta* 2000;45:2121–30.
- [103] Cong HN, Sene C, Chartier P. Cadmium sulfide thickness effect on the photoresponse of the CdS spray/poly(3-methylthiophene) solid state junction. *Sol Energy Mater Sol Cells* 1993;29:209–19.
- [104] Cong HN, Dieng M, Sene C, Chartier P. Hybrid organic-inorganic solar cells: case of the all thin film PMeT(Y)/CdS(X) junctions. *Sol Energy Mater Sol Cells* 2000;63:23–35.
- [105] Dhawale DS, Dubal DP, Jamadade VS, Salunkhe RR, Joshi SS, Lokhande CD. Room temperature LPG sensor based on n-CdS/p-polyaniline heterojunction. *Sens Actuators B* 2010;145:205–10.
- [106] Chartier P, Cong HN, Sene C. Hybrid organic-inorganic photovoltaic junctions: case of the all thin-film CdSe/poly(3-methylthiophene) junction. *Sol Energy Mater Sol Cells* 1998;52:413–21.
- [107] Joshi SS, Gujar TP, Shinde VR, Lokhande CD. Fabrication of n-CdTe/p-polyaniline heterojunction-based room temperature LPG sensor. *Sens Actuators B* 2008;132:349–55.
- [108] Gamboa SA, Sebastian PJ, Mathew X, Nguyen-Cong H, Chartier P. A CdTe/PMeT photovoltaic structure formed by electrodeposition and processing. *Sol Energy Mater Sol Cells* 1999;59:115–24.
- [109] Patil SV, Deshmukh PR, Lokhande CD. Fabrication and liquefied petroleum gas (LPG) sensing performance of p-polyaniline/n-PbS heterojunction at room temperature. *Sens Actuators B* 2011;156:450–5.
- [110] Bereznev S, Konovalov I, Öpik A, Kois J, Mellikov E. Hybrid copper-indium disulfide/polypyrrole photovoltaic structures prepared by electrodeposition. *Sol Energy Mater Sol Cells* 2005;87:197–206.
- [111] Bereznev S, Kois J, Golovtsov I, Öpik A, Mellikov E. Electrodeposited (Cu-In-Se)/polypyrrole PV structures. *Thin Solid Films* 2006;511–512:425–9.

- [112] Cai L, Liu X, Wang L, Liu B. Iodine-free organic dye sensitized solar cells with *in situ* polymerized hole transporting material from alkoxy-substituted TriEDOT. *Polym Bull* 2011;68:1857–65.
- [113] Min HS, Park BY, Taherabadi L, Wang C, Yeh Y, Zaouk R, Madou MJ, Dunn B. Fabrication and properties of a carbon/polypyrrole three-dimensional microbattery. *J Power Sources* 2008;178:795–800.
- [114] Wang D, Li F, Zhao J, Ren W, Chen Z, Tan J, Wu ZS, Gentle I, Li GQ, Cheng HM. Fabrication of graphene/polyaniline composite paper via *in situ* anodic electropolymerization for high-performance flexible electrode. *ACS Nano* 2009;3:1745–52.
- [115] Chen K, Chen L, Chen Y, Bai H, Li L. Three-dimensional porous graphene-based composite materials: electrochemical synthesis and application. *J Mater Chem* 2012;22:20968–76.
- [116] Xue M, Li F, Zhu J, Song H, Zhang M, Cao T. Structure-based enhanced capacitance: *in situ* growth of highly ordered polyaniline nanorods on reduced graphene oxide patterns. *Adv Funct Mater* 2012;22:1284–90.
- [117] Davies A, Audette P, Farrow B, Hassan F, Chen Z, Choi JY, Yu A. Graphene-based flexible supercapacitors: pulse-electropolymerization of polypyrrole on free-standing graphene films. *J Phys Chem C* 2011;115:17612–20.
- [118] Zhang S, Shao Y, Liu J, Aksay IA, Lin Y. Graphene-polypyrrole nanocomposite as a highly efficient and low cost electrically switched ion exchanger for removing ClO_4^- from wastewater. *ACS Appl Mater Interfaces* 2011;3:3633–7.
- [119] Qu L, Liu J, Wang Z, Zhao Y, Cheng H, Hu C, Jiang L, Qu L. Three-dimensional graphene/polypyrrole hybrid electrochemical actuator. *Nanoscale* 2012;4:7563–8.
- [120] Song Y, Xu JL, Liu XX. Electrochemical anchoring of dual doping polypyrrole on graphene sheets partially exfoliated from graphite foil for high-performance supercapacitor electrode. *J Power Sources* 2014;249:48–58.
- [121] Lin Y, Cui X. Electrosynthesis, characterization, and application of novel hybrid materials based on carbon nanotube-polyaniline-nickel hexacyanoferrate nanocomposites. *J Mater Chem* 2006;16:585–92.
- [122] Zhang H, Cao G, Wang Z, Yang Y, Shi Z, Gu Z. Tube-covering-tube nanostructured polyaniline/carbon nanotube array composite electrode with high capacitance and superior rate performance as well as good cycling stability. *Electrochim Commun* 2008;10:1056–9.
- [123] Zhang H, Cao G, Wang W, Yuan K, Xu B, Zhang W, Cheng J, Yang Y. Influence of microstructure on the capacitive performance of polyaniline/carbon nanotube array composite electrodes. *Electrochim Acta* 2009;54:1153–9.
- [124] Chen Y, Gao H, Luo Y. Coaxial carbon nanotube–polythiophene core–shell nanowire for efficient hole transport in heterojunction photovoltaic device. *Appl Phys Lett* 2011;99:143309/1–3.
- [125] Xiao Y, Lin JV, Tai SY, Chou SW, Yue G, Wu J. Pulse electropolymerization of high performance PEDOT/MWCNT counter electrodes for Pt-free dye-sensitized solar cells. *J Mater Chem* 2012;22:19919–25.
- [126] Agui L, Penafaral C, Yanezsedeno P, Pingarron J. Poly-(3-methylthiophene)/carbon nanotubes hybrid composite-modified electrodes. *Electrochim Acta* 2007;52:7946–52.
- [127] Gao M, Huang S, Dai L, Wallace G, Gao R, Wang Z. Aligned coaxial nanowires of carbon nanotubes sheathed with conducting polymers. *Angew Chem Int Ed* 2000;112:3810–3.
- [128] Fang Y, Liu J, Yu DJ, Wicksted JP, Kalkan K, Topal CO, Flanigan BN, Wu J, Li J. Self-supported supercapacitor membranes: polypyrrole-coated carbon nanotube networks enabled by pulsed electrodeposition. *J Power Sources* 2010;195:674–9.
- [129] Hu Y, Zhao Y, Li Y, Li H, Shao H, Qu L. Defective super-long carbon nanotubes and polypyrrole composite for high-performance supercapacitor electrodes. *Electrochim Acta* 2012;66:279–86.
- [130] Baibarac M, Lira-Cantú M, Oró-Solé J, Casañ-Pastor N, Gomez-Romero P. Electrochemically functionalized carbon nanotubes and their application to rechargeable lithium batteries. *Small* 2006;2:1075–82.
- [131] Baibarac M, Lira-Cantú M, Oró Sol J, Baltog I, Casañ-Pastor N, Gomez-Romero P. Poly(N-vinyl carbazole) and carbon nanotubes based composites and their application to rechargeable lithium batteries. *Compos Sci Technol* 2007;67:2556–63.
- [132] Fan LZ, Hu YS, Maier J, Adelhelm P, Smarsly B, Antonietti M. High electroactivity of polyaniline in supercapacitors by using a hierarchically porous carbon monolith as a support. *Adv Funct Mater* 2007;17:3083–7.
- [133] Moghaddam RB, Pickup PG. Electrochemical impedance study of the polymerization of pyrrole on high surface area carbon electrodes. *Phys Chem Chem Phys* 2010;12:4733–41.
- [134] Baibarac M, Baltog I, Godon C, Lefrant S, Chauvet O. Covalent functionalization of single-walled carbon nanotubes by aniline electrochemical polymerization. *Carbon* 2004;42:3143–52.
- [135] Gupta V, Miura N. Polyaniline/single-wall carbon nanotube (PANI/SWCNT) composites for high performance supercapacitors. *Electrochim Acta* 2006;52:1721–6.
- [136] Niu Z, Luan P, Shao Q, Dong H, Li J, Chen J, Zhao D, Cai L, Zhou W, Chen X, Xie S. A “skeleton/skin” strategy for preparing ultrathin free-standing single-walled carbon nanotube/polyaniline films for high performance supercapacitor electrodes. *Energy Environ Sci* 2012;5:8726–33.
- [137] Ertas M, Walczak RM, Das RK, Rinzler AG, Reynolds JR. Supercapacitors based on polymeric dioxyppyrroles and single walled carbon nanotubes. *Chem Mater* 2012;24:433–43.
- [138] Patel RJ, Tighe TB, Ivanov IN, Hickner MA. Electro-optical properties of electropolymerized poly(3-hexylthiophene)/carbon nanotube composite thin films. *J Polym Sci B Polym Phys* 2011;49:1269–75.
- [139] Mukai K, Yamato K, Asaka K, Hata K, Oike H. Actuator of double layer film composed of carbon nanotubes and polypyrrroles. *Sens Actuators B* 2012;161:1010–7.
- [140] Baibarac M, Baltog I, Lefrant S. Raman spectroscopic evidence for interfacial interactions in poly(bithiophene)/single-walled carbon nanotube composites. *Carbon* 2009;47:1389–9138.
- [141] Lin YJ, Wang L, Chiu WY. Novel poly(3-methylthiophene)- TiO_2 hybrid materials for photovoltaic cells. *Thin Solid Films* 2006;511–512:199–202.
- [142] Ma L, Li Y, Yu X, Yang Q, Noh CH. Using room temperature ionic liquid to fabricate PEDOT/TiO₂ nanocomposite electrode-based electrochromic devices with enhanced longterm stability. *Sol Energy Mater Sol Cells* 2008;92:1253–9.
- [143] Latonen RM, Kvärnström C, Ivaska A. Electrochemical preparation of oligo(azulene) on nanoporous TiO₂ and characterization of the composite layer. *J Appl Electrochem* 2010;40:1583–91.
- [144] Wu CT, Chen PY, Chen JG, Suryanarayanan V, Ho KC. Detection of nicotine based on molecularly imprinted TiO₂-modified electrodes. *Anal Chim Acta* 2009;633:119–26.
- [145] Yoon JH, Kim DM, Yoon SS, Won MS, Shim YB. Comparison of solar cell performance of conducting polymer dyes with different functional groups. *J Power Sources* 2011;196:8874–80.
- [146] Cecchet F, Bignozzi CA, Paolucci F, Marcaccio M. Electrochemical and electrochromic investigation of poly-bithiophene films on a mesoporous TiO₂ surface. *Synth Met* 2006;156:27–31.
- [147] Hao Y, Yang M, Li W, Qiao X, Zhang L, Cai S. A photoelectrochemical solar cell based on ZnO/dye/polypyrrole film electrode as photoanode. *Sol Energy Mater Sol Cells* 2000;60:349–59.
- [148] O'Regan B, Grätzel M. A low-cost, high-efficiency solar cell based on dye-sensitized colloidal TiO₂ films. *Nature* 1991;353:737–40.
- [149] Xi D, Zhang H, Furst S, Chen B, Pei Q. Electrochemical synthesis and photovoltaic property of cadmium sulfide–polybithiophene interdigitated nanohybrid thin films. *J Phys Chem C* 2008;112:19765–9.
- [150] Elzanowska H, Miasek E, Birss VI. Electrochemical formation of Ir oxide/polyaniline composite films. *Electrochim Acta* 2008;53:2706–15.
- [151] Chen X, Li C, Grätzel M, Kostecki R, Mao SS. Nanomaterials for renewable energy production and storage. *Chem Soc Rev* 2012;41:7909–37.
- [152] De Tacconi NR, Chenthamarakshan C, Yogeeshwaran G, Watcharenwong A, de Zoysa R, Basit N, Rajeshwar K. Nanoporous TiO₂ and WO₃ films by anodization of titanium and tungsten substrates: influence of process variables on morphology and photoelectrochemical response. *J Phys Chem B* 2006;110:25347–55.
- [153] Roy P, Berger S, Schmuki P. TiO₂ nanotubes: synthesis and applications. *Angew Chem Int Ed* 2011;50:2904–39.
- [154] Xia X, Chao D, Qi X, Xiong Q, Zhang Y, Tu J, Zhang H, Fan HJ. Controllable growth of conducting polymers shell for constructing high-quality organic/inorganic core/shell nanostructures and their optical-electrochemical properties. *Nano Lett* 2013;13:4562–8.
- [155] Velazquez JM, Gaikwad AV, Rout TK, Rzayev J, Banerjee S. A substrate-integrated and scalable templated approach based on rusted steel for the fabrication of polypyrrole nanotube arrays. *ACS Appl Mater Interfaces* 2011;3:1238–44.
- [156] Mariani G, Wang Y, Wong PS, Lech A, Hung CH, Shapiro J, Prikhodko S, El-Kady M, Kaner RB, Huffaker DL. Three-dimensional core–shell hybrid solar cells via controlled *in situ* materials engineering. *Nano Lett* 2012;12:3581–6.
- [157] Babakhani B, Ivey DG. Improved capacitive behavior of electrochemically synthesized Mn oxide/PEDOT electrodes utilized as electrochemical capacitors. *Electrochim Acta* 2010;55:4014–24.

- [158] Bahloul A, Nessark B, Briot E, Groult H, Mauger A, Zaghib K, Julien CM. Polypyrrole-covered MnO₂ as electrode material for supercapacitor. *J Power Sources* 2013;240:267–72.
- [159] Xia XH, Tu JP, Zhang J, Wang XL, Zhang WK, Huang H. A highly porous NiO/polyaniline composite film prepared by combining chemical bath deposition and electro-polymerization and its electrochromic performance. *Nanotechnology* 2008;19:465701/1–7.
- [160] Xia XH, Tu JP, Zhang J, Huang XH, Wang XL, Zhang WK, Huang H. Multicolor and fast electrochromism of nanoporous NiO/poly(3,4-ethylenedioxythiophene) composite thin film. *Electrochim Commun* 2009;11:702–5.
- [161] Huang XH, Tu JP, Xia XH, Wang XL, Xiang JY, Zhang L. Porous NiO/poly(3,4-ethylenedioxythiophene) films as anode materials for lithium ion batteries. *J Power Sources* 2010;195:1207–10.
- [162] Nam HS, Kim KM, Kim SH, Kim BC, Wallace GG, Ko JM. Supercapacitive properties of polyaniline/hydrous RuO₂ composite electrode. *Polym Bull* 2011;68:553–60.
- [163] Concepción Arenas M, Hu H, Antonio del Río J, Sánchez A, Nicho ME. Electrical properties of porous silicon/polypyrrole heterojunctions. *Sol Energy Mater Sol Cells* 2006;90:2413–20.
- [164] Harraz FA, Salem MS, Sakka T, Ogata YH. Hybrid nanostructure of polypyrrole and porous silicon prepared by galvanostatic technique. *Electrochim Acta* 2008;53:3734–40.
- [165] Peng X, Huo K, Fu J, Zhang X, Gao B, Chu PK. Coaxial PANI/TiN/PANI nanotube arrays for high-performance supercapacitor electrodes. *Chem Commun* 2013;49:10172–4.
- [166] Li X, Teng W, Zhao Q, Wang L. Efficient visible light-induced photoelectrocatalytic degradation of rhodamine B by polyaniline-sensitized TiO₂ nanotube arrays. *J Nanopart Res* 2011;13:6813–20.
- [167] Su L, Gan YX. Experimental study on synthesizing TiO₂ nanotube/polyaniline (PANI) nanocomposites and their thermoelectric and photosensitive property characterization. *Composites B* 2012;43:170–82.
- [168] Cai G, Tu J, Zhou D, Zhang J, Xiong Q, Zhao X, Guo Z. Multicolor electrochromic film based on TiO₂@polyaniline core/shell nanorod array. *J Phys Chem C* 2013;117:15967–75.
- [169] Yu M, Zeng Y, Zhang C, Lu X, Zeng C, Yao C, Yang Y, Tong Y. Titanium dioxide@polypyrrole core-shell nanowires for all solid-state flexible supercapacitors. *Nanoscale* 2013;5:10806–10.
- [170] Shi H, Zhao G, Liu M, Zhu Z. A novel photoelectrochemical sensor based on molecularly imprinted polymer modified TiO₂ nanotubes and its highly selective detection of 2,4-dichlorophenoxyacetic acid. *Electrochim Commun* 2011;13:1404–7.
- [171] Kowalski D, Schmuki P. Polypyrrole self-organized nanopore arrays formed by controlled electropolymerization in TiO₂ nanotube template. *Chem Commun* 2010;46:8585–7.
- [172] Kowalski D, Tighineanu A, Schmuki P. Polymer nanowires or nanopores? Site selective filling of titania nanotubes with polypyrrole. *J Mater Chem* 2011;21:17909–15.
- [173] Jia Y, Xiao P, He H, Yao J, Liu F, Wang Z, Li Y. Photoelectrochemical properties of polypyrrole/TiO₂ nanotube arrays nanocomposite under visible light. *Appl Surf Sci* 2012;258:6627–31.
- [174] Dziewoński PM, Grzeszczuk M. Towards TiO₂-conducting polymer hybrid materials for lithium ion batteries. *Electrochim Acta* 2010;55:3336–47.
- [175] Kowalski D, Schmuki P. Advanced geometries of PEDOT formed in titania nanotubes. *ChemPhysChem* 2012;13:3790–3.
- [176] Kowalski D, Albu SP, Schmuki P. Current dependent formation of PEDOT inverse nanotube arrays. *RSC Adv* 2013;3:2154–7.
- [177] Wang D, Liu Y, Wang C, Zhou F, Liu W. Highly flexible coaxial nanohybrids made from porous TiO₂ nanotubes. *ACS Nano* 2009;3:1249–57.
- [178] Pang Y, Li X, Shi G, Wang F, Jin L. Electrochromic properties of poly(3-chlorothiophene) film electrodeposited on a nanoporous TiO₂ surface via a room temperature ionic liquid and its application in an electrochromic device. *Thin Solid Films* 2008;516:6512–6.
- [179] Liang H, Li X. Visible-induced photocatalytic reactivity of polymer-sensitized titania nanotube films. *Appl Catal B Environ* 2009;86:8–17.
- [180] Janáky C, de Tacconi NR, Chanmanee W, Rajeshwar K. Electrodeposited polyaniline in a nanoporous WO₃ matrix: an organic/inorganic hybrid exhibiting both p- and n-type photoelectrochemical activity. *J Phys Chem C* 2012;116:4234–42.
- [181] Döbelin M, Tena-Zaera R, Carrasco PM, Sarasua JR, Cabañero G, Mecerreyres D. Electrochemical synthesis of poly(3,4-ethylenedioxythiophene) nanotube arrays using ZnO templates. *J Polym Sci A Polym Chem* 2010;48:4648–53.
- [182] Wang ZL, Guo R, Li GR, Lu HL, Liu ZQ, Xiao FM, Zhang M, Tong YX. Polyaniline nanotube arrays as high-performance flexible electrodes for electrochemical energy storage devices. *J Mater Chem* 2012;22:2401–4.
- [183] Tang Q, Lin L, Zhao X, Huang K, Wu J. p-n heterojunction on ordered ZnO nanowires/polyaniline microrods double array. *Langmuir* 2012;28:3972–8.
- [184] Hao Y, Pei J, Wei Y, Cao Y, Jiao S, Zhu F, Li J, Xu D. Efficient semiconductor-sensitized solar cells based on poly(3-hexylthiophene)@CdSe@ZnO core-shell nanorod arrays. *J Phys Chem C* 2010;114:8622–5.
- [185] Sun B, Hao Y, Guo F, Cao Y, Zhang Y, Li Y, Xu D. Fabrication of poly(3-hexylthiophene)/CdS/ZnO core-shell nanotube array for semiconductor-sensitized solar cell. *J Phys Chem C* 2012;116:1395–400.
- [186] Mohan Kumar G, Raman K, Kawakita J, Ilanchezhiyan P, Jayavel R. Fabrication of polypyrrole/ZnCoO nanohybrid systems for solar cell applications. *Dalton Trans* 2010;39:8325–30.
- [187] Kateb M, Ahmadi V, Mohseni M. Fast switching and high contrast electrochromic device based on PEDOT nanotube grown on ZnO nanowires. *Sol Energy Mater Sol Cells* 2013;112:57–64.
- [188] Janáky C, de Tacconi N, Chanmanee W, Rajeshwar K. Conjugated polymers and oxide nanoarchitectures into intimate contact: light induced electrodeposition of polypyrrole and polyaniline on nanoporous WO₃ or TiO₂. *J Phys Chem C* 2012;116:19145–55.
- [189] Feng W, Wan AS, Garfunkel E. Interfacial bonding and morphological control of electropolymerized polythiophene films on ZnO. *J Phys Chem C* 2013;117:9852–63.
- [190] Sakmeche N, Aeyach S, Aaron J, Jouini M, Lacroix J, Lacaze P. Improvement of the electrosynthesis and physicochemical properties of poly[3,4-ethylenedioxythiophene] using a sodium dodecyl sulfate micellar aqueous medium. *Langmuir* 1999;15:2566–74.
- [191] Zhang Z, Yuan Y, Liang L, Cheng Y, Xu H, Shi G, Jin L. Preparation and photoelectrochemical properties of a hybrid electrode composed of polypyrrole encapsulated in highly ordered titanium dioxide nanotube array. *Thin Solid Films* 2008;516:8663–7.
- [192] Xie Y, Du H. Electrochemical capacitance performance of polypyrrole-titania nanotube hybrid. *J Solid State Electrochem* 2012;16:2683–9.
- [193] Debiemme-Chouvy C, Tran TTM. An insight into the overoxidation of polypyrrole materials. *Electrochim Commun* 2008;10:947–50.
- [194] Tóth PS, Janáky C, Berkesi O, Tamm T, Visy C. On the unexpected cation exchange behavior, caused by covalent bond formation between PEDOT and Cl[−] ions: extending the conception for the polymer-dopant interactions. *J Phys Chem B* 2012;116:5491–500.
- [195] Janáky C, Bencsik G, Rácz A, Visy C, de Tacconi NR, Chanmanee W, Rajeshwar K. Electrochemical grafting of poly(3,4-ethylenedioxythiophene) into a titanium dioxide nanotube host network. *Langmuir* 2010;26:13697–702.
- [196] Bella F, Bongiovanni R. Photoinduced polymerization: an innovative, powerful and environmentally friendly technique for the preparation of polymer electrolytes for dye-sensitized solar cells. *J Photochem Photobiol C* 2013;16:1–21.
- [197] Noufi R, Frank AJ, Nozil AJ. Stabilization of n-type silicon photoelectrodes to surface oxidation in aqueous electrolyte solution and mediation of oxidation reaction by surface attached organic conducting polymer. *J Am Chem Soc* 1981;103:1849–50.
- [198] Fan FRF, Wheeler BL, Bard AJ, Noufi R. Semiconductor electrodes: XXXIX. Techniques for stabilization of n-silicon electrodes in aqueous solution photoelectrochemical cells. *J Electrochim Soc* 1981;128:2042–5.
- [199] Skotheim T, Lundstrom I, Prejza J. Stabilization of n-Si photoanodes to surface corrosion in aqueous electrolyte with a thin film of polypyrrole. *J Electrochim Soc* 1981;128:1625–6.
- [200] Noufi R, Tench D, Warren LF. Protection of n-GaAs photoanodes with photoelectrochemically generated polypyrrole films. *J Electrochim Soc* 1980;127:2310–1.
- [201] Frank A, Honda K. Oxygen and hydrogen generation from water on polymer-protected CdS photoanodes. *J Electroanal Chem* 1983;150:673–8.
- [202] Frank A, Glenis S, Nelson A. Conductive polymer-semiconductor junction: characterization of poly(3-methylthiophene)-cadmium sulfide based photoelectrochemical and photovoltaic cells. *J Phys Chem* 1989;3818–25.
- [203] Horowitz G, Tourillon G, Garnier F. Protection of n-GaAs photoanodes by photoelectrochemical grafting of poly(3-methylthiophene) and poly(3,4-dimethylthiophene) films. *J Electrochim Soc* 1984;131:151–6.

- [204] Horowitz G, Garnier F. Polythiophene-GaAs p-n heterojunction solar cells. *Sol Energy Mater* 1986;13:47–55.
- [205] Kamat PV, Basheer R, Fox MA. Polymer-modified electrodes. Electrochemical and photoelectrochemical polymerization of 1-vinylpyrene. *Macromolecules* 1985;18:1367–71.
- [206] Bereznay S, Konovalov I, Öpik A, Kojs J. Hybrid CuInS₂/polypyrrole and CuInS₂/poly(3,4-ethylenedioxythiophene) photovoltaic structures. *Synth Met* 2005;152:81–4.
- [207] Okano M, Itoh K, Fujishima A, Honda K. Generation of organic conducting patterns on semiconductors by photoelectrochemical polymerization of pyrrole. *Chem Lett* 1986;469–72.
- [208] Okano M, Itoh K, Fujishima A, Honda K. Photoelectrochemical polymerization of pyrrole on TiO₂ and its application to conducting pattern generation. *J Electrochem Soc* 1987;134:837–41.
- [209] Okano M, Kikuchi E, Itoh K, Fujishima A. Photoelectrochemical polymerization of pyrrole on ZnO and its application to conducting pattern generation. *J Electrochem Soc* 1988;135:1641–5.
- [210] Di Franco F, Bocchetta P, Santamaria M, Di Quarto F. Light induced electropolymerization of poly(3,4-ethylenedioxythiophene) on niobium oxide. *Electrochim Acta* 2010;56:737–44.
- [211] Di Quarto F, Figà V, Bocchetta P, Santamaria M. Photoelectrochemical synthesis of polypyrrrole on anodic Ta₂O₅ films. *Electrochim Solid State Lett* 2007;10:H305–8.
- [212] Yang Z, Ni X. Photovoltaic hybrid films with polythiophene growing on monoclinic WO₃ semiconductor substrates. *Langmuir* 2012;28:4829–34.
- [213] Yildiz A, Sobczynski A, Bard A, Campion A, Fox MA, Mallouk TE, Webber SE, White JM. Sensitized polypyrrrole-coated semiconducting powders as materials in photosystems for hydrogen generation. *Langmuir* 1989;5:148–9.
- [214] Fox MA, Worthen KL. Comparison of the physical properties of polypyrrrole produced by anodic oxidation and by photoelectrochemical activation of TiO₂. *Chem Mater* 1991;3:253–7.
- [215] Jarkov A, Bereznay S, Volobujeva O, Traksmaa R, Tverjanovich A, Öpik A, Mellikov E. Photo-assisted electrodeposition of polypyrrrole back contact to CdS/CdTe solar cell structures. *Thin Solid Films* 2013;535:198–201.
- [216] Ramanavicius A, Karabanovas V, Ramanaviciene A, Rotomskis R. Stabilization of (CdSe)ZnS quantum dots with polypyrrrole formed by UV/Vis irradiation initiated polymerization. *J Nanosci Nanotechnol* 2009;9:1909–15.
- [217] Goubard F, Aubert PH, Boukerma K, Pauthe E, Chevrot C. Elaboration of nanohybrid materials by photopolymerisation of 3,4-ethylenedioxythiophene on TiO₂. *Chem Commun* 2008;3139–41.
- [218] Weng Z, Ni X. Oxidative polymerization of pyrrole photocatalyzed by TiO₂ nanoparticles and interactions in the composites. *J Appl Polym Sci* 2008;110:109–16.
- [219] Zhang W, Cheng Y, Yin X, Liu B. Solid-state dye-sensitized solar cells with conjugated polymers as hole-transporting materials. *Macromol Chem Phys* 2011;212:15–23.
- [220] Heo JH, Im SH, Noh JH, Mandal TN, Lim CS, Chang JA, Lee YH, Kim HJ, Sarkar A, Nazeeruddin MK, Grätzel M, Seok S. Efficient inorganic–organic hybrid heterojunction solar cells containing perovskite compound and polymeric hole conductors. *Nat Photonics* 2013;7:486–91.
- [221] Wang J, Ni X. Photoresponsive polypyrrrole-TiO₂ nanoparticles film fabricated by a novel surface initiated polymerization. *Solid State Commun* 2008;146:239–44.
- [222] Strandwitz NC, Nonoguchi Y, Boettcher SW, Stucky GD. In situ photopolymerization of pyrrole in mesoporous TiO₂. *Langmuir* 2010;26:5319–22.
- [223] Takagi S, Makuta S, Veamatahau A, Otsuka Y, Tachibana Y. Organic/inorganic hybrid electrochromic devices based on photoelectrochemically formed polypyrrrole/TiO₂ nanohybrid films. *J Mater Chem* 2012;22:22181–9.
- [224] Dehadt J, Beouch L, Peralta S, Plesse C, Aubert PH, Chevrot C, Goubard F. Facile route to prepare film of poly(3,4-ethylene dioxythiophene)-TiO₂ nanohybrid for solar cell application. *Thin Solid Films* 2011;519:1876–81.
- [225] Liu P, Yang HX, Ai XP, Li GR, Gao XP. A solar rechargeable battery based on polymeric charge storage electrodes. *Electrochim Commun* 2012;16:69–72.
- [226] Otsuka Y, Okamoto Y, Akiyama HY, Umekita K, Tachibana Y, Kubabata S. Photoinduced formation of polythiophene/TiO₂ nanohybrid heterojunction films for solar cell applications. *J Phys Chem C* 2008;112:4767–75.
- [227] Sidorov D, Smertenko P, Piryatinski Y, Yoshida T, Pud A. Electrochemically assembled planar hybrid poly(3-methylthiophene)/ZnO nanostructured composites. *Electrochim Acta* 2012;81:83–9.
- [228] Senadeera R, Fukuri N, Saito Y, Kitamura T, Wada Y, Yanagida S. Volatile solvent-free solid-state polymer-sensitized TiO₂ solar cells with poly(3,4-ethylenedioxythiophene) as a hole-transporting medium. *Chem Commun* 2005;2259–61.
- [229] Rajeshwar K, Osugi ME, Chanmanee W, Chenthamarakshan CR, Zanoni MVB, Kajitivichyanukul P, Krishnan-Ayer R. Heterogeneous photocatalytic treatment of organic dyes in air and aqueous media. *J Photochem Photobiol C* 2008;9:171–92.
- [230] Manseki K, Jarernboon W, Youhai Y, Jiang KJ, Suzuki K, Masaki N, Kim Y, Xia J, Yanagida S. Solid-state dye-sensitized solar cells fabricated by coupling photoelectrochemically deposited poly(3,4-ethylenedioxythiophene) (PEDOT) with silver-paint on cathode. *Chem Commun* 2011;47:3120.
- [231] Murakoshi K, Kogure R, Wada Y, Yanagida S. Solid state dye-sensitized TiO₂ solar cell with polypyrrrole as hole transport layer. *Chem Lett* 1997;471–2.
- [232] Murakoshi K, Kogure R, Wada Y, Yanagida S. Fabrication of solid-state dye-sensitized TiO₂ solar cells combined with polypyrrrole. *Sol Energy Mater Sol Cells* 1998;55:113–25.
- [233] Saito Y, Azuchi T, Kitamura T, Hasegawa Y, Wada Y, Yanagida S. Photo-sensitizing ruthenium complexes for solid state dye solar cells in combination with conducting polymers as hole conductors. *Coord Chem Rev* 2004;248:1469–78.
- [234] Mozer AJ, Wada Y, Jiang KJ, Masaki N, Yanagida S, Mori SN. Efficient dye-sensitized solar cells based on 2-thiophen-2-yl-vinyl-conjugated ruthenium photosensitizer and a conjugated polymer hole conductor. *Appl Phys Lett* 2006;89, 043509/1–3.
- [235] Caramori S, Cazzanti S, Marchini L, Argazzi R, Bignozzi CA, Martineau D, Gros PC, Beley M. Dye-sensitized solar cells based on PEDOT as a hole conductive medium. *Inorg Chim Acta* 2008;361:627–34.
- [236] Kim HS, Wamser CC. Photoelectropolymerization of aniline in a dye-sensitized solar cell. *Photochem Photobiol Sci* 2006;5:955–60.
- [237] Saito Y, Fukuri N, Sanadeera R, Kitamura T, Wada Y, Yanagida S. Solid state dye sensitized solar cells using in situ polymerized PEDOTs as hole conductor. *Electrochim Commun* 2004;6:71–4.
- [238] Yanagida S, Yu Y, Manseki K. Iodine/iodide-free dye-sensitized solar cells. *Acc Chem Res* 2009;42:1827–38.
- [239] Song IY, Park SH, Lim J, Kwon YS, Park T. A novel hole transport material for iodine-free solid state dye-sensitized solar cells. *Chem Commun* 2011;47:10395–7.
- [240] Liu X, Zhang W, Uchida S, Cai L, Liu B, Ramakrishna S. An efficient organic-dye-sensitized solar cell with in situ polymerized poly(3,4-ethylenedioxythiophene) as a hole-transporting material. *Adv Mater* 2010;22:E150–5.
- [241] Janáky C, Chanmanee W, Rajeshwar K. Mechanistic aspects of photoelectrochemical polymerization of polypyrrrole on a TiO₂ nanotube array. *Electrochim Acta* 2014;122:303–9.
- [242] Fonseca L, Rinaldi A, Rubira A, Cotica L, Medeiros S, Paesano A, Santos IA, Girotto EM. Structural, magnetic, and electrochemical properties of poly(o-anisidine)/maghemite thin films. *Mater Chem Phys* 2006;97:252–5.
- [243] Prakash GKS, Suresh P, Viva F, Olah GA. Novel single step electrochemical route to γ -MnO₂ nanoparticle-coated polyaniline nanofibers: thermal stability and formic acid oxidation on the resulting nanocomposites. *J Power Sources* 2008;181:79–84.
- [244] Sun LJ, Liu XX. Electrodepositions and capacitive properties of hybrid films of polyaniline and manganese dioxide with fibrous morphologies. *Eur Polym J* 2008;44:219–24.
- [245] Sharma RK, Rastogi AC, Desu SB. Manganese oxide embedded polypyrrrole nanocomposites for electrochemical supercapacitor. *Electrochim Acta* 2008;53:7690–5.
- [246] Zou W, Wang W, He B, Sun M, Yin Y. Supercapacitive properties of hybrid films of manganese dioxide and polyaniline based on active carbon in organic electrolyte. *J Power Sources* 2010;195:7489–93.
- [247] Liu R, Duay JW, Lee SB. Electrochemical formation mechanism for the controlled synthesis of heterogeneous MnO₂/poly(3,4-ethylenedioxythiophene) nanowires. *ACS Nano* 2011;5:5608–19.
- [248] Duay J, Gillette E, Liu R, Lee SB. Highly flexible pseudocapacitor based on freestanding heterogeneous MnO₂/conductive polymer nanowire arrays. *Phys Chem Chem Phys* 2012;14:3329–37.
- [249] Liu XX, Bian LJ, Zhang L, Zhang LJ. Composite films of polyaniline and molybdenum oxide formed by electrodeposition in aqueous media. *J Solid State Electrochem* 2007;11:1279–86.

- [250] Peng X, Li W, Liu X, Hua P. Electrodeposition of NiO_x/PANI composite film and its catalytic properties towards electrooxidations of polyhydroxyl compounds. *J Appl Polym Sci* 2007;105:2260–4.
- [251] Peng XY, Liu XX, Hua PJ, Diamond D, Lau KT. Electrochemical codeposition of nickel oxide and polyaniline. *J Solid State Electrochem* 2009;14:1–7.
- [252] Ehsani A, Mahjani MG, Jafarian M, Naeemy A. Electrosynthesis of polypyrrole composite film and electrocatalytic oxidation of ethanol. *Electrochim Acta* 2012;71:128–33.
- [253] Shen PK, Huang HT, Tseung ACC. A study of tungsten trioxide and polyaniline composite films. *J Electrochem Soc* 1992;139:1840–5.
- [254] Zou BX, Liang Y, Liu XX, Diamond D, Lau KT. Electrodeposition and pseudocapacitive properties of tungsten oxide/polyaniline composite. *J Power Sources* 2011;196:4842–8.
- [255] Hepel M, Seymour E, Yogeve D, Fendler JH. Electrochemical quartz crystal microbalance monitoring of cadmium sulfide generation in polypyrrole and polypyrrole-poly(styrenesulfonate) thin films. *Chem Mater* 1992;4:209–16.
- [256] Refczynska M, Mieczkowski J, Skompska M. Synthesis, characterization and photoelectrochemical properties of poly(3,4-dioctyloxythiophene)-CdS hybrid electrodes. *Electrochim Acta* 2008;53:2984–93.
- [257] Armel V, Winther-Jensen O, Kerr R, MacFarlane DR, Winther-Jensen B. Designed electrodeposition of nanoparticles inside conducting polymers. *J Mater Chem* 2012;22:19767–73.
- [258] Guascito M, Boffi P, Malitesta C. Conducting polymer electrodes modified by metallic species for electrocatalytic purposes: spectroscopic and microscopic characterization. *Mater Chem Phys* 1996;44:17–24.
- [259] Cioffi N, Torsi L, Losito I, Di Franco C, De Bari I, Chiavarone L, Scamarcio G, Tsakova V, Sabbatini L, Zamboni PG. Electrosynthesis and analytical characterisation of polypyrrole thin films modified with copper nanoparticles. *J Mater Chem* 2001;11:1434–40.
- [260] Xue T, Loo LS, Wang X, Kyu Kwak S, Lee JM. Electrodeposition of mesoporous bilayers of polyaniline supported Cu_2O semiconductor films from lyotropic liquid crystalline phase. *Chem Eng Sci* 2012;80:452–9.
- [261] Andreoli E, Annibaldi V, Rooney DA, Breslin CB. Electrochemical fabrication of copper-based hybrid microstructures and mechanism of formation of related hierarchical structures on polypyrrole films. *J Phys Chem C* 2011;115:20076–83.
- [262] Du Z, Zhang S, Jiang T, Wu X, Zhang L, Fang H. Facile synthesis of SnO_2 nanocrystals coated conducting polymer nanowires for enhanced lithium storage. *J Power Sources* 2012;219:199–203.
- [263] Liu R, Duay J, Lane T, Lee SB. Synthesis and characterization of $\text{RuO}_2/\text{poly}(3,4\text{-ethylenedioxythiophene})$ composite nanotubes for supercapacitors. *Phys Chem Chem Phys* 2010;12:4273–84.
- [264] Zhao D, Guo X, Gao Y, Gao F. An electrochemical capacitor electrode based on porous carbon spheres hybridized with polyaniline and nanoscale ruthenium oxide. *ACS Appl Mater Interfaces* 2012;4:5583–9.
- [265] Li X, Gan W, Zheng F, Li L, Zhu N, Huang X. Preparation and electrochemical properties of $\text{RuO}_2/\text{polyaniline}$ electrodes for supercapacitors. *Synth Met* 2012;162:953–7.
- [266] Prasad K, Miura N. Polyaniline- MnO_2 composite electrode for high energy density electrochemical capacitor. *Electrochim Solid-State Lett* 2004;7:A425–8.
- [267] Rios EC, Correa AA, Cristovan FH, Pocrifka LA, Rosario AV. Poly(3,4-ethylenedioxythiophene)/ MnO_2 composite electrodes for electrochemical capacitors. *Solid State Sci* 2011;13:1978–83.
- [268] Rios EC, Rosario AV, Mello RMQ, Micaroni L. Poly(3-methylthiophene)/ MnO_2 composite electrodes as electrochemical capacitors. *J Power Sources* 2007;163:1137–42.
- [269] Liu FJ. Electrodeposition of manganese dioxide in three-dimensional poly(3,4-ethylenedioxythiophene)-poly(styrene sulfonic acid)-polyaniline for supercapacitor. *J Power Sources* 2008;182:383–8.
- [270] Tang P, Zhao Y, Xu C. Step-by-step assembled poly (3,4-ethylenedioxythiophene)/manganese dioxide composite electrodes: tuning the structure for high electrochemical performance. *Electrochim Acta* 2013;89:300–9.
- [271] Lu SY, Lin IH. Characterization of polypyrrole-CdSe/CdTe nanocomposite films prepared with an all electrochemical deposition process. *J Phys Chem B* 2003;107:6974–8.
- [272] Lee S, Cho MS, Lee H, Nam JD, Lee Y. A facile synthetic route for well defined multilayer films of graphene and PEDOT via an electrochemical method. *J Mater Chem* 2012;22:1899–903.
- [273] Tang Y, Wu N, Luo S, Liu C, Wang K, Chen L. One-step electrodeposition to layer-by-layer graphene-conducting-polymer hybrid films. *Macromol Rapid Commun* 2012;33:1780–6.
- [274] Huynh WU, Dittmer JJ, Alivisatos P. Hybrid nanorod-polymer solar cells. *Science* 2002;295:2425–7.
- [275] Xu T, Qiao Q. Conjugated polymer-inorganic semiconductor hybrid solar cells. *Energy Environ Sci* 2011;4:2700–20.
- [276] Zhao L, Lin Z. Crafting semiconductor organic-inorganic nanocomposites via placing conjugated polymers in intimate contact with nanocrystals for hybrid solar cells. *Adv Mater* 2012;24:4353–68.
- [277] Nogueira AF, Longo C, De Paoli MA. Polymers in dye sensitized solar cells: overview and perspectives. *Coord Chem Rev* 2004;248:1455–68.
- [278] Liu X, Cheng Y, Wang L, Cai L, Liu B. Light controlled assembling of iodine-free dyesensitized solar cells with poly(3,4-ethylenedioxythiophene) as a hole conductor reaching 7.1% efficiency. *Phys Chem Chem Phys* 2012;14:7098–103.
- [279] Cells SDS, Burschka J, Dualah E, Kessler F, Baranoff E, Yi C, Nazeerudin MK, Grätzel M. Tris(2-(1H-pyrazol-1-yl)pyridine)cobalt(III) as p-type dopant for organic semiconductors and its application in highly efficient solid-state dye-sensitized solar cells. *J Am Chem Soc* 2011;133:18042–5.
- [280] Im SH, Lim CS, Chang JA, Lee YH, Maiti N, Kim HJ, Nazeerudin MK, Grätzel M, Seok S. Toward interaction of sensitizer and functional moieties in hole-transporting materials for efficient semiconductor-sensitized solar cells. *Nano Lett* 2011;11:4789–93.
- [281] Kamat P. Quantum dot solar cells. The next big thing in photovoltaics. *J Phys Chem Lett* 2013;4:908–18.
- [282] Burschka J, Pellet N, Moon S-J, Humphry-Baker R, Gao P, Nazeeruddin MK, Grätzel M. Sequential deposition as a route to high-performance perovskite-sensitized solar cells. *Nature* 2013;499:316–9.
- [283] Park NG. Organometal perovskite light absorbers toward a 20% efficiency low-cost solid-state mesoscopic solar cell. *J Phys Chem Lett* 2013;4:2423–9.
- [284] Bi D, Yang L, Boschloo G, Hagfeldt A, Johansson EMJ. Effect of different hole transport materials on recombination in $\text{CH}_3\text{NH}_3\text{PbI}_3$ perovskite-sensitized mesoscopic solar cells. *J Phys Chem Lett* 2013;4:1532–6.
- [285] Lee W, Roh SJ, Hyung KH, Park J, Lee SH, Han SH. Photoelectrochemically polymerized polythiophene layers on ruthenium photosensitizers in dye-sensitized solar cells and their beneficial effects. *Sol Energy* 2009;83:690–5.
- [286] Lim I, Yoon SJ, Lee W, Nah YC, Shrestha NK, Ahn H, Han SH. Interfacially treated dye-sensitized solar cell with in situ photopolymerized iodine doped polythiophene. *ACS Appl Mater Interfaces* 2012;4:4838–41.
- [287] Zhang J, Li X, Guo W, Hreid T, Hou J, Su H, Yuan Z. Electropolymerization of a poly(3,4-ethylenedioxythiophene) and functionalized, multi-walled, carbon nanotubes counter electrode for dye-sensitized solar cells and characterization of its performance. *Electrochim Acta* 2011;56:3147–52.
- [288] Guan G, Yang Z, Qin L, Sun X, Zhang Z, Ren J, Peng H. Oriented PEDOT:PSS on aligned carbon nanotubes for efficient dye-sensitized solar cells. *J Mater Chem A* 2013;1:13268–73.
- [289] Yue G, Wu J, Xiao Y, Lin J, Huang M, Lan Z, Fan L. Functionalized graphene/poly(3,4-ethylenedioxythiophene):polystyrene-sulfonate as counter electrode catalyst for dye-sensitized solar cells. *Energy* 2013;54:315–21.
- [290] McGehee MD. Nanostructured organic-inorganic hybrid solar cells. *MRS Bull* 2009;34:95–100.
- [291] Grant CD, Schwartzberg AM, Smestad GP, Kowalik J, Tolbert LM, Zhang JZ. Characterization of nanocrystalline and thin film TiO_2 solar cells with poly (3-undecyl-2,2-bithiophene) as a sensitizer and hole conductor. *J Electroanal Chem* 2002;522:40–8.
- [292] Coakley KM, Liu Y, McGehee MD, Frindell KL, Stucky GD. Infiltrating semiconducting polymers into self-assembled mesoporous titania films for photovoltaic applications. *Adv Funct Mater* 2003;13:301–6.
- [293] Olson DC, Lee YJ, White MS, Kopidakis N, Shaheen SE, Ginley DS, Voigt JA, Hsu JWP. Effect of polymer processing on the performance of poly(3-hexylthiophene)/ ZnO nanorod photovoltaic devices. *J Phys Chem C* 2007;111:16640–5.
- [294] Tepavcevic S, Darling SB, Dimitrijevic NM, Rajh T, Sibener SJ. Improved hybrid solar cells via in situ UV polymerization. *Small* 2009;5:1776–83.

- [295] Atienzar P, Ishwara T, Horie M, Durrant JR, Nelson J. Hybrid polymer–metal oxide solar cells by *in situ* chemical polymerization. *J Mater Chem* 2009;19:5377–80.
- [296] Xia J, Masaki N, Lira-Cantu M, Kim Y, Jiang K, Yanagida S. Influence of doped anions on poly(3,4-ethylenedioxothiophene) as hole conductors for iodine-free solid-state dye-sensitized solar cells. *J Am Chem Soc* 2008;130:1258–63.
- [297] Xia J, Masaki N, Lira-Cantu M, Kim Y, Jiang K, Yanagida S. Effect of doping anions' structures on poly(3,4-ethylenedioxothiophene) as hole conductors in solid-state dye-sensitized solar cells. *J Phys Chem C* 2008;112:11569–74.
- [298] Kim Y, Sung YE, Xia JB, Lira-Cantu M, Masaki N, Yanagida S. Solid-state dye-sensitized TiO_2 solar cells using poly(3,4-ethylenedioxothiophene) as substitutes of iodine/iodide electrolytes and noble metal catalysts on FTO counter electrodes. *J Photochem Photobiol A* 2008;193:77–80.
- [299] Yang L, Zhang J, Shen Y, Park B, Bi D, Haggman L, Johansson EMJ, Boschloo G, Hagfeldt A, Vlachopoulos N, Snedden A, Kloot L, Jarboui A, Chams A, Perruchot C, Jouini M. New approach for preparation of efficient solid-state dye-sensitized solar cells by photoelectrochemical polymerization in aqueous micellar solution. *J Phys Chem Lett* 2013;4:4026–31.
- [300] Mozer AJ, Panda DK, Gambhir S, Winther-Jensen B, Wallace GG. Microsecond dye regeneration kinetics in efficient solid state dye-sensitized solar cells using a photoelectrochemically deposited PEDOT hole conductor. *J Am Chem Soc* 2010;132:9543–5.
- [301] Snook GA, Kao P, Best AS. Conducting-polymer-based supercapacitor devices and electrodes. *J Power Sources* 2011;196:1–12.
- [302] Cong HP, Ren XC, Wang P, Yu SH. Flexible graphene–polyaniline composite paper for high-performance supercapacitor. *Energy Environ Sci* 2013;6:1185–91.
- [303] Feng XM, Li RM, Ma YW, Chen RF, Shi NE, Fan QL, Huang W. One-step electrochemical synthesis of graphene/polyaniline composite film and its applications. *Adv Funct Mater* 2011;21:2989–96.
- [304] Cai Z, Li L, Ren J, Qiu L, Lin H, Peng H. Flexible, weavable and efficient microsupercapacitor wires based on polyaniline composite fibers incorporated with aligned carbon nanotubes. *J Mater Chem A* 2013;1:258–61.
- [305] Liu R, Lee SB. MnO_2 /poly(3,4-ethylenedioxothiophene) coaxial nanowires by one-step coelectrodeposition for electrochemical energy storage. *J Am Chem Soc* 2008;130:2942–53.
- [306] Zang J, Bao SJ, Li CM, Bian H, Cui X, Bao Q, Sun CQ, Guo J, Lian K. Well-aligned cone-shaped nanostructure of polypyrrole/RuO₂ and its electrochemical supercapacitor. *J Phys Chem C* 2008;112:14843–7.
- [307] Ambade RB, Ambade SB, Shrestha NK, Nah YC, Han SH, Lee W, Lee SH. Polythiophene infiltrated TiO_2 nanotubes as high-performance supercapacitor electrodes. *Chem Commun* 2013;49:2308–10.
- [308] Wei H, Yan X, Wu S, Luo Z, Wei S, Guo Z. Electropolymerized polyaniline stabilized tungsten oxide nanocomposite films: electrochromic behavior and electrochemical energy storage. *J Phys Chem C* 2012;116:25052–64.
- [309] Pieta P, Obraztsov I, D'Souza F, Kutner W. Composites of conducting polymers and various carbon nanostructures for electrochemical supercapacitors. *ECS J Solid State Sci Technol* 2013;2:M3120–34.
- [310] Nagai H, Segawa H. Energy-storable dye-sensitized solar cell with a polypyrrole electrode. *Chem Commun* 2004:974–5.
- [311] Yoneyama H, Kishimoto A, Kuwabata S. Charge–discharge properties of polypyrrole films containing manganese dioxide particles. *J Chem Soc Chem Commun* 1991:986–7.
- [312] Park KI, Song HM, Kim Y, Mho S, Cho Il W, Yeo IH. Electrochemical preparation and characterization of V_2O_5 /polyaniline composite film cathodes for Li battery. *Electrochim Acta* 2010;55:8023–9.
- [313] Boyano I, Bengoechea M, de Meatzia I, Miguel O, Cantero I, Ochoateco E, Rodriguez J, Lira-Cantu M, Gomez-Romero P. Improvement in the PPY/ V_2O_5 hybrid as a cathode material for Li ion batteries using PSA as an organic additive. *J Power Sources* 2007;166:471–7.
- [314] Liu B, Soares P, Checkles C, Zhao Y, Yu G. Three-dimensional hierarchical ternary nanostructures for high-performance Li-ion battery anodes. *Nano Lett* 2013;13:3414–9.
- [315] Winther-Jensen B, Winther-Jensen O, Forsyth M, Macfarlane DR. High rates of oxygen reduction over a vapor phase-polymerized PEDOT electrode. *Science* 2008;321:671–4.
- [316] Rajeshwar K, Janáky C, Lin WY, Roberts DA, Wampler W. Photocatalytically prepared metal nanocluster-oxide semiconductor–carbon nanocomposite electrodes for driving multielectron transfer. *J Phys Chem Lett* 2013;4:3468–78.
- [317] Zou BX, Liu XX, Diamond D, Lau KT. Electrochemical synthesis of WO_3 /PANI composite for electrocatalytic reduction of iodate. *Electrochim Acta* 2010;55:3915–20.
- [318] Bencsik G, Lukács Z, Visy C. Photo-electrochemical sensor for dissolved oxygen, based on a poly(3,4-ethylenedioxothiophene)/iron oxalate hybrid electrode. *Analyst* 2010;135:375–80.
- [319] Shi J, Guo D, Wang Z, Li H. Electrocatalytic oxidation of formic acid on platinum particles dispersed in SWNT/PANI composite film. *J Solid State Electrochem* 2005;9:634–8.
- [320] Wu G, Li L, Li JH, Xu BQ. Methanol electrooxidation on Pt particles dispersed into PANI/SWNT composite films. *J Power Sources* 2006;155:118–27.
- [321] Wang Z, Yuan J, Li M, Han D, Zhang Y, Shen Y, Niu L, Ivaska A. Electropolymerization and catalysis of well-dispersed polyaniline/carbon nanotube/gold composite. *J Electroanal Chem* 2007;599:121–6.
- [322] Wang Q, Yun Y. A nanomaterial composed of cobalt nanoparticles, poly(3,4-ethylenedioxothiophene) and graphene with high electrocatalytic activity for nitrite oxidation. *Microchim Acta* 2012;177:411–8.
- [323] Su PG, Huang LN. Humidity sensors based on TiO_2 nanoparticles/polypyrrole composite thin films. *Sens Actuators B* 2007;123:501–7.
- [324] Boback J, Ivaska A, Lewenstam A. Potentiometric ion sensors based on conducting polymers. *Electroanalysis* 2003;15:366–74.
- [325] Ramanavicius A, Ramanaviciene A, Malinauskas A. Electrochemical sensors based on conducting polymer/polypyrrole. *Electrochim Acta* 2006;51:6025–37.
- [326] Janáky C, Visy C. Conducting polymer-based hybrid assemblies for electrochemical sensing: a materials science perspective. *Anal Bioanal Chem* 2013;405:489–511.
- [327] Grankvist CG. Electrochromic tungsten oxide films: review of progress 1993–1998. *Sol Energy Mater Sol Cells* 2000;60:201–62.
- [328] Amb CM, Dyer AL, Reynolds JR. Navigating the color palette of solution-processable electrochromic polymers. *Chem Mater* 2011;23:397–415.
- [329] Kobayashi N, Teshima K, Hirohashia R. Conducting polymer image formation with photoinduced electron transfer reaction. *J Mater Chem* 1998;8:497–506.
- [330] Thakur VK, Ding G, Ma J, Lee PS, Lu X. Hybrid materials and polymer electrolytes for electrochromic device applications. *Adv Mater* 2012;24:4071–96.
- [331] Cai GF, Tu JP, Zhou D, Zhang JH, Wang XL, Gu CD. Dual electrochromic film based on WO_3 /polyaniline core/shell nanowire array. *Sol Energy Mater Sol Cells* 2014;122:51–8.
- [332] Yoneyama H, Takahashi N, Kuwabata S. Formation of a light image in a polyaniline film containing titanium (IV) oxide particles. *Chem Commun* 1992;716–7.